



Module 3202: Biosphere - Agricultural Applications with SAR Data

Tanja Riedel

Robert Eckardt

Earth Observation

Institute of Geography

Friedrich-Schiller-University Jena

Content of Module Biosphere

- ↗ Forest biomass estimation using SAR data (Module 3210)
- ↗ Agricultural applications with SAR data (Module 3220)

Educational Objectives

- ↗ To learn how SAR data are usable for agricultural applications
- ↗ To understand advantages of SAR techniques over traditional measuring techniques and optical systems
- ↗ To understand the limitations of SAR techniques
- ↗ To learn optimal sensor and acquisition parameters for agricultural applications

Tutorial

- ↗ Extraction of temporal crop signatures and crop type classification using multitemporal C-band data acquired over Nordhausen, Thuringia, Germany (Nest software)

Requirements

- ↗ You know and understand the mathematical and physical basics
[\(Module ID 1100: Mathematics & physics\)](#)
- ↗ You know and understand SAR technology
[\(Module ID 1300: SAR basics\)](#)
- ↗ You know and understand main SAR processing steps
[\(Module ID 1200: Data processing\)](#)
- ↗ You know and understand main image interpretation techniques
[\(Module ID 2100: Image processing\)](#)
- ↗ You know the basics of SAR polarimetry
[\(Module ID 2300: SAR polarimetry\)](#)
- ↗ **For tutorial:** You know basic functions of the NEST software
[\(Tutorial: Data processing with 'NEST'\)](#)

Further Reading

Overview

- Brisco, B. & R.J. Brown (1998): Agricultural Applications with Radar. In: Henderson, F.M. & A.J. Lewis (Eds.): *Principles & Applications of Imaging Radar. Manual of Remote Sensing*. Third Edition, Volume 2. Wiley & Sons, New York.
- Ferrazzoli, P. (2001). SAR for agriculture: advances, problems and prospects. In: *Proceedings of the Third International Symposium on Retrieval of Bio- and Geophysical Parameters from SAR Data for Land Applications* (ESA SP-475, pp. 47-56), September 11-14, 2001, Sheffield, UK.
- Lopez-Sanchez, J. M., & Ballester-Berman, J. D. (2009). Potentials of polarimetric SAR interferometry for agriculture monitoring. *Radio Science*, 44(2), DOI: 10.1029/2008RS004078.
- McNairn, H., & Brisco, B. (2004): The application of C-band polarimetric SAR for agriculture: a review. *Canadian Journal of Remote Sensing*, 30(3), 525-542.

Application Examples

- Baghdadi, N., Boyer, N., Todoroff, P., El Hajj, M., & Bégué, A. (2009). Potential of SAR sensors TerraSAR-X, ASAR/ENVISAT and PALSAR/ALOS for monitoring sugarcane crops on Reunion Island. *Remote Sensing of Environment*, 113, 1724–1738.
- Bouvet, A., & Le Toan, T. (2011). Use of ENVISAT/ASAR wide-swath data for timely rice fields mapping in the Mekong River Delta. *Remote Sensing of Environment*, 115, 1090–1101.

Further Reading

- Brown, S. C. M., Quegan, S., Morrison, K., Bennett, J. C., & Cookmartin, G. (2003). High-resolution measurements of scattering in wheat canopies - Implications for crop parameter retrieval. *IEEE Transactions on Geoscience and Remote Sensing*, 41(7), 1602–1610.
- Chakraborty, M., Manjunath, K. R., Panigrahy, S., Kundu, N., & Parihar, J. S. (2005). Rice crop parameter retrieval using multi-temporal, multi-incidence angle RADARSAT SAR data. *ISPRS Journal of Photogrammetry and Remote Sensing*, 59, 310–322.
- Chen, C., & McNairn, H. (2006). A neural network integrated approach for rice crop monitoring. *International Journal of Remote Sensing*, 27(7), 1367-1393.
- De Mattheis, P., Schiavon, G., & Solimini, D. (1994). Effect of scattering mechanisms on polarimetric features of crops and trees. *International Journal of Remote Sensing*, 15(14), 2917-2930.
- Hoekman, D. H., & Vissers, M. A. M. (2003). A new polarimetric classification approach evaluated for agricultural crops. *IEEE Transactions on Geoscience and Remote Sensing*, 41(12), 2881–2889.
- Li, K., Brisco, B., Yun, S., & Touzi, R (2012). Polarimetric decomposition with RADARSAT-2 for rice mapping and monitoring. *Canadian Journal of Remote Sensing*, 38, 169–179.
- Macelloni, G., Paloscia, S., Pampaloni, P., Marliani, F., & Gai, M. (2001). The relationship between the backscattering coefficient and the biomass of narrow and broad leaf crops. . *IEEE Transactions on Geoscience and Remote Sensing*, 39(4), 873–884.
- McNairn, H., Champagne, C., Shang, J., Holmstrom, D., & Reichert, G. (2009). Integration of optical and Synthetic Aperture Radar (SAR) imagery for delivering operational annual crop inventories. *ISPRS Journal of Photogrammetry & Remote Sensing*, 64(5). 434-449.

Further Reading

- Pei, Z., Zhang, S., Guo, L., McNairn, H., Shang, J., & Jiao, X. (2011). Rice identification and change detection using TerraSAR-X data. *Canadian Journal of Remote Sensing*, 37(1), 151-156.
- Saich, P., & Borgeaud, M. (2000). Interpreting ERS SAR signatures of agricultural crops in Flevoland, 1993–1996. *IEEE Transactions on Geoscience and Remote Sensing*, 38(2), 651–657.
- Satalino, G., Mattia, F., Le Toan, T., & Rinaldi, M. (2009). Wheat crop mapping by using ASAR AP data. *IEEE Transactions on Geoscience and Remote Sensing*, 47(2), 527–530.
- Silva, W. F., Rudorff, B. F. T., Formaggio, A. R., Paradella, W. R., & Mura, J. C. (2009). Discrimination of agricultural crops in a tropical semiarid region of Brazil based on L-band polarimetric airborne SAR data. *ISPRS Journal of Photogrammetry and Remote Sensing*, 64, 458–463.
- Skriver, H., Svendsen, M. T., & Thomsen, A. G. (1999). Multitemporal C- and L-band polarimetric signatures of crops. *IEEE Transactions on Geoscience and Remote Sensing*, 37(5), 2413–2429.
- Voormansik, K., Jagdhuber, T., Olesk, A., Hajnsek, I., & Papathanassiou, K. P. (2013). Towards a detection of grassland cutting practices with dual polarimetric TerraSAR-X data. *International Journal of Remote Sensing*, 34(22), 8081-8103.
- Wang, D., Lin, H., Chen, J., Zhang, Y., & Zeng, Q. (2010). Application of multi-temporal Envisat ASAR data to agricultural area mapping in the Pearl River Delta. *International Journal of Remote Sensing*, 31(6), 1555–1572.
- Zhang, Y., Wang, C., Wu, J., Qi, J., & Salas, W. A. (2009). Mapping paddy rice with multitemporal ALOS/PALSAR imagery in southeast China. *International Journal of Remote Sensing*, 30(23), 6301-6315.



See also references
slide 150 - 158

Structure

- ↗ Introduction
- ↗ Major parameters affecting radar backscatter from crops
 - ↗ Sensor parameters
 - ↗ Target parameters
- ↗ Agricultural applications
 - ↗ Crop type mapping
 - ↗ Crop management / biophysical parameter retrieval
 - ↗ Soil parameter retrieval
- ↗ Optimal system configuration for agricultural applications

Structure

- ↗ Introduction
- ↗ Major parameters affecting radar backscatter from crops
 - ↗ Sensor parameters
 - ↗ Target parameters
- ↗ Agricultural applications
 - ↗ Crop type mapping
 - ↗ Crop management / biophysical parameter retrieval
 - ↗ Soil parameter retrieval
- ↗ Optimal system configuration for agricultural applications

Global agriculture and food demand

- ↗ Approximately one billion people (roughly one in seven) on earth don't have enough food right now (Foley et al., 2011)
- ↗ ~ 1/3 of the food produced is lost or wasted each year (FAO, 2013a)
- ↗ Agricultural production needs to increase by 60% over the next 40 years to meet rising food demand (OECD-FAO, 2012)

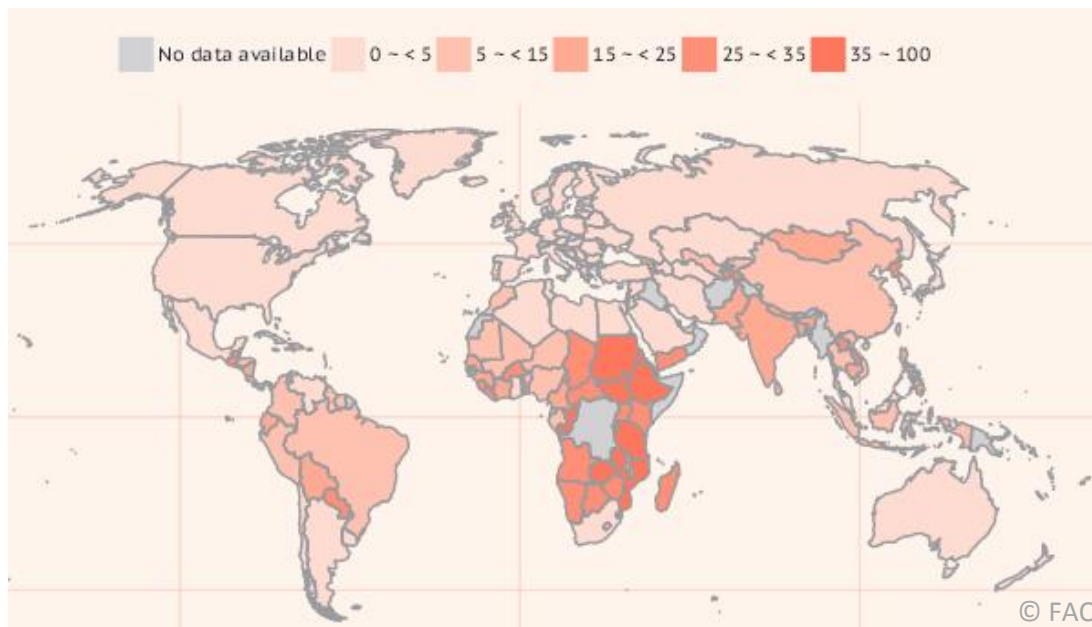


Fig.: Map of hunger: % prevalence of undernourishment, 2012 (FAO, 2013b)

The state of global agriculture

Agriculture occupies about 38% of Earth's terrestrial surface

- Croplands ~ 12% of ice-free land
- Pasture ~ 26% of ice-free land
- ~ 25% of all agricultural land is highly degraded

Foley et al., 2011

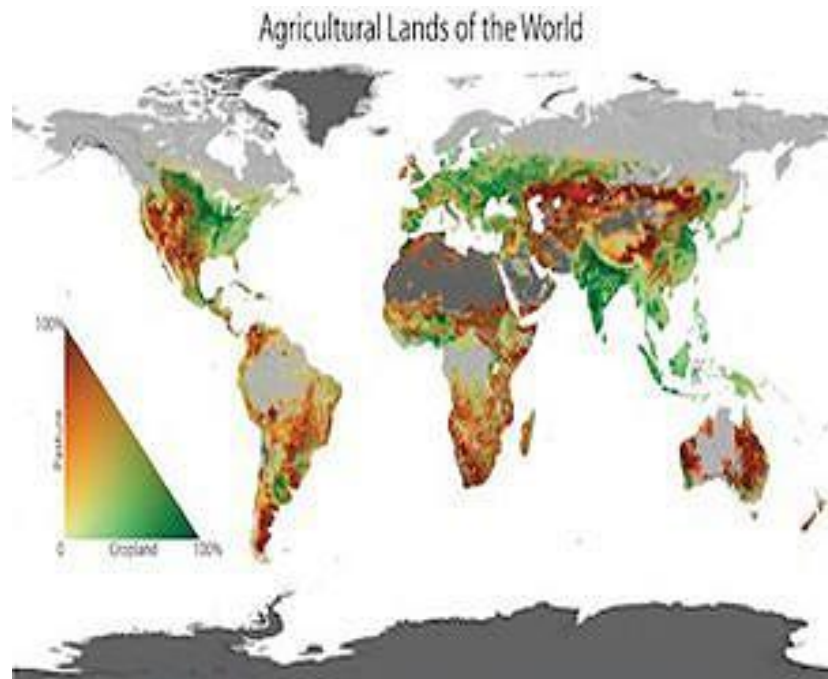


Fig.:

http://www.seddaily.com/reports/Southampton_researchers_help_to_outline_world_land_and_water_resources_for_food_and_agriculture_999.html

The state of global agriculture

Global crop use and allocation

- Human food: 62%
- Animal feed: 35% (although animal feed produces human food indirectly, e.g. meat and dairy products, efficiency is much less)
- Bioenergy, seed and other industrial products: 3%

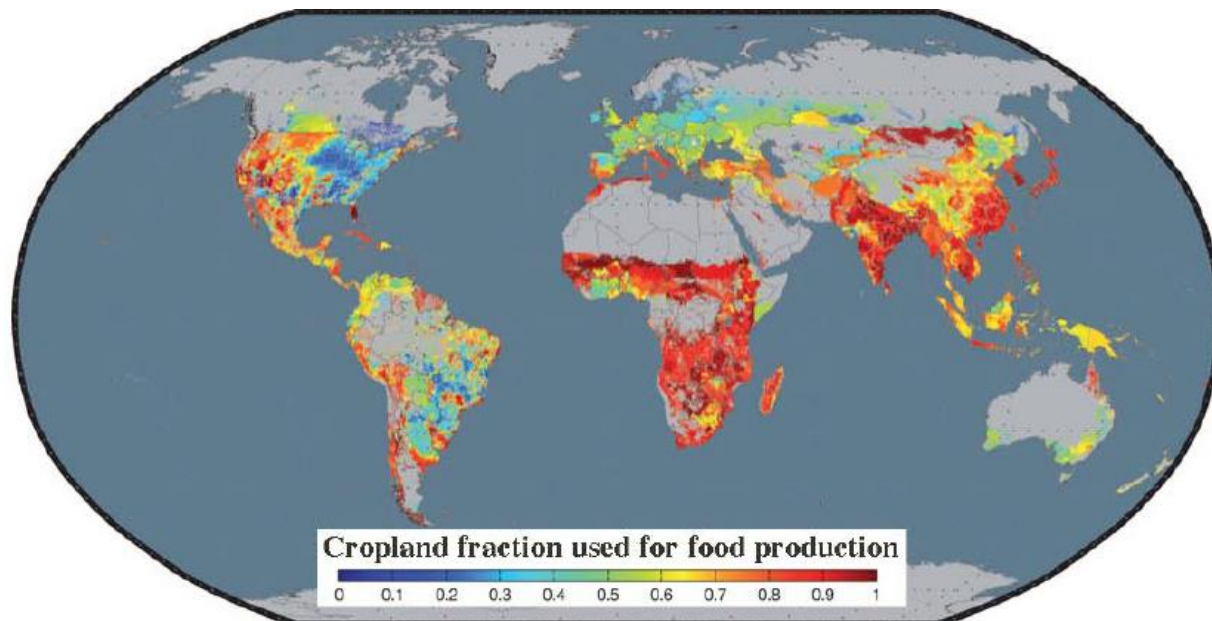


Fig.: Foley et al., 2011

Foley et al., 2011

Environmental impacts of agriculture

Negative impacts of current agriculture praxis

- ↗ Biodiversity is threatened by land clearing and habitat fragmentation
- ↗ Greenhouse gas (GHG) emissions from land clearing, crop production and fertilization contribute already to 1/3 of global GHG emissions
- ↗ Global nitrogen and phosphorus cycles have been disrupted, with impacts on water quality aquatic ecosystems and marine fisheries
- ↗ Freshwater resources are depleted as nearly 80 percent of freshwater currently used by humans is for irrigation

Atzberger, 2013

Future pathways

Need for increasing agricultural production – main drivers

- ↗ Population growth
- ↗ Increasing consumption of calorie- and meat-intensive diets
- ↗ Increasing use of cropland for bioenergy production

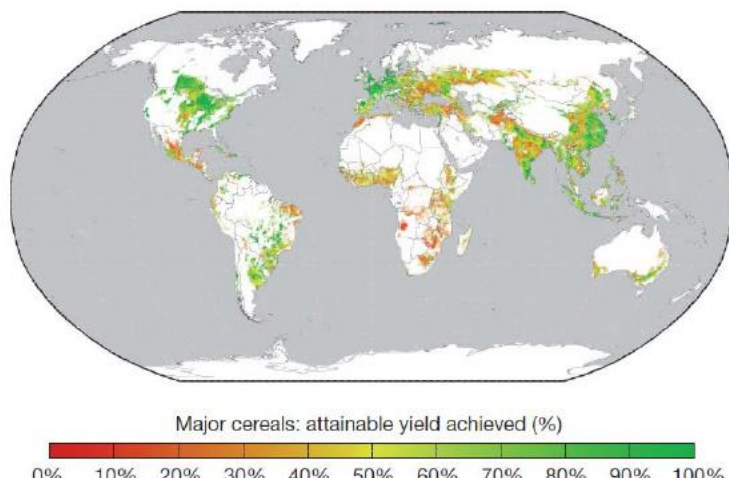
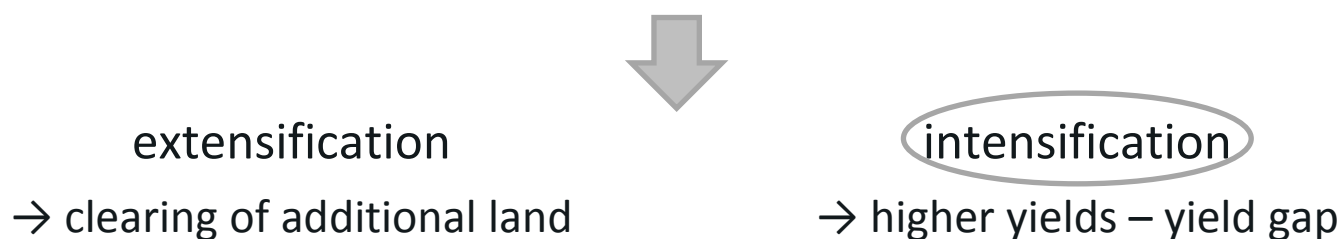


Fig.: Atzberger, 2013

Future pathways

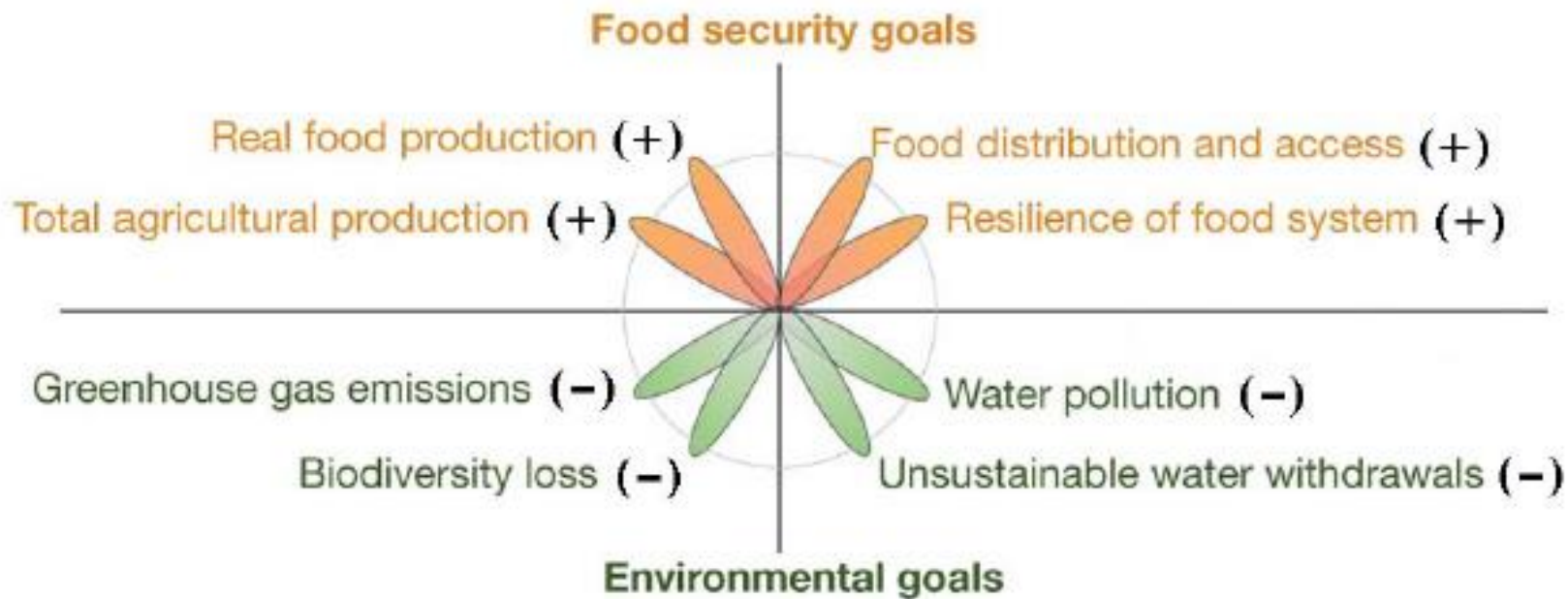


Fig.: Future environmental (bottom) and food security goals (top). The signs after the different items indicate if an increase is necessary (+), respectively, or a reduction (-) (Atzberger, 2013)

Agricultural monitoring

Challenge

- Biological lifecycle of crops – strong seasonal patterns
- Agricultural production depends on
 - Physical landscape (e.g., soil type)
 - Climatic driving variables
 - Agricultural management practices
- Unfavourable growing conditions → change of productivity within short time

Highly variable in space and time!!!



Major factor for agricultural monitoring:

Timeliness

Atzberger, 2013

Remote sensing for agricultural monitoring

Earth observation provides an unique and cost-efficient tool to acquire timely and spatially consistent information over large areas with a high revisit frequency

Advantages of SAR (compared to optical remote sensing)

- ↗ **All-weather capability**
 - ⇒ Frequent measurements during the short dynamic growing season of crops is possible
- ↗ Independence of sun illumination → day and night operation
- ↗ Sensitivity to dielectric (water content, biomass) and geometrical (plant/canopy structure, surface roughness) properties of the target → complementary information to optical data

Remote sensing for agricultural monitoring

Disadvantages of SAR data

- ↗ Complex interactions
(difficult in understanding, complex processing)
- ↗ Speckle effects
- ↗ Topographic effects, radar shadow
- ↗ Effect of surface roughness

LeToan, 2008

Remote sensing for agricultural monitoring

End Users

Remote sensing - a tool for management and optimization of resources

| End users | Demand | Objective |
|---|---|---|
| Authorities or government agencies at national-regional-local scale | Crop-type mapping and classification | Justification of subsidies and fraud detection |
| | Water resources consumption | Control in regions suffering droughts or with scarce water resources |
| | Yield prediction & losses | Economic and market predictions, price regulations, etc. production adjustment payments |
| Farmers with extensive fields | Timely information about crop condition | Planning and triggering of farming practices according to specific phenological stages |
| | Water requirements | Irrigation only when and where necessary |
| | Final crop productivity | Benefits |

Tab.: Lopez-Sanchez, 2010 (adapted)

Remote sensing for agricultural monitoring

Most frequent applications of EO-data in agriculture

(Findings of the pre-workshop survey of the International GEO Workshop on Synthetic Aperture Radar (SAR) to support agricultural monitoring, Canada, 2009)

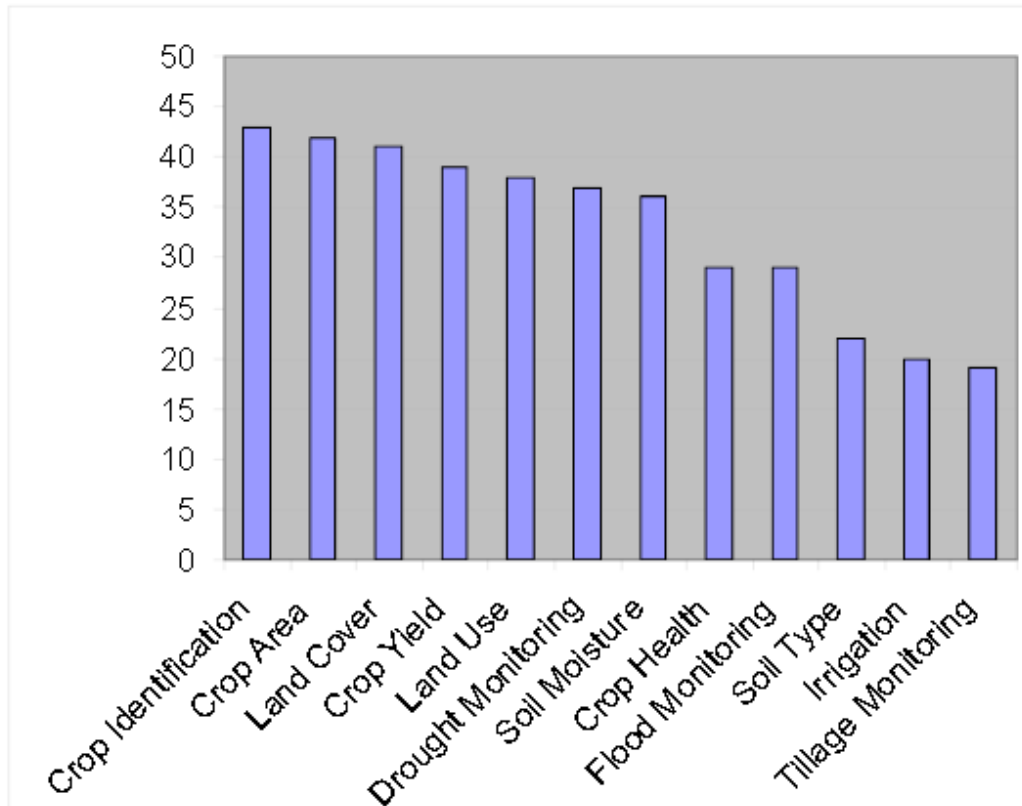


Fig.: Top twelve applications of agricultural monitoring data - (Government of Canada, 2010)

Structure

- ↗ Introduction
- ↗ Major parameters affecting radar backscatter from crops
 - ↗ Sensor parameters
 - ↗ Target parameters
- ↗ Agricultural applications
 - ↗ Crop type mapping
 - ↗ Crop management / biophysical parameter retrieval
 - ↗ Soil parameter retrieval
- ↗ Optimal system configuration for agricultural applications

Radar backscatter from crops

Depends upon a wide range of parameters of the vegetation, soil, topography and the sensor itself

↗ Challenges

- ↗ Dielectric & geometric attributes of crops vary significantly within short time
- ↗ Phenological cycle is very short (few months only)

↗ Where do we know the importance of each parameter?

- ↗ Complex measurement campaigns
- ↗ Radar backscatter models
- ↗ Backscatter mechanism analyses

→ See module 2300:
Radar polarimetry

Radar backscatter from crops

Scattering mechanisms important for agricultural crops

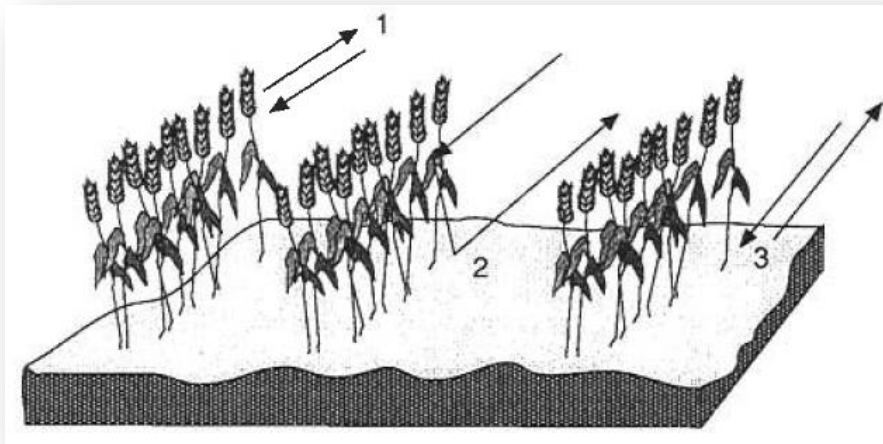


Fig.: Sources of radar backscatter from cultivated crops (Brisco & Brown 1998)

- 1 – Direct backscattering from the vegetation constituents such as leaves, stems, heads (including multiple scattering)
- 2 – Double-bounce reflections between the soil surface and the crop canopy
- 3 – Direct backscattering from the underlying ground (including multiple scattering)

Radar backscatter from crops

The importance of each **scattering mechanism** depends on

- ↗ System parameters
 - ↗ Frequency
 - ↗ Polarisation
 - ↗ Incident angle
 - ↗ Target parameters
 - ↗ Dielectric properties (soil / plant moisture)
 - ↗ Geometrical properties (surface roughness, plant / canopy structure)
- ⇒ Vary with crop type, phenological stage ...

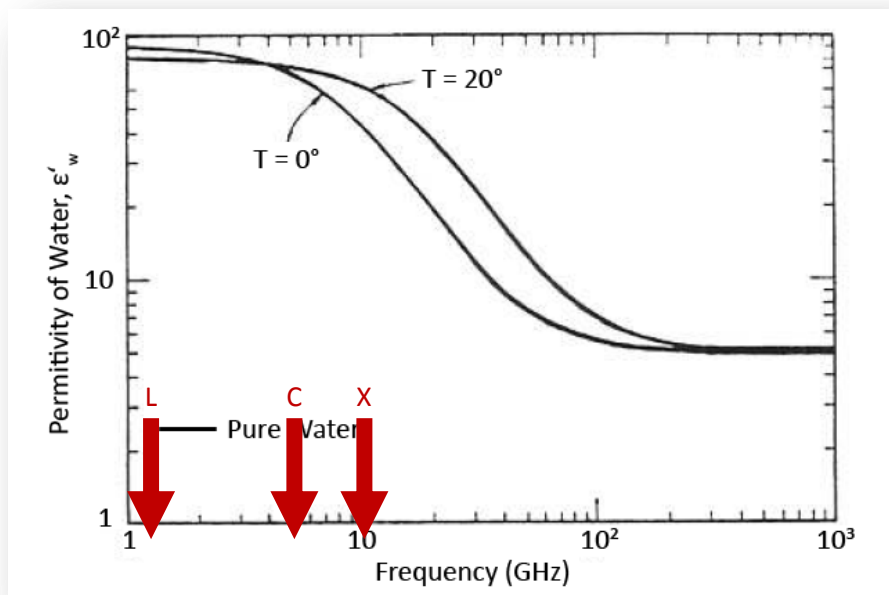
Structure

- ↗ Introduction
- ↗ Major parameters affecting radar backscatter from crops
 - ↗ Sensor parameters
 - ↗ Target parameters
- ↗ Agricultural applications
 - ↗ Crop type mapping
 - ↗ Crop management / biophysical parameter retrieval
 - ↗ Soil parameter retrieval
- ↗ Optimal system configuration for agricultural applications

System parameters - frequency

Dependence of radar backscatter from frequency due to relationship between

- Dielectric constant of water and frequency



*Plant water content
vary as a function of
crop type, growth stage
and crop condition*

Fig.: Real part of the dielectric constant of pure water vs. frequency for 0°C & (redrawn from Ulaby et al. 1986)

- Frequency and plant part size and/or penetration depth

System parameters - frequency

Decreasing frequency

- ↗ Signal **penetration** into crops/soil **increases**
 - ↗ Size of target components (leafs, ears etc.) relative to wavelength becomes smaller → „**smoother**“ target
-
- ⇒ Higher frequencies (e.g. X-Band) → dominated by **canopy scattering**
 - ⇒ Lower frequencies (e.g. L- or P-Band) → dominant or significant **soil backscatter** contributions

System parameters - frequency

Airborne E-SAR data acquired on June 14, 2000 near Alling, Bavaria, Germany



Fig.: VV-polarized E-SAR data (© DLR) at X-, C- and L-band

⇒ L-band: less information on crop type

System parameters - frequency

Airborne E-SAR data acquired on June 14, 2000 near Alling, Bavaria, Germany

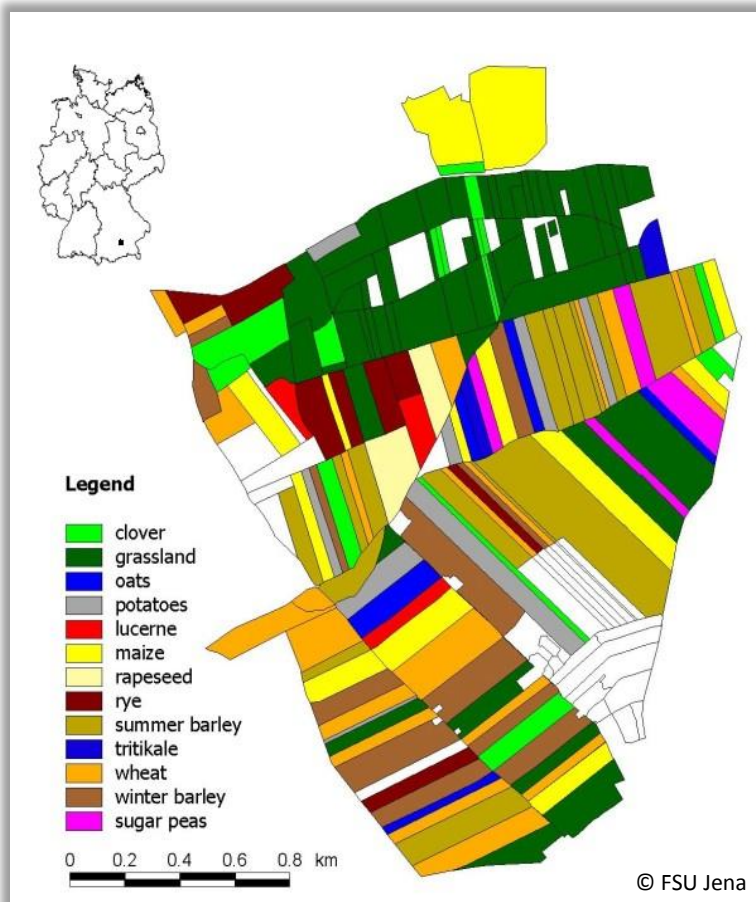


Fig.: X-VV / C-VV / L-VV composite (left) and crop type map (right)

System parameters - polarization

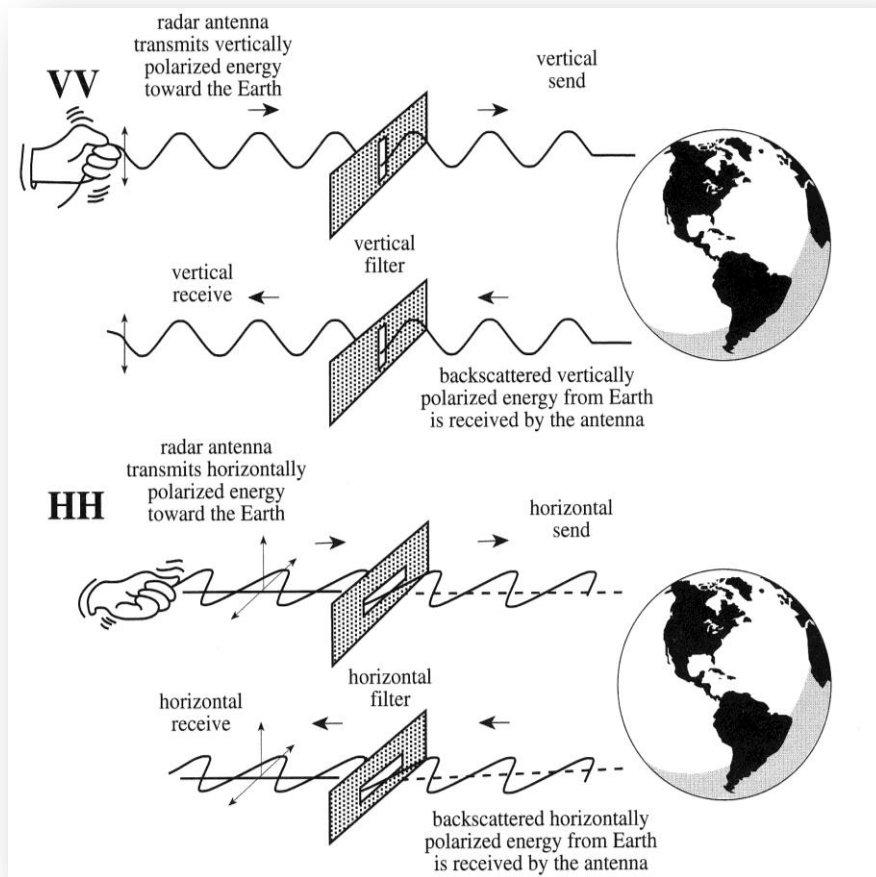


Fig.: Polarisation (Jensen, 2000).

HH: the emitted and backscattered signals have horizontal polarization.

HV: the emitted signal has horizontal and the backscattered signal has vertical polarization.

VH: the emitted signal has vertical and the backscattered signal has horizontal polarization.

VV: both emitted and reflected signals have vertical polarization.

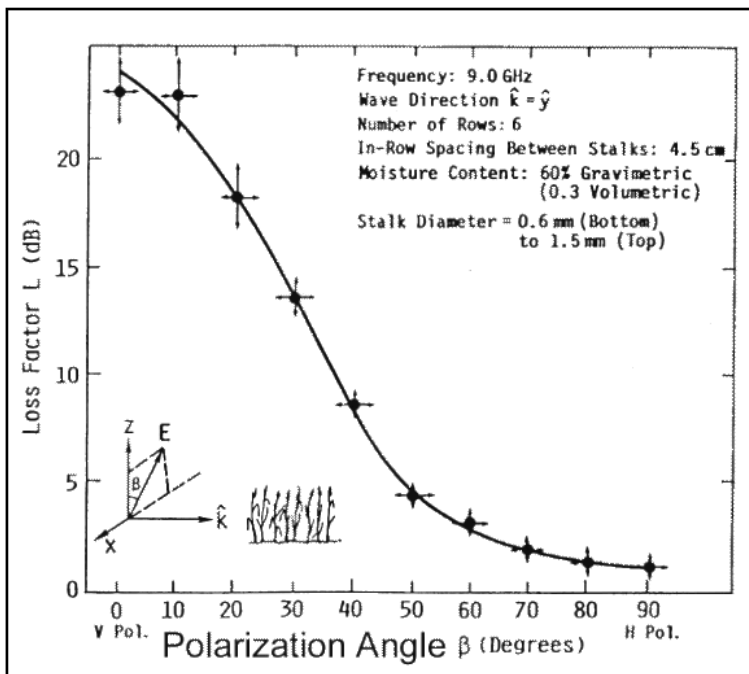


See module 1300:
SAR basics

System parameters - polarization

Different attenuation of **grain** crops at HH versus VV

- Grain → dominantly vertical oriented components (esp. stems)
- VV-polarisation: strong attenuation of radar signal
- HH-polarisation: more information about underlying soil



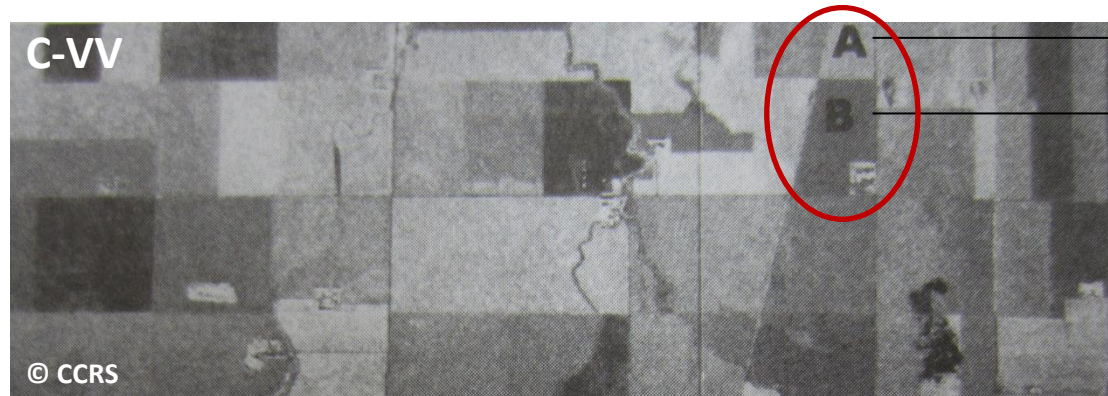
HH/VV-ratio used for

- *classification*
(slide 73)
- *biomass estimation*
(slides 115 / 116)

Fig.: Lopes, 1983

System parameters - polarisation

- ↗ Polarisation dependence of grain



- ↗ VV-polarisation:
stronger interaction
with vegetation
structure
- ↗ HH-polarisation:
stronger soil
contribution – similar
roughness and
moisture

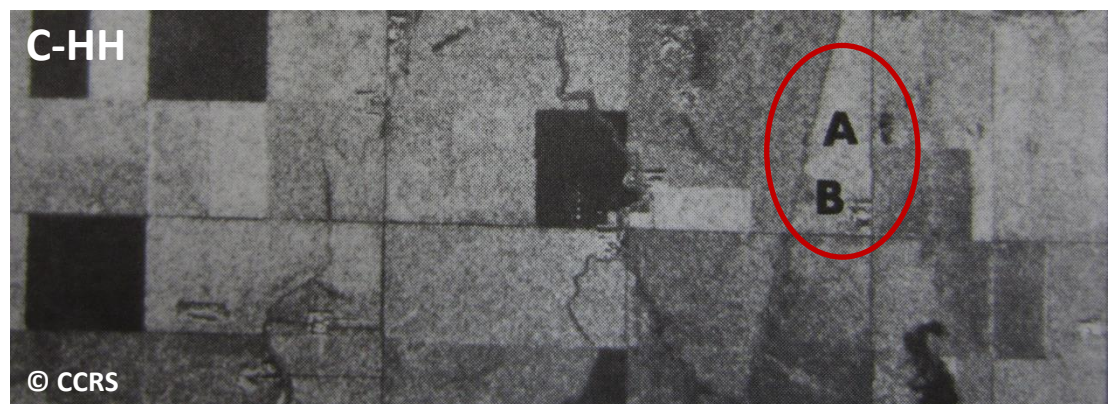


Fig.: C-VV and C-HH SAR images acquired on July 13, 1989 over an agricultural area near Melfort, Saskatchewan (Brisco & Brown, 1998)

System parameters - polarisation

Airborne E-SAR data acquired on June 14, 2000 near Alling, Bavaria, Germany



Fig.: E-SAR data (© DLR) at L-band

⇒ Dependence of information content on polarization

System parameters - polarisation

Airborne E-SAR data acquired on June 14, 2000 near Alling, Bavaria, Germany

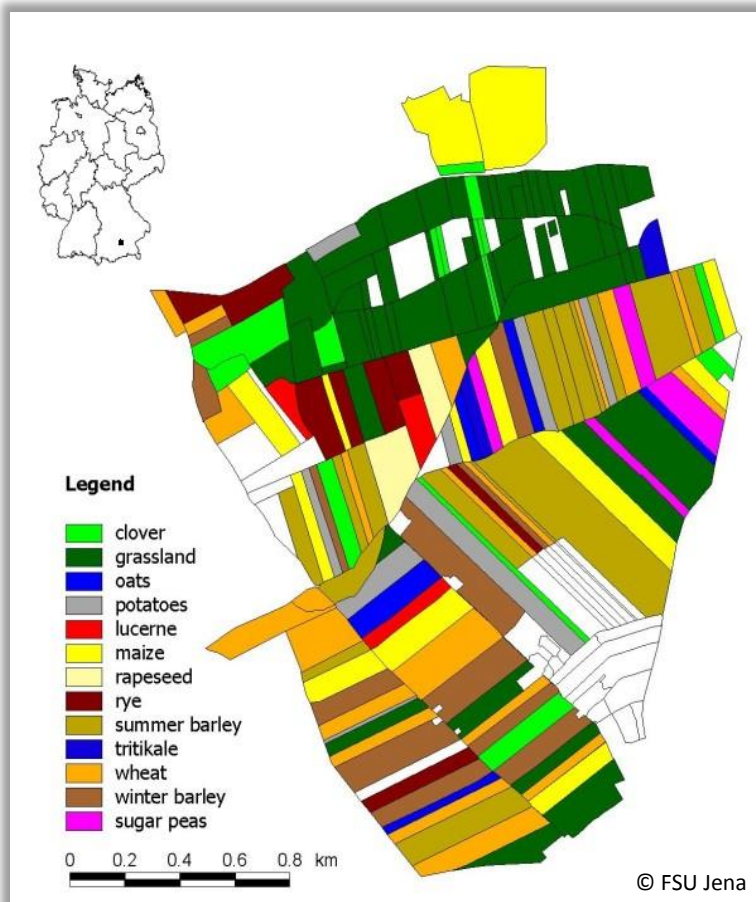


Fig.: L-VV-L-HV-L-HH composite (left) and crop map (right)

System parameters - polarisation

Airborne E-SAR data acquired on June 14, 2000 near Alling, Bavaria, Germany

- ↗ Polarisation dependence of radar backscatter for two corn fields

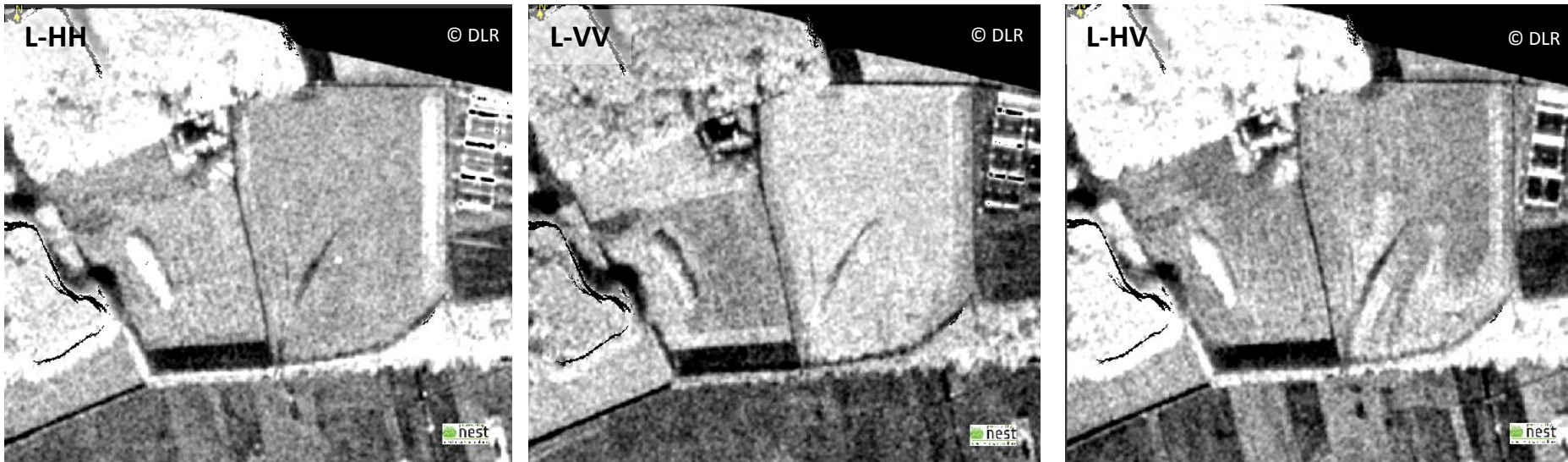


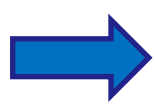
Fig.: E-SAR data (© DLR) at L-band

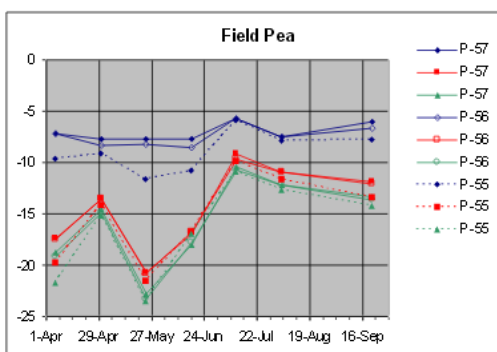
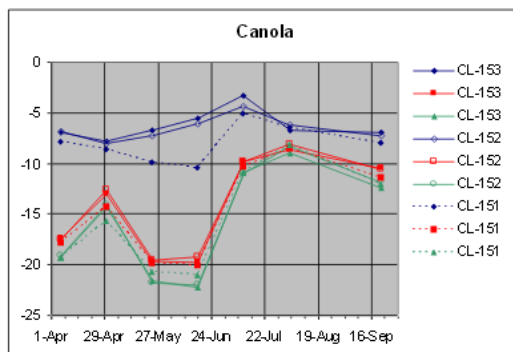
⇒ VV-polarisation: strong effect of row orientation

System parameter – polarisation

Fully polarimetric SAR images

- additional information gain, e.g. on scattering mechanisms

 See module 2300:
polarimetry



Surface Scattering - $|HH+VV|^2$
Dihedral Scattering - $|HH-VV|^2$
Volume Scattering - $|HVI|^2$

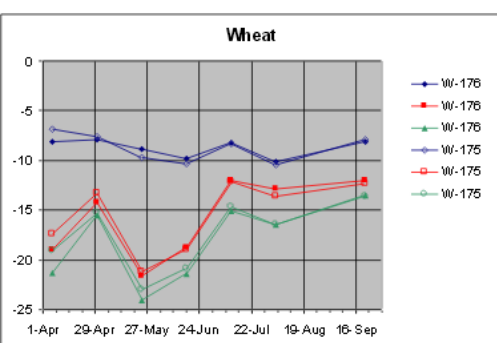
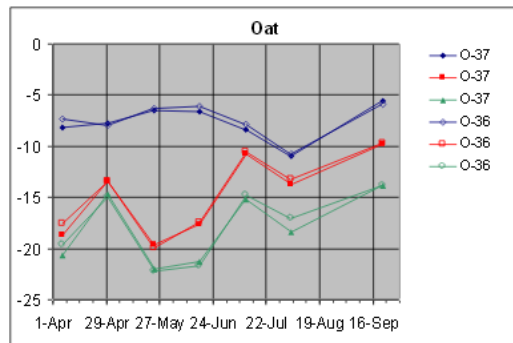


Fig.: Staples et al., 2010

System parameters - incident angle

General:

- ↗ Shallow incident angles ($> 40^\circ$)
 - ↗ Higher sensitivity to crop conditions
 - ↗ Why?: path length through vegetation increases
- ↗ Steep incident angles ($< 30^\circ$)
 - ↗ More useful for soil moisture measurement
 - ↗ Why?: effects of soil roughness and vegetation attenuation decreases

System parameters - incident angle

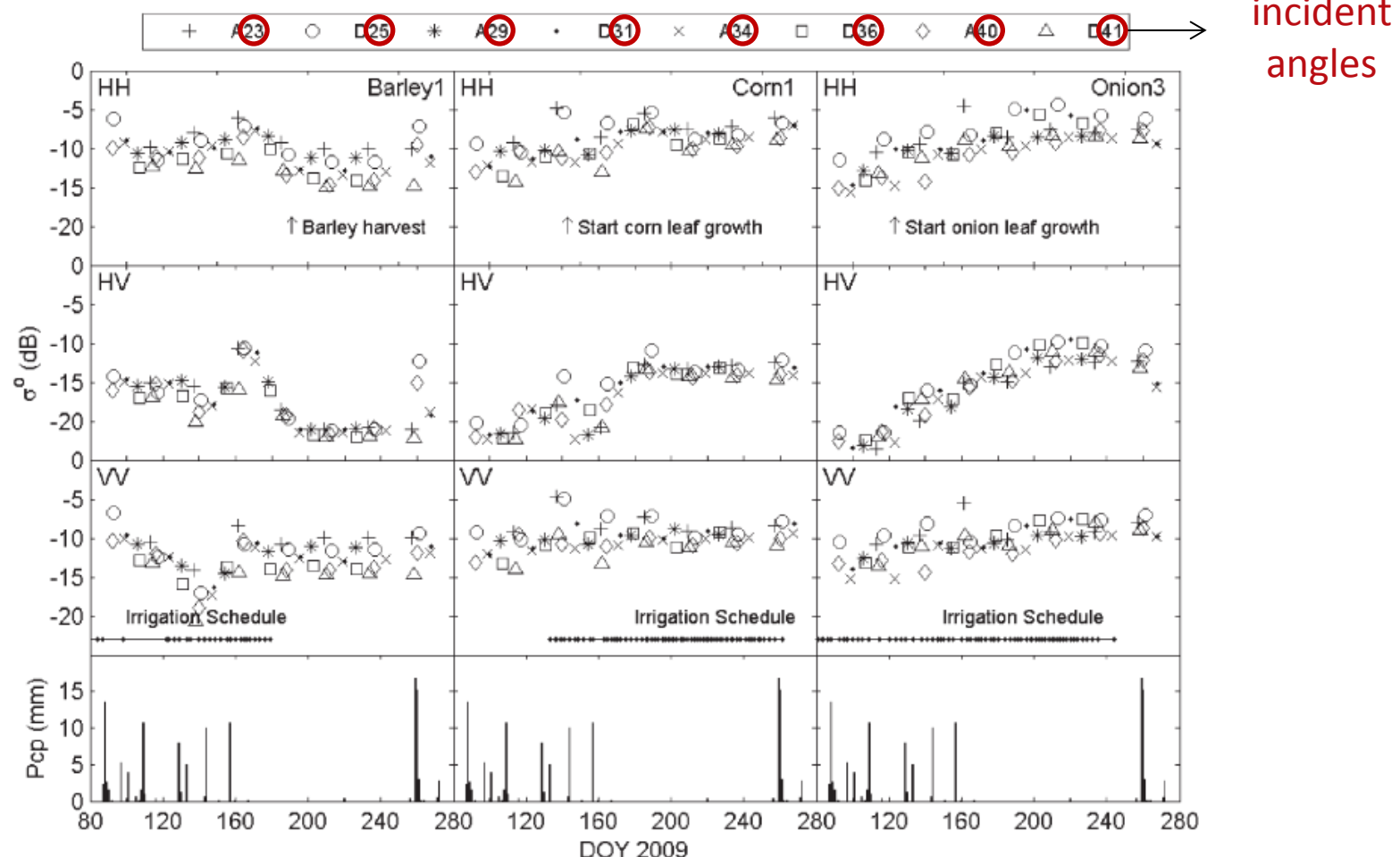


Fig.: RADARSAT-2 backscatter of three crop types at various incident angles (Moran et al., 2012)

System parameters - incident angle

- ↗ TerraSAR-X data acquired at different incident angles (2 days in between)
- ↗ Test site Nordhausen, Thuringia, Germany

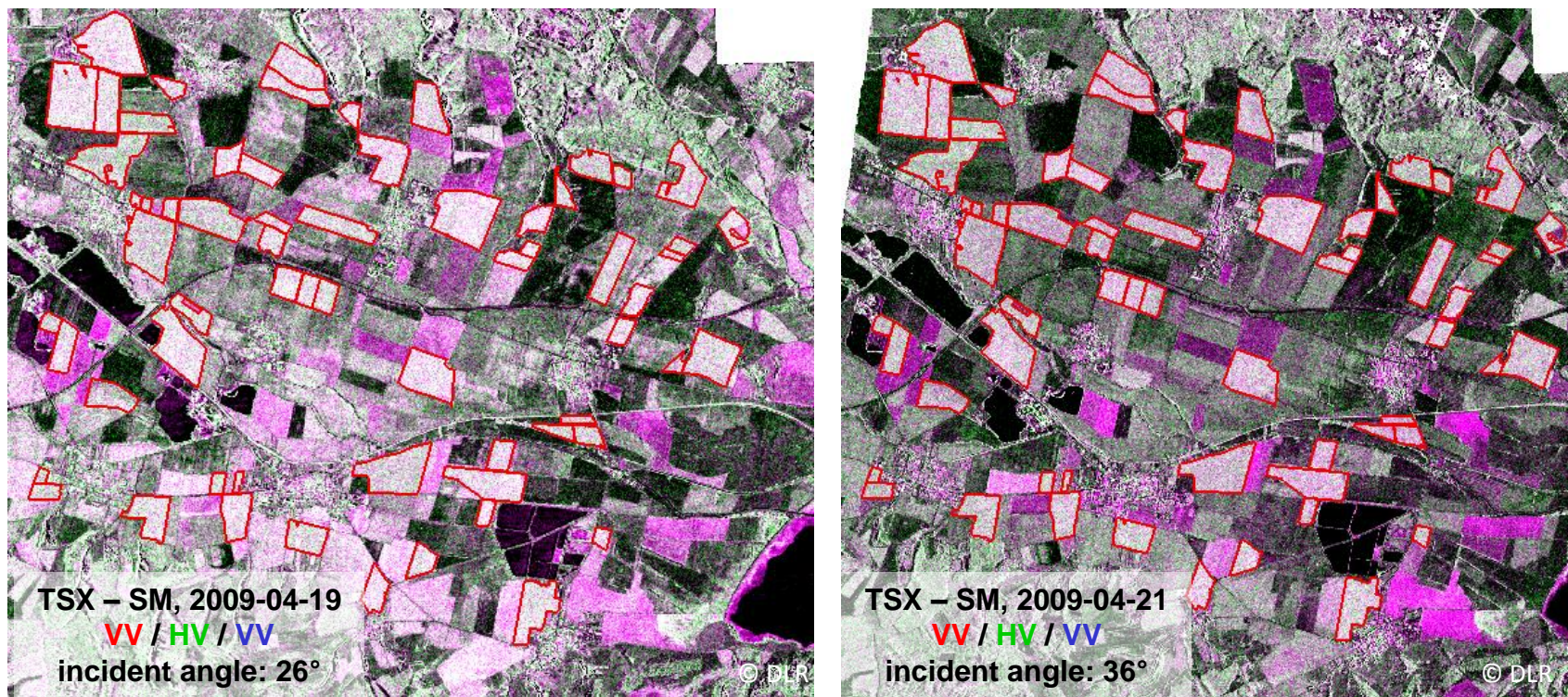


Fig.: TSX RGB-composites overlaid with reference data for rape in red

- ↗ Shallow incident angles: higher separability of corn fields, especially at VV
- ↗ Later in season: higher separability at HV, all incident angles

System parameters - incident angle

- TerraSAR-X data acquired at different incident angles (2 days in between)
- Test site Nordhausen, Thuringia, Germany

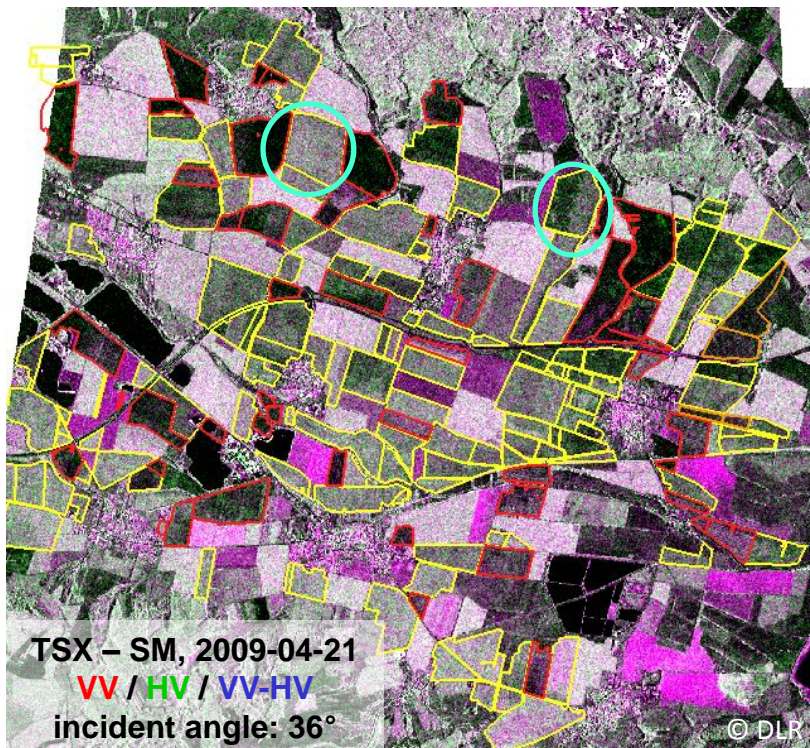
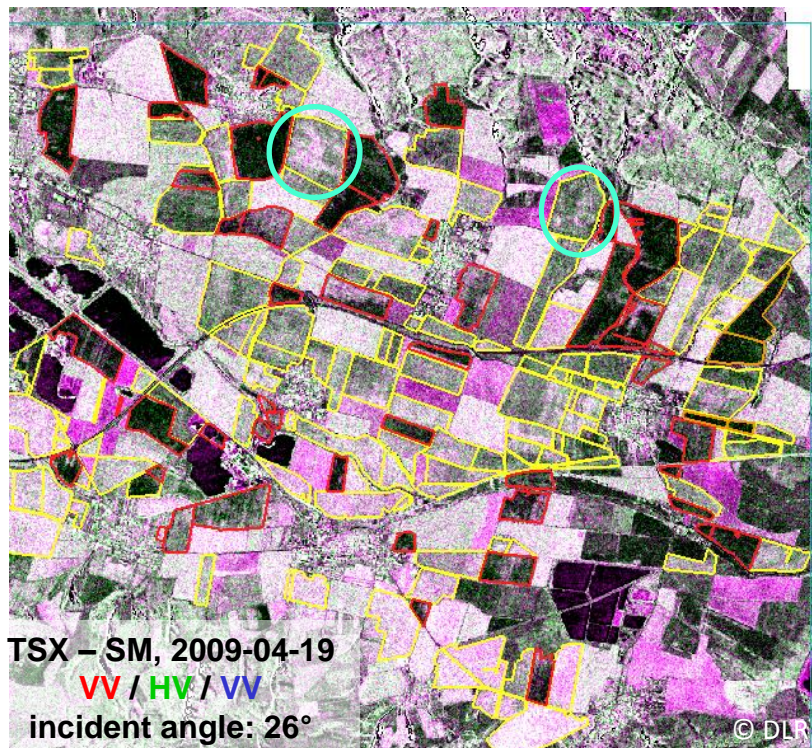


Fig.: TSX RGB-composites overlaid with reference data: winter wheat → yellow / winter barley → red / winter triticale → orange

- Steep incident angles, VV: higher intra-field variability → higher sensitivity to soil moisture variation

System parameters - incident angle

- ↗ TerraSAR-X data acquired at different incident angles (2 days in between)
- ↗ Test site Nordhausen, Thuringia, Germany

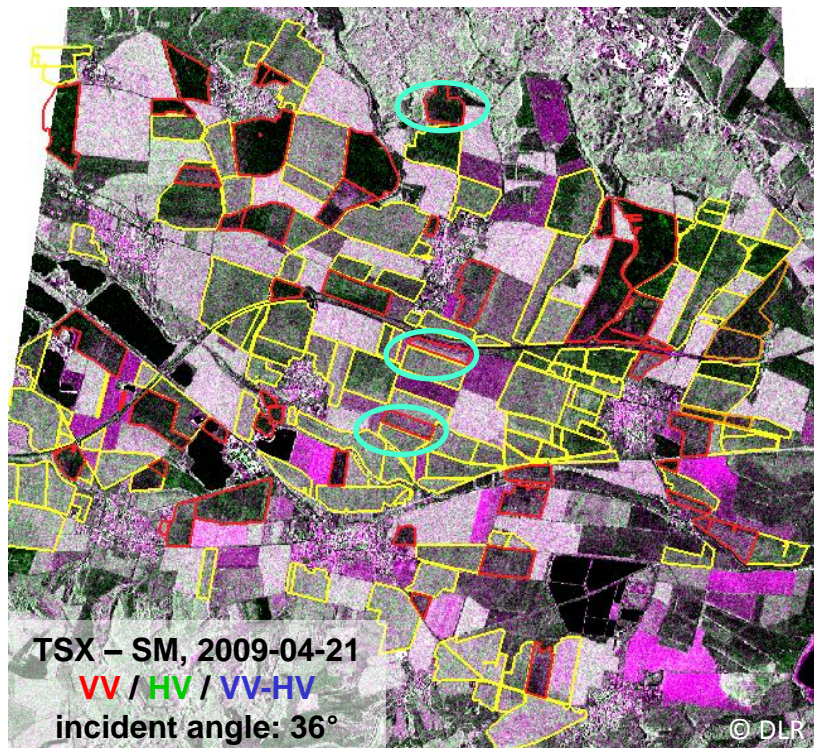
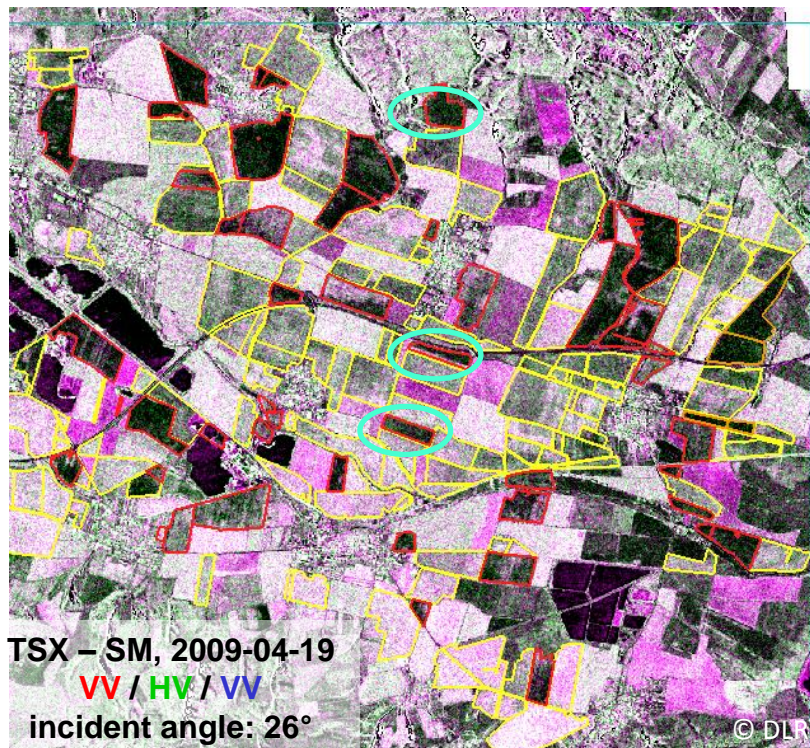


Fig.: TSX RGB-composites overlaid with reference data: winter wheat → yellow / winter barley → red / winter triticale → orange

- ↗ Steep incident angles: better separability of wheat vs. barley / triticale
→ confirmed by statistics and classifications

System parameters - incident angle

- ↗ Multiangular Radarsat-2 images, test-site Pleine-Fougères, France
- ↗ Acquisition time: end of March → most fields were covered by small crops with less density

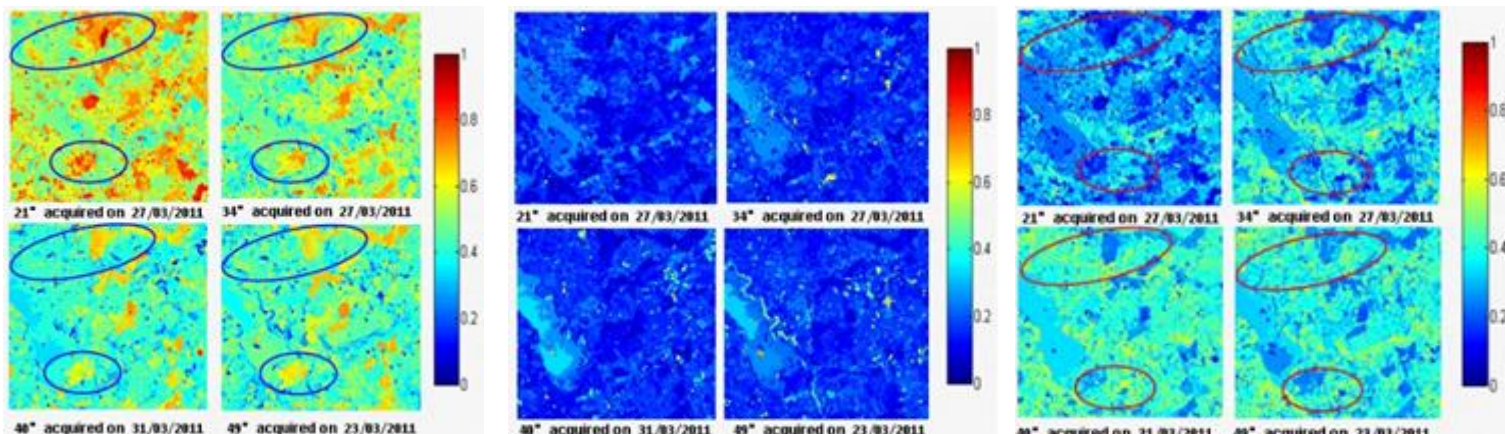


Fig.: Normalised components of Vanzyl non-negative eigenvalue decomposition – (a) single bounce, (b) double bounce, (c) volume scattering (Wang et al., 2013)

- Dominant single bounce scattering at all incidence angles
- Increase in incidence angle (path length through vegetation increases):

See module 2300:
polarimetry

- ↗ Single bounce scattering: decrease (saturation $\sim 40^\circ$)
- ↗ Volume scattering: increase (saturation $\sim 40^\circ$)
- ↗ Double bounce scattering: no significant variations

Structure

- ↗ Introduction
- ↗ Major parameters affecting radar backscatter from crops
 - ↗ Sensor parameters
 - ↗ Target parameters
- ↗ Agricultural applications
 - ↗ Crop type mapping
 - ↗ Crop management / biophysical parameter retrieval
 - ↗ Soil parameter retrieval
- ↗ Optimal system configuration for agricultural applications

What are target parameters?

Dielectric and geometrical characteristics of crops (plant parameters) and soils (soil parameters)

Important target parameters:

↗ Plant / canopy parameters

Crop type, phenological stage, water content, biomass, LAI, height, stem diameter, row orientation and distance, orientation of plant constituents (e.g. ear bending), plant surface water (dew, intercepted rainfall)...

↗ Soil parameters

Soil moisture, surface roughness, soil texture

Complex interactions of the target parameters



Important: experimental field work and modelling approaches

Target parameters – crop type

Each crop type - characteristic temporal signature

- Depends on frequency, polarisation and incidence angle
- Strongly affected by other target parameters (and external factors, e.g. rain)

Temporal signatures may vary significantly for different fields, growing seasons

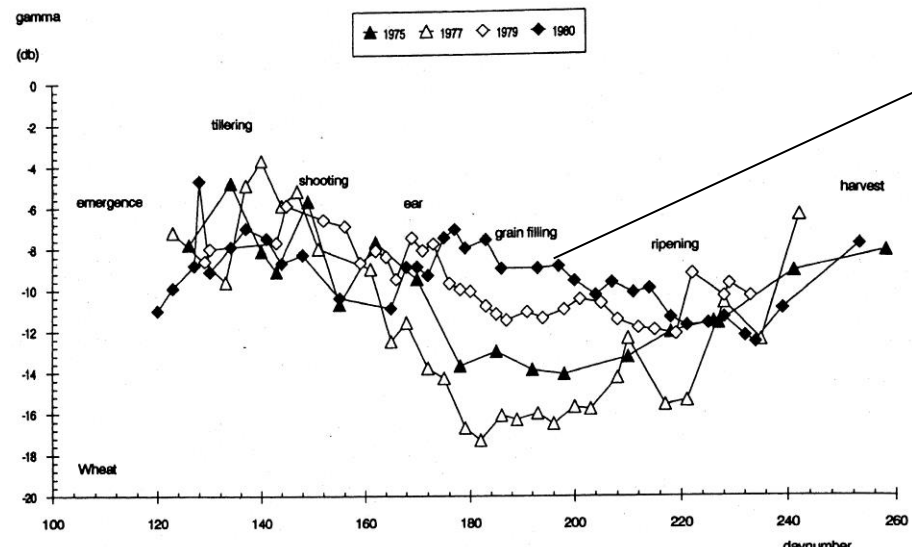


Fig.: Temporal signature of wheat - ground-based X-VV data acquired at 50° incidence angle (Bouman & van Kasteren, 1990)

- 1980
- No common wheat signature
- Pattern largely resembles the backscattering curve of neighboring bare soil plots
- Explanation: very rainy year
 - High soil moisture content
 - Extremely low soil coverage, height and biomass

Scattering behaviour of selected crop types

Corn

- ↗ Grain with the highest production worldwide in 2012 (FAO, 2013)
- ↗ Important staple food and feed crop
- ↗ Cultivated throughout the world (40% in United States)

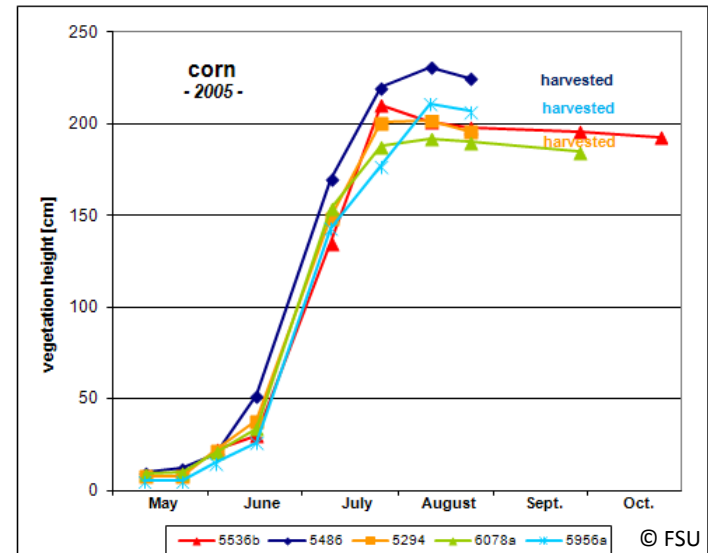
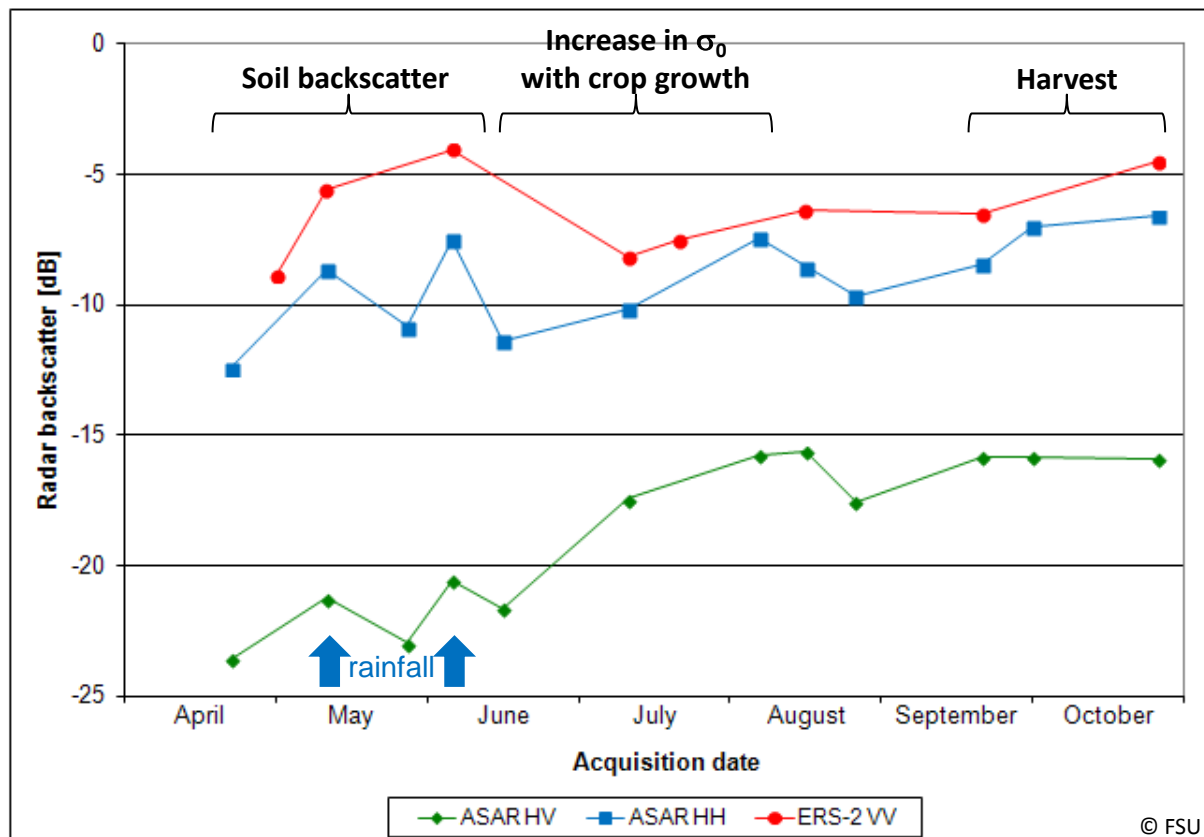


Fig.: Seasonal development of vegetation height for single corn fields, test site Nordhausen, Thuringia, Germany (© FSU)

Scattering behaviour of selected crop types

Corn – C-band



- HV vs. HH: higher range of variation with increasing vegetation height (see figure previous slide) / biomass
- VV: missing data for mid of June

Fig.: C-band temporal signatures of corn in 2005 (regional mean values), test site Nordhausen, Thuringia, Germany (© FSU)

Scattering behaviour of selected crop types

Rice

- Second-highest production worldwide in 2012 (FAO, 2013b)
- Staple food for more than half of the world's population
- Most important crop type in Asia (90% of world production)

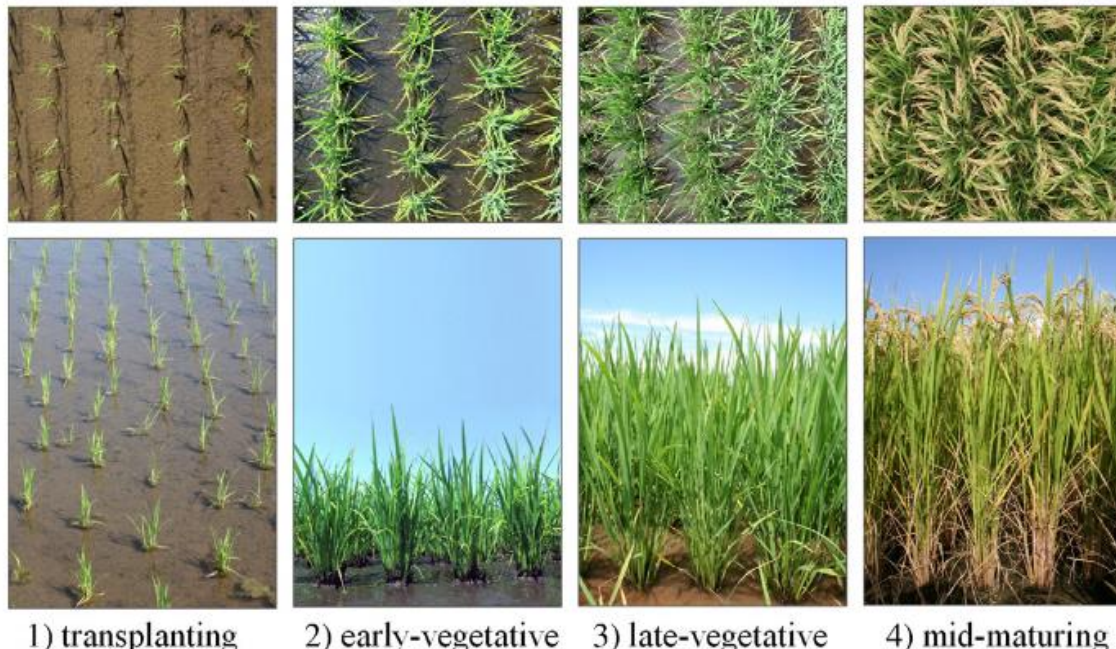


Fig.: Examples of rice canopies:
nadir and side view of typical rice
canopies at (1) transplanting, (2)
early-vegetative, (3) late-vegeta-
tive and (4) mid-maturing stages,
respectively (Inoue et al., 2013)

Scattering behaviour of selected crop types

Rice – X-band, scatterometer data

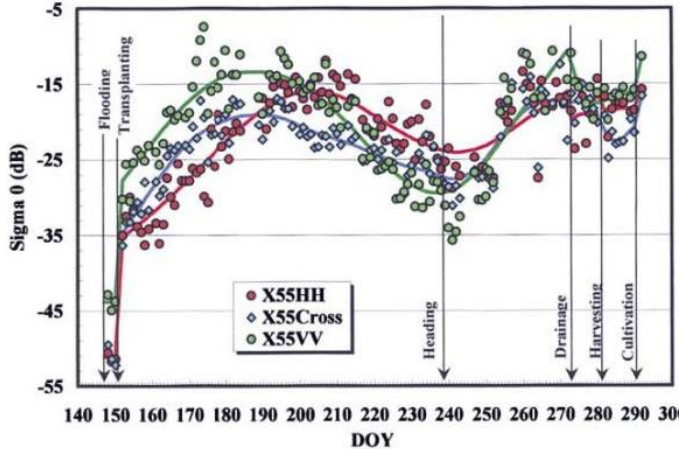
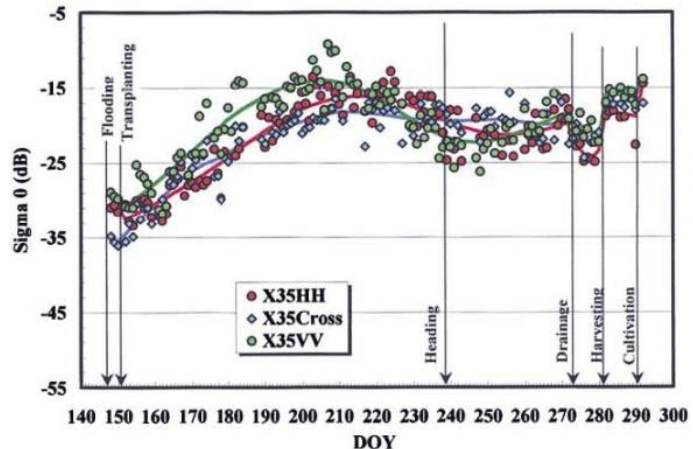
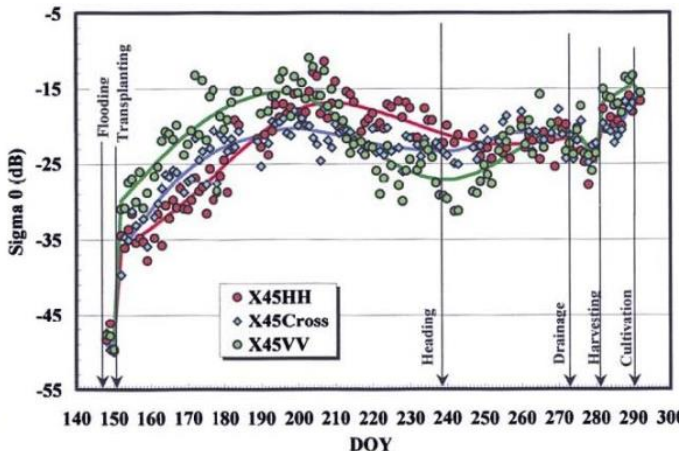
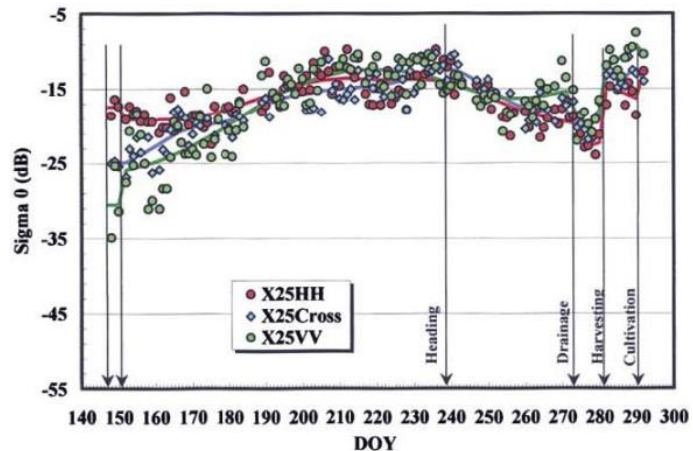


Fig.: Seasonal change in radar backscatter from rice fields for co- and cross-polarization at different incident angles (Inoue et al., 2002)

Scattering behaviour of selected crop types

Rice – X-band, TerraSAR-X data

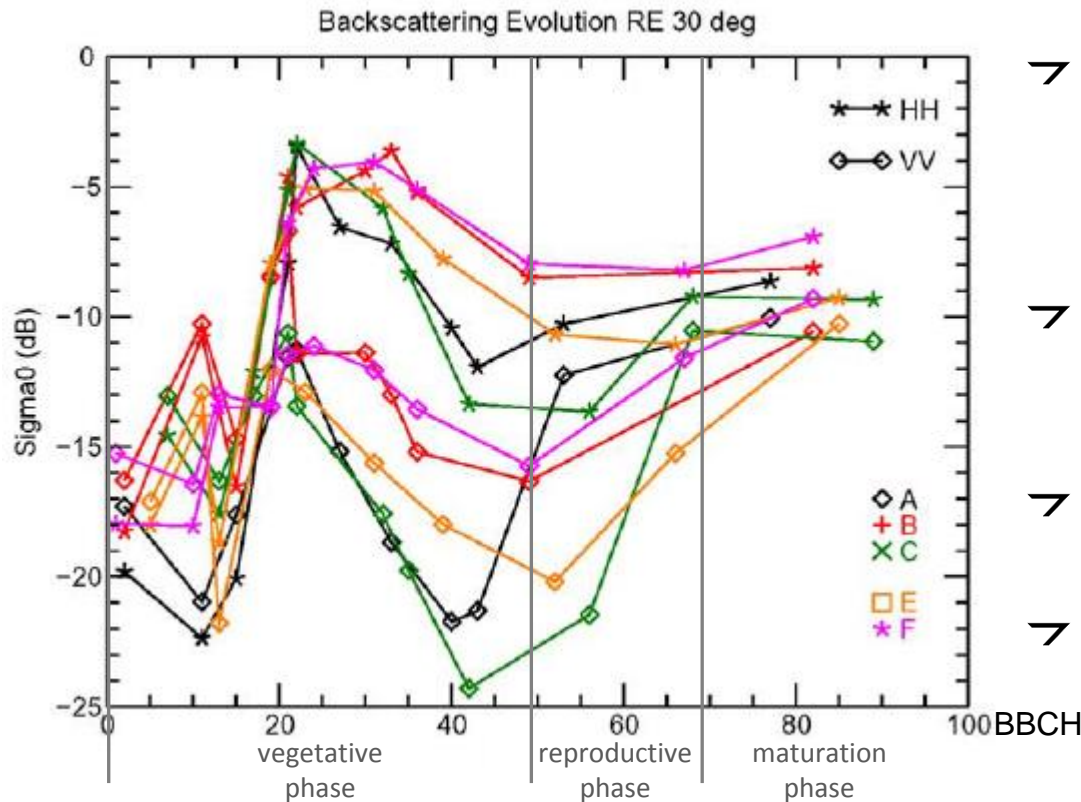


Fig.: Temporal signatures of a single rice fields at X-HH and X-VV(adapted after Lopez-Sanchez et al., 2012a)

- BBCH 0 – 20: backscattering from flooded ground (higher backscatter values due to wind effects)
- BBCH 20 – 30: plant emerge → double bounce flooded ground / stems
- BBCH 30 – 40 to 50: decrease in backscatter → extinction
- 40 to 50 – end of growth cycle: increase in backscatter; plant structure becomes more and more random, decrease in plant moisture

Scattering behaviour of selected crop types

Wheat

- ↗ Grain with the third-highest production worldwide in 2012 (FAO, 2013b)

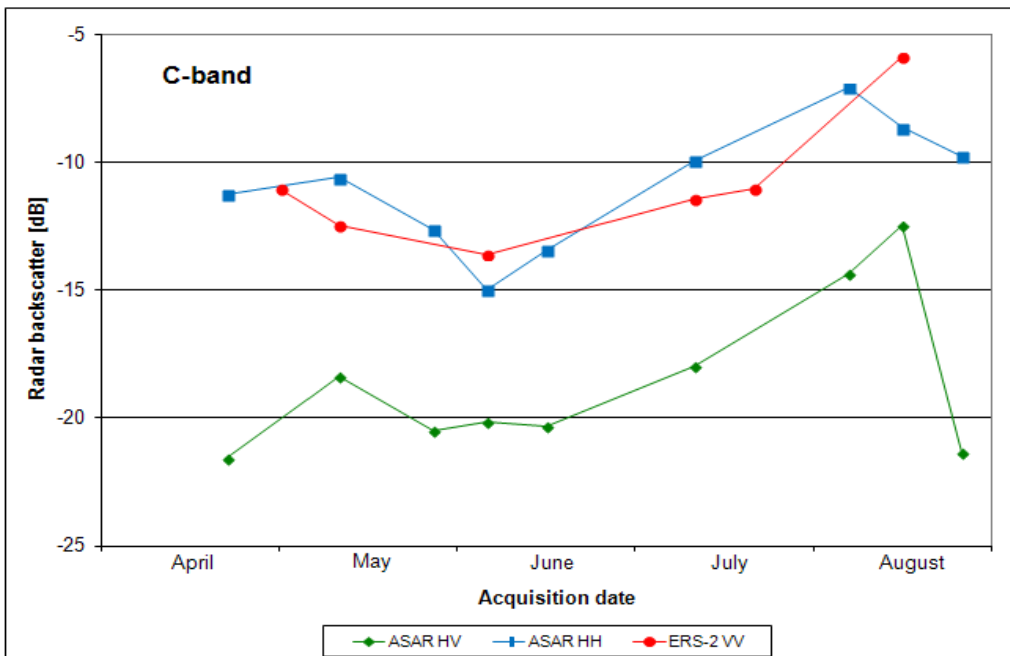


Fig.: Scattering behaviour of a wheat canopy, test site Nordhausen, Thuringia, Germany (© FSU)



C-band, HH & VV polarisation:

- ↗ Crop growth → decrease in σ_0 → attenuated soil backscatter
- ↗ Ripening → decrease in canopy moisture → canopy becomes more transparent → increase in σ_0

C-Band, HV polarisation: strong impact of ear bending on σ_0 (Ferrazzoli, 2001)

Scattering behaviour of selected crop types

Rape – C-band

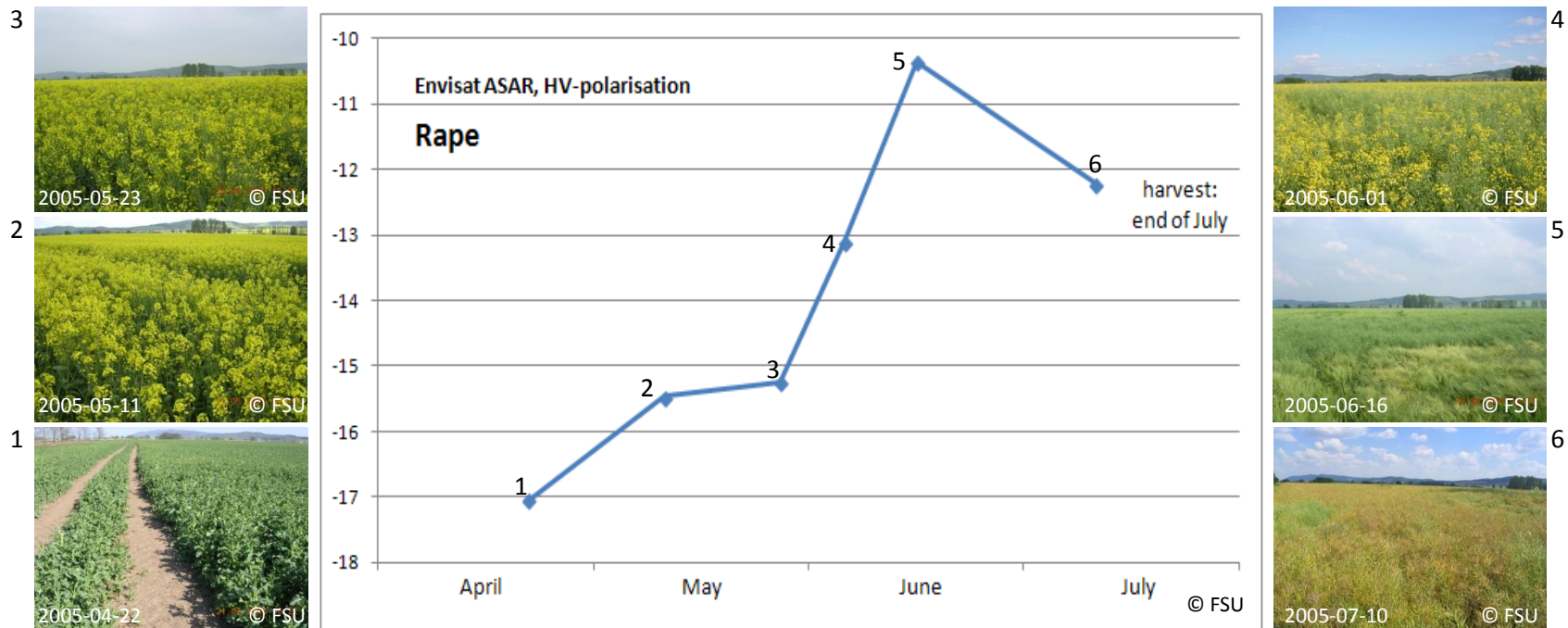


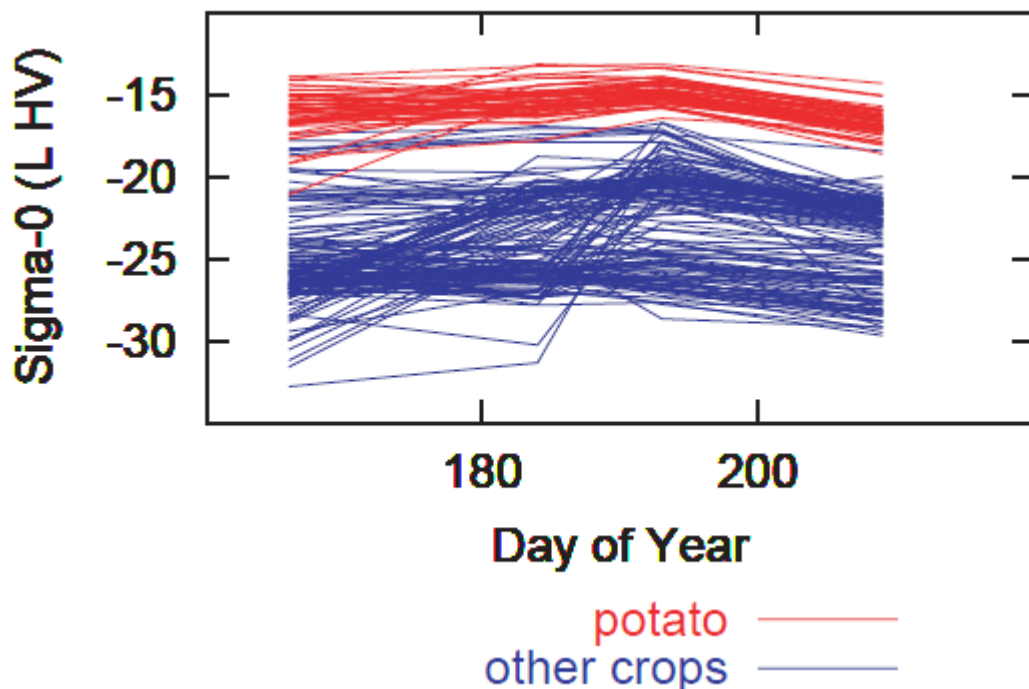
Fig.: Temporal signature of a single rape field in 2005, test site Nordhausen, Thuringia, Germany (© FSU)

C-HV: June / July:

- Higher radar backscatter than other crops
- Crosspolar scattering of twigs and pods

Scattering behaviour of selected crop types

Potatoes – L-band, AIRSAR data



- Shallow incidence angle: σ_0 developed potato fields $> \sigma_0$ other crops/ soil
- Crosspolar scattering of twigs

Fig.: Temporal signatures of single potato fields at L-HV collected at Flevoland in 1991 (Ferrazzoli, 2001)

Ferrazzoli, 2001

Target parameters – other important plant/canopy parameters

- ↗ Plant parameters
 - ↗ Plant height
 - ↗ LAI
 - ↗ Biomass
 - ↗ Plant water content
 - ↗ Stem diameter
 - ↗ ...
- ↗ Management practice → important parameters affecting the radar signal
 - ↗ Tillage practices (e.g. plantation of potatoes on ridges)
 - ↗ Row direction
 - ↗ Row distance
- ↗ Important external factors influencing the target parameters
 - ↗ Rainfall
 - ↗ Wind



See also biophysical parameter retrieval

Target parameters – plant / canopy parameters

Row spacing

- Close row spacing → enhancement of typical crop characteristics in the temporal signatures

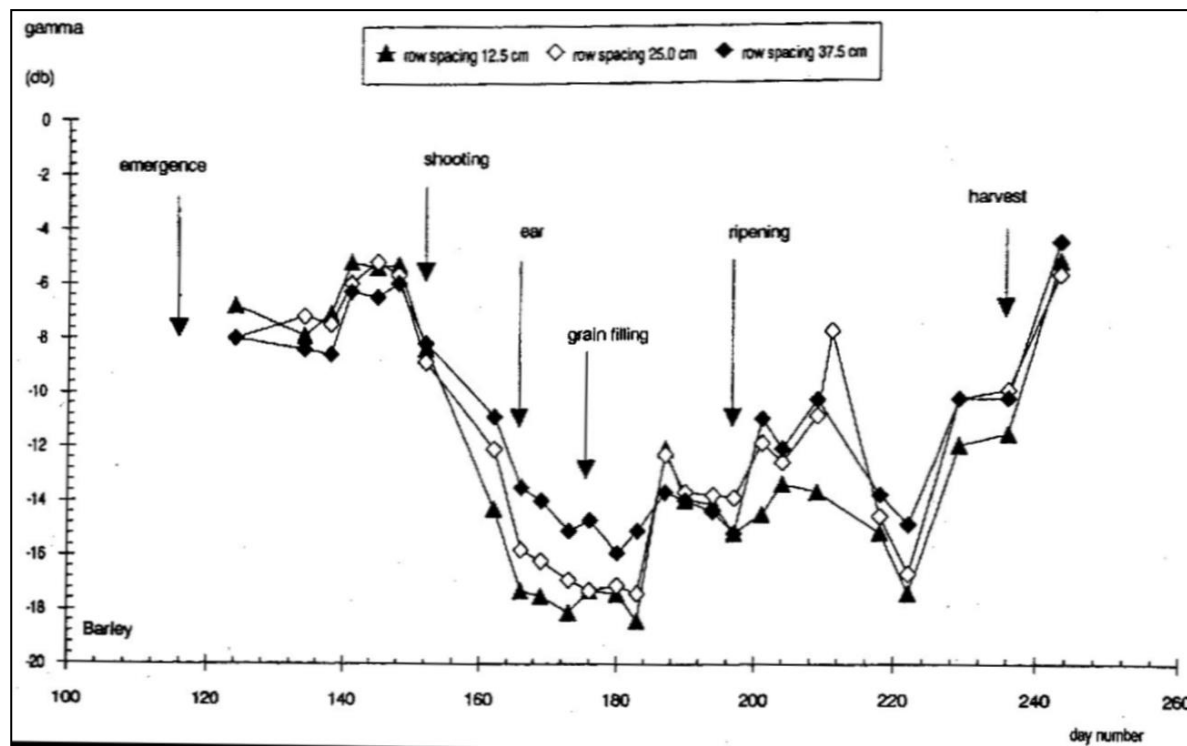
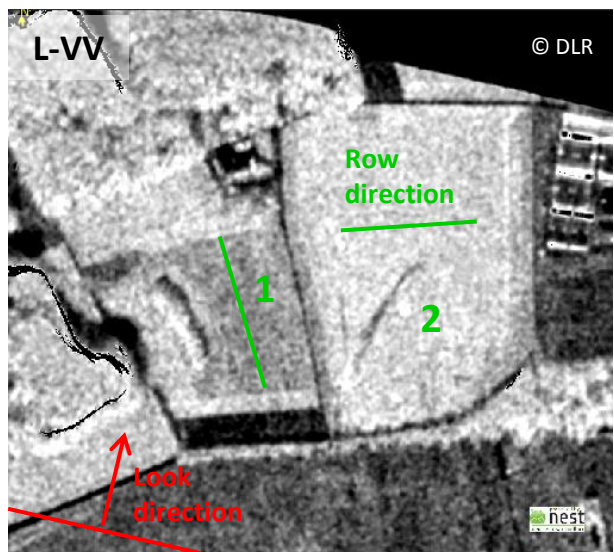


Fig: X-VV scatterometer data of barley with different row spacing in the course of the growing season of 1977 at 50° incidence angle (Bouman & van Kasteren, 1990)

Target parameters – plant/canopy parameters

Row orientation

- ↗ Especially for crops with distinct row structure, e.g. corn, potatoes, cotton
- ↗ Reported differences in radar backscatter: 5 – 10 dB (max. up to 20 dB)
- ↗ Look direction perpendicular to the row direction → can be 5–10 dB higher than the look directions just 5°– 15° off perpendicular
- ↗ Reduced effects at cross-polarization → important for classification



- ↗ Differences in radar backscatter: 3,6 dB
- ↗ Pauli decomposition → field 2: stronger double bounce interactions
- ↗ Plant height: ~ 80 cm

Fig.: E-SAR data (© DLR) at L-VV, June 14, 2000, test site Alling, Germany

Target parameters – plant/canopy parameters

Row orientation

- Test site: Flevoland, The Netherlands
- Strong directional scattering for fields with a cultivation direction approximately perpendicular to the look direction
- Fields include potato and carrot fields with very strong row structures as well as onion, sugar beet and wheat fields with rows having amplitudes comparable or even smaller than the random roughness
- Directional scattering effects → similar level at HH and HV, no effects at cross-polarization

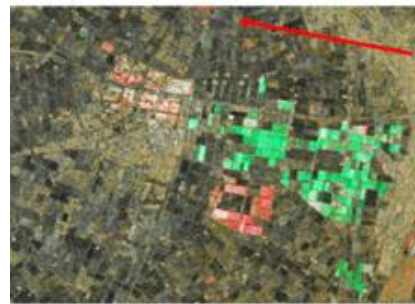


Fig.: ENVISAT ASAR and ERS-2 Tandem HSI (Hue–Saturation–Intensity) composite of the backscatter ratio (hue), backscatter change (saturation) and backscattering in the first image of the pair (intensity) over Dronten site on 3-May-2009. Red indicates higher intensity for ENVISAT ASAR, and green higher intensity for ERS-2 (Wegmüller et al., 2012)

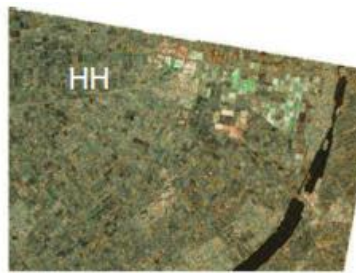


Fig.: RADARSAT-2 FQ8 sub-band HSI images (first sub-band image combined with last sub-band image) acquired on 1st May 2009 at HH (top left), VV (top right), HV (bottom left) and VH (bottom right) polarization (Wegmüller et al., 2012)

Wegmüller et al., 2011

Target parameters – plant/canopy parameters

Ear orientation

- Ear bending → increase in HV-polarisation (Ferrazzoli, 2001)
- Effect of ear orientation with regard to sensor → see figure below

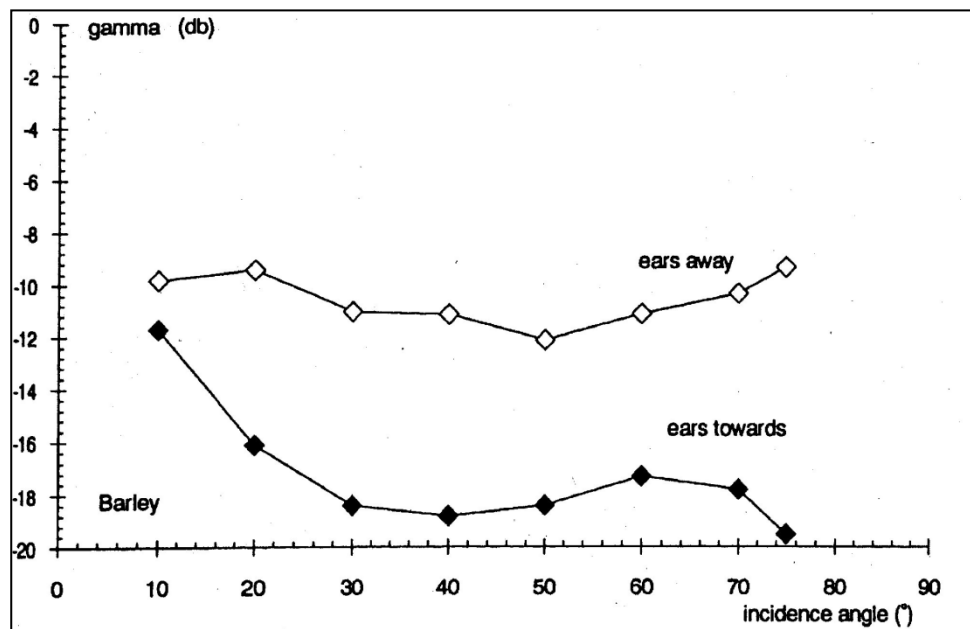


Fig: X-VV scatterometer data of barley in the stage of ear filling (Bouman & van Kasteren, 1990)

- Ears were bent → almost horizontal orientation
- Change of ear orientation due to wind
 - Day 182: ears were directed towards the sensor
 - Day 186: ears were directed away from the sensor

Target parameters – plant/canopy parameters

Lodging

- ↗ Definition: collapse of the stalk of a plant (stalk lodging) or the entire plant (root lodging), especially cereals
- ↗ Variety dependent
- ↗ Causes: high plant populations, high nitrogen fertilization, external factors such as rain and wind ...
- ↗ Effect on radar signal → increase in σ_0 , but impact depends on growth stage, crop type etc.

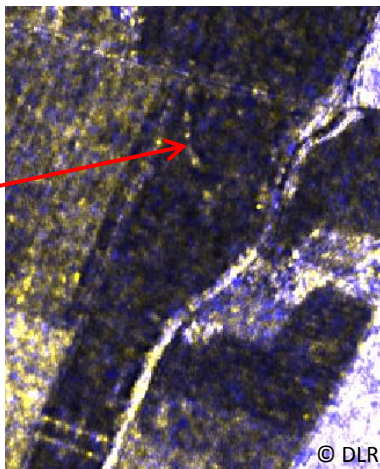
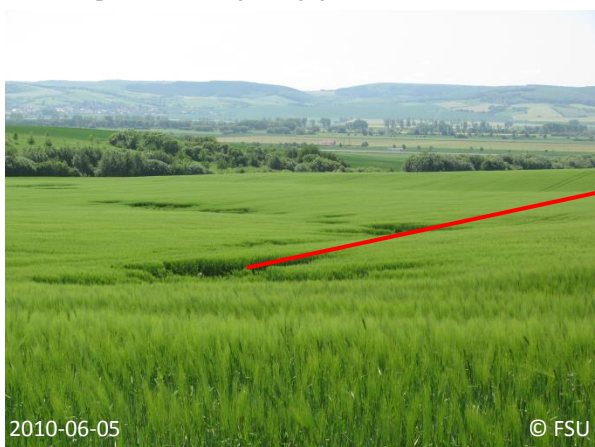
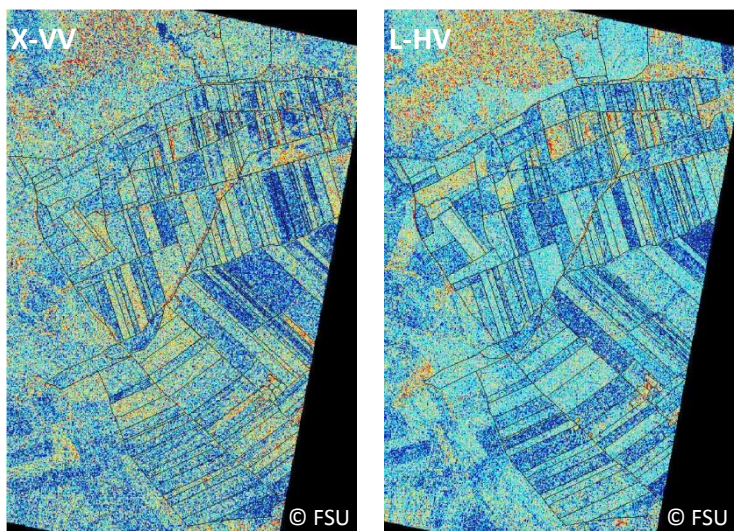


Fig: Increase in radar backscatter of winter barley due to lodging, test site Nordhausen, Germany – TerraSAR-X SM data acquired on June 05, 2010, HH / HH / HV (© FSU Jena)

Target parameters – external factors

Wind / rain

- ↗ Impact on geometric attributes, e.g. ear bending, lodging (see previous slides)
- ↗ Rainfall → increase in soil moisture & presence of plant surface water
- ↗ Increase in radar backscatter → but: impact depends on crop type, growth stage (contribution of soil backscatter to radar signal, amount of intercepted water, ...)



Impact of rain depends on frequency, polarisation, crop type, growth stage – X-VV & L-HV:

- ↗ Grassland / spiked grains: significant increase in σ_0
- ↗ Broadleaf crops / panicle grain: low variations

Fig: Diurnal variations in backscatter due to interception on June 14, 2000, test site Alling, Germany: E-SAR (© DLR) ratio-pictures between 6 and 12 am after a rain event at X-VV (left) and L-HV (right) (negative values → increase due to moisture; positive values → decrease)(© FSU Jena)

Target parameters – external factors

Wind / rain

- Example: Impact on temporal crop signatures

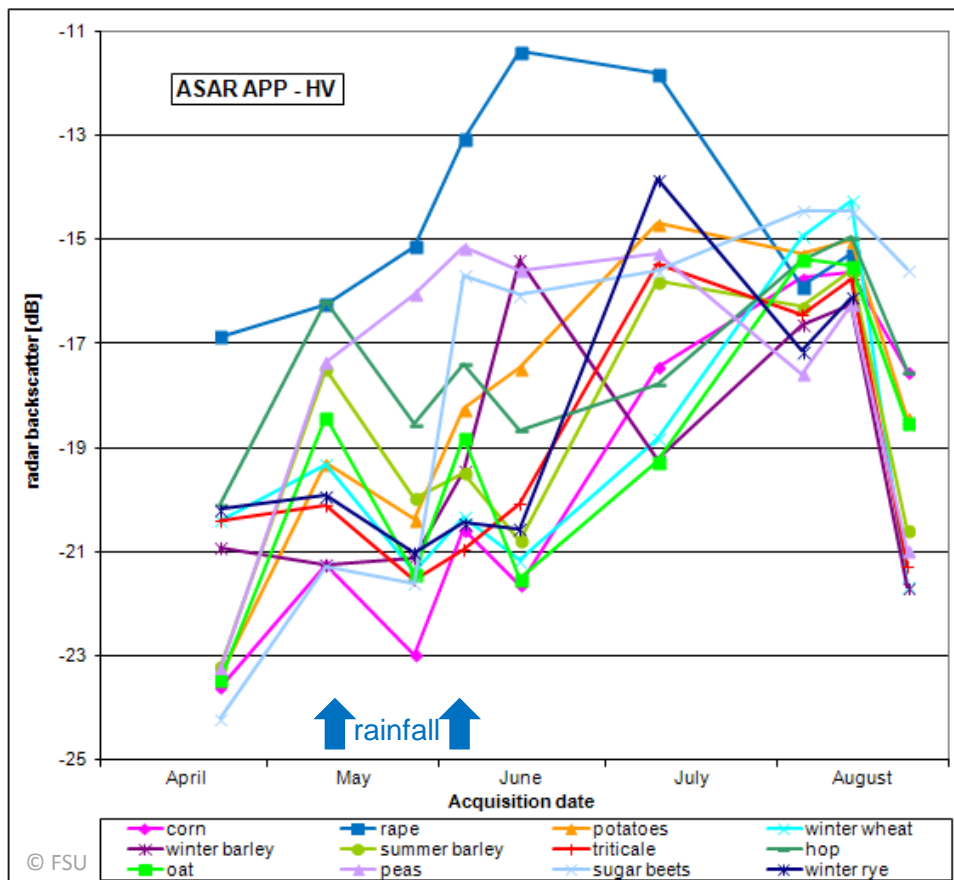


Fig: Impact of rain on temporal crop signatures at C-HV, 2005, test site Nordhausen, Germany (© FSU Jena)

Structure

- ↗ Introduction
- ↗ Major parameters affecting radar backscatter from crops
 - ↗ Sensor parameters
 - ↗ Target parameters
- ↗ Agricultural applications
 - ↗ Crop type mapping
 - ↗ Crop management / biophysical parameter retrieval
 - ↗ Soil parameter retrieval
- ↗ Optimal system configuration for agricultural applications

Crop type mapping

Need

- ↗ (Rapid) estimation of crop surface coverage
 - ↗ Important tool in the effective management and administration
 - ↗ Allows the planning of distribution resources, subsidy levels and storage facilities at national / international level (e.g. EU-wide)
- ↗ Monitoring of crop productivity
 - ↗ Yield models are crop-specific
 - ↗ Knowledge of acreage and yield (see biophysical parameters) is required

Traditional measurement methods

- ↗ Field inspections → not area-wide, cost- and time-consuming
- ↗ Information from farmer (not available for every country)

Crop type mapping

Advantages / disadvantages compared to optical data

- ↗ Major advantage
 - ↗ **All-weather capability**
 - ↗ Generation of dense time series → multitemporal analysis
 - ↗ SAR data take at optimal acquisition times (class-separability varies significantly during growing season)
- ↗ Disadvantage
 - ↗ Lower classification accuracies → compensated by usage of multitemporal, multipolarisation and / or multifrequency SAR data
 - ↗ Speckle effects
 - ↗ Topographic effects, radar shadow
 - ↗ Complex processing

Crop type mapping

Data requirements

- ↗ **Image product**
 - ↗ RAW / PRI data
 - ↗ SLC data → required for polarimetric analyses
- ↗ **Frequency**
 - ↗ Optimal: multifrequency data
 - ↗ In case of single frequency: depends on crop type, growth stage etc. – general:
 - ↗ Broad-leaf crops, e.g. corn, soybeans: longer wavelengths (good classification results were achieved for X-band data, too)
 - ↗ Narrow-leaf crops, e.g. grains: X-band, C-Band



See module 2300:
Radar polarimetry

Crop type mapping

Data requirements

↗ Polarisation

- ↗ Usage of intensities
 - ↗ In case of single polarisation: HV data preferable – high temporal resolution is required
 - ↗ Dual-pol data: quad-pol slightly better results
 - ↗ VV / HV better than HH / HV for most crop types
- ↗ Polarimetry → HH / VV / HV (/VH) SLC data required
(dual polarimetry: two polarisations)

↗ Incidence angles

- ↗ Common suggestion: Usage of shallow incidence angles (reduced soil contribution) or multiangular datasets
- ↗ Other studies: No clear pattern → depends on crop type etc.



Example see slide 77

Crop type mapping

Data requirements

↗ Timing

- ↗ Class separability varies significant during the growing season → optimal acquisition times → depends on crop type (e.g. C-band, grain: time window associated with heading)
- ↗ General: middle season
- ↗ Ripening → diminishing separability
- ↗ Early season → large confusion of spring crops (sparse and small vegetation, partly bare fields)
- ↗ Usage of multitemporal time series (highest increase in classification accuracy using 3 - 5 acquisitions)
- ↗ Polarimetric data → number of acquisitions could be reduced

↗ Spatial resolution

- ↗ High spatial resolution compared to parcel size

Crop type mapping

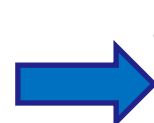
General remarks

- ↗ Optimal: usage of multifrequency / multipolarimetric SAR data → classification results comparable to optical data could be achieved
- ↗ Many individual crops could be classified to accuracies better than 90%.
- ↗ Separation of different cereals is often most critical

Crop type mapping

Methods – classification approaches

- ↗ Standard maximum likelihood
 - e.g. *Skriver et al., 2011*
- ↗ Decision tree classification
 - e.g. *McNairn, 2009; Quegan et al., 2003*
- ↗ Random forest
 - e.g. *Deschamps et al., 2012; Loosvelt et al., 2012*
- ↗ Support vector machines
 - e.g. *Tan et al., 2011*
- ↗ Neural networks
 - e.g. *Stankiewicz, 2006*
- ↗ Wishart classifier for polarimetric datasets
 - e.g. *Skriver et al., 2011*
- ↗ ...



See module 2102:
Classification
methods



See module 2300:
SAR polarimetry

Crop type mapping

Potential of multipolarized SAR data

- ↗ Rape: cross-polarized backscatter from twigs and pods
- ↗ Corn: dominant soil backscatter
- ↗ Cereals: attenuated soil backscatter
- ↗ Sugar beets: soil backscattering and scattering from leaves

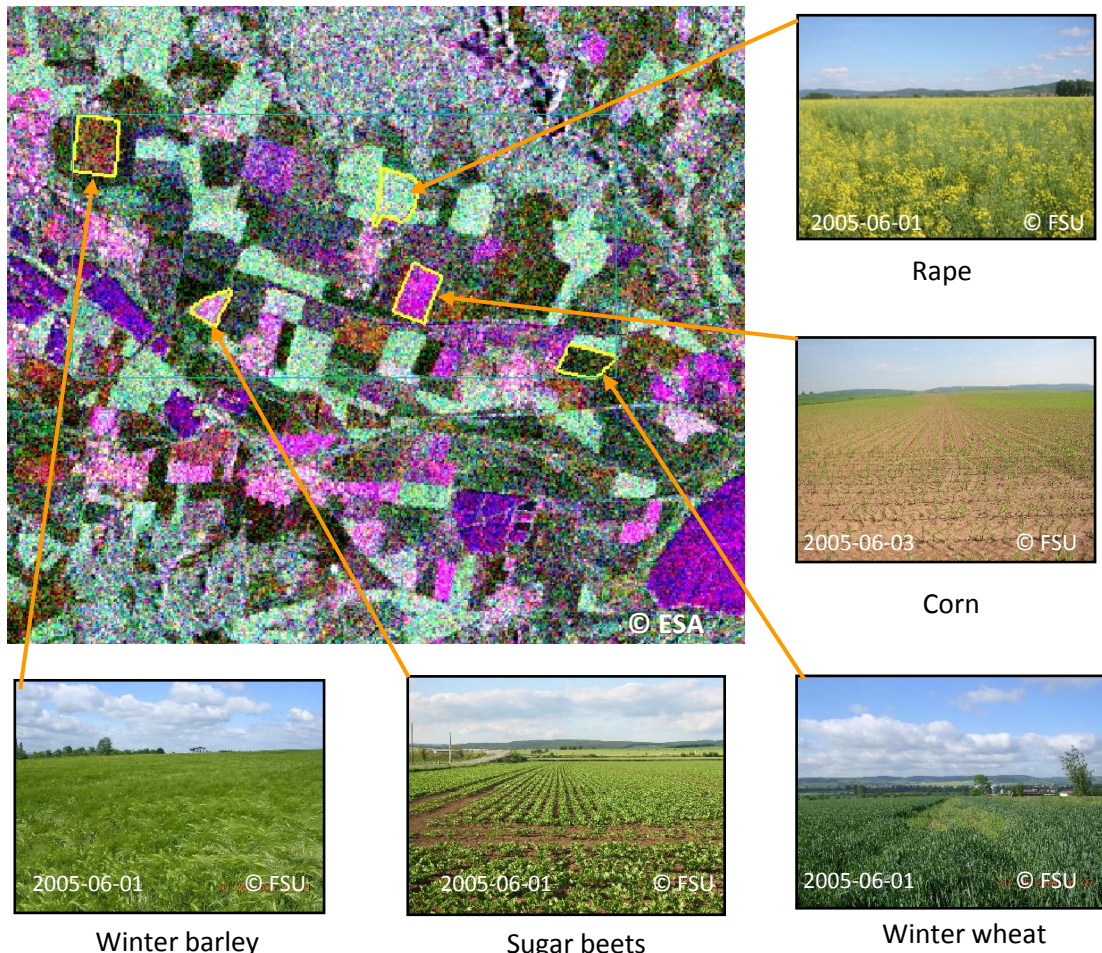


Fig: Potential of multipolarized SAR data for crop-type classification – C-band RGB composite **ASAR HH / ASAR HV / ERS-2** acquired on June 6, 2005 over the Nordhausen test site, Germany (© FSU Jena)

Crop type mapping – selected image features

Separability of grassland and agriculture

Grassland at X-HV
and C-HV:

Low radar backscatter
during entire year

- Low mean annual variability (MAV)
- Low multitemporal maximum (MMAX)
- C-HV: more suitable
- Misclassification with clover

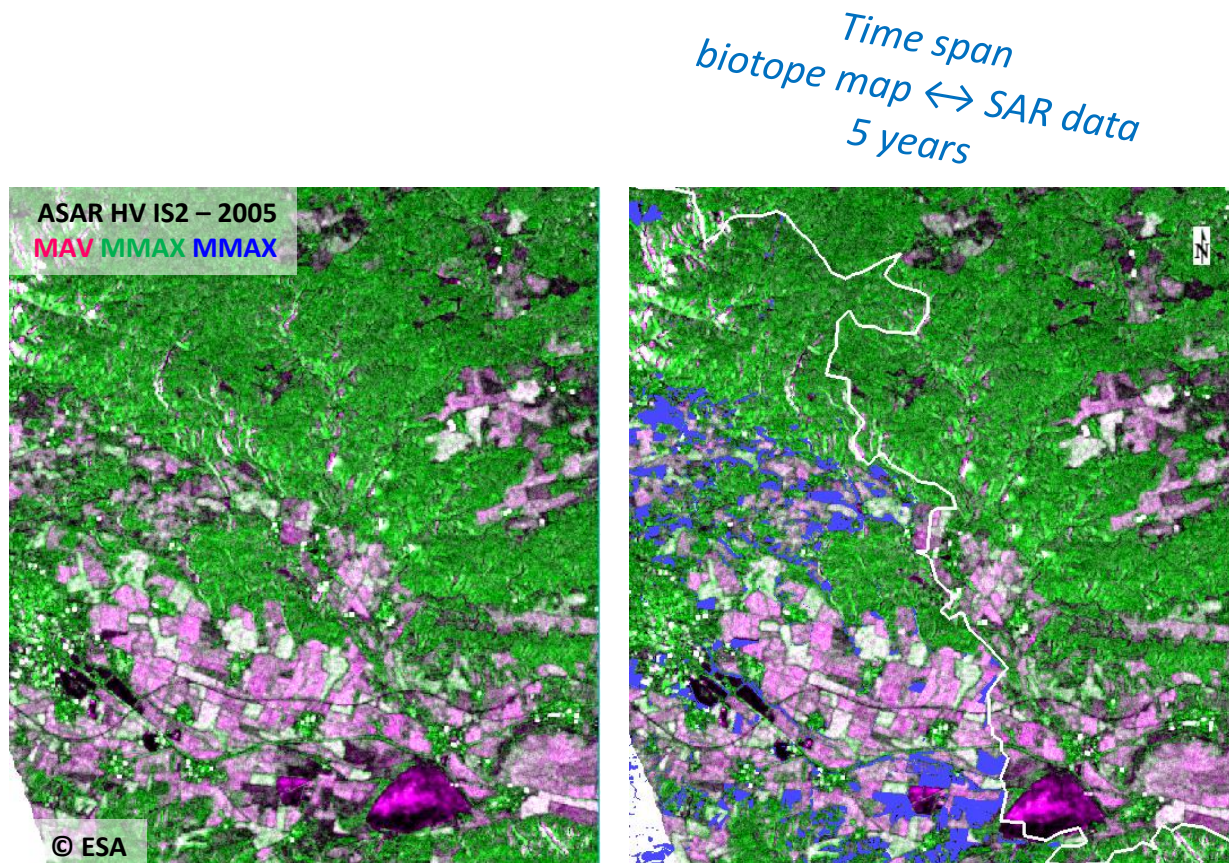


Fig: Potential of multitemporal image features to separate agriculture and grassland, test site Nordhausen, Germany – left: ASAR RGB composite from 2005; right: overlay with biotope map of Thuringia (grassland in blue) and the border of Thuringia (white) (© FSU Jena)

Crop type mapping – selected image features

Winter vs. spring crops

Early growing season

Spring crops → bare fields
→ surface scattering

Winter crops → some degree of volume scattering

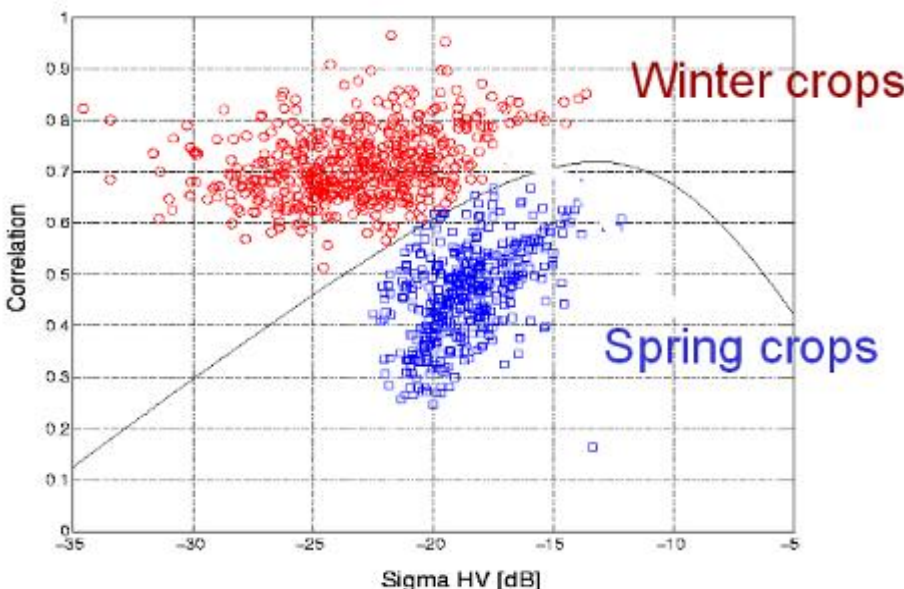


Fig.: HH-VV correlation versus HV backscatter for winter (red) and spring (blue) crops – airborne EMISAR data, April 17, Foulum test site (Quegan et al., 2003)

| Parameter 1 | Parameter 2 | Spring OK (No. & %) | Spring Bad (No. & %) | Winter OK (No. & %) | Winter Bad (No. & %) | Overall (%) |
|-------------|-------------|---------------------|----------------------|---------------------|----------------------|-------------|
| VV | HV | 524 (94.2) | 32 (5.8) | 395 (88.0) | 54 (12.0) | 92.6 |
| Correlation | HV | 524 (94.2) | 32 (5.8) | 432 (96.2) | 17 (3.8) | 95.1 |
| Alpha | Entropy | 535 (96.2) | 21 (3.8) | 413 (92.0) | 36 (8.0) | 94.2 |
| Correlation | Entropy | 539 (96.9) | 17 (3.1) | 392 (87.3) | 57 (12.7) | 92.6 |
| HV-HH | HV-VV | 512 (92.0) | 44 (8.0) | 421 (93.7) | 28 (6.3) | 92.8 |
| RR-RL | HV-VV | 506 (91.0) | 50 (9.0) | 428 (95.3) | 21 (4.7) | 92.9 |
| HH | HV | 452 (81.3) | 104 (18.7) | 424 (94.4) | 25 (5.6) | 87.1 |
| Entropy | RR-RL | 531 (95.5) | 25 (4.5) | 418 (93.1) | 31 (6.9) | 94.4 |

Tab.: Potential of various parameters for differentiation of winter and spring crops – airborne EMISAR data, April 17, Foulum test site (Quegan et al., 2003)

Quegan et al., 2003

Crop type mapping – selected image features

Rice

- Mapping of paddy rice fields
- HH/VV ratio at X- or C-band
- Dynamic range (sowing – plant maturity phase)
 - C-band: 4 – 7 dB
 - X-band: 8 – 12 dB

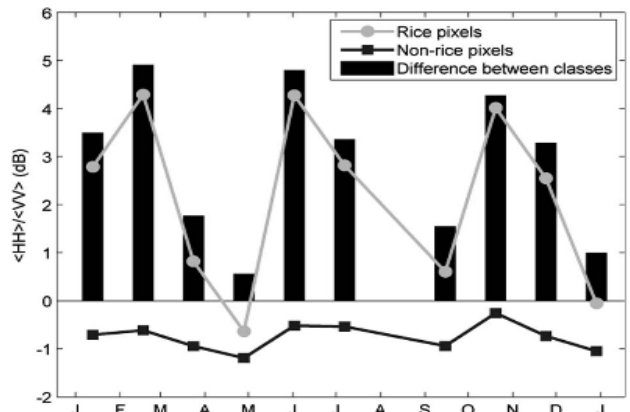


Fig.: Envisat ASAR polarization ratio of the mean intensities HH/VV for pixels defined as (grey circles) rice and (black square) non-rice in the GIS database. Black bars represent the difference of this ratio between the two classes (Bouvet et al., 2009)



Fig.: TerraSAR-X false colour composite image (HH / VV / HH-VV) of a test site in the mouth of the Guadalquivir river, SW of Spain, acquired on August 4. Cultivated rice fields are identified in pink colour (Lopez-Sanchez et al., 2011)

Crop type mapping – selected image features

Winter cereals: wheat vs. barley

- ↗ X-band, VV-polarization (or HV if VV is not available)
- ↗ Ratio of April and July data
- ↗ Winter barley
 - ↗ Earlier ripening → increase in radar backscatter
 - ↗ Strong ear bending → rise in HV

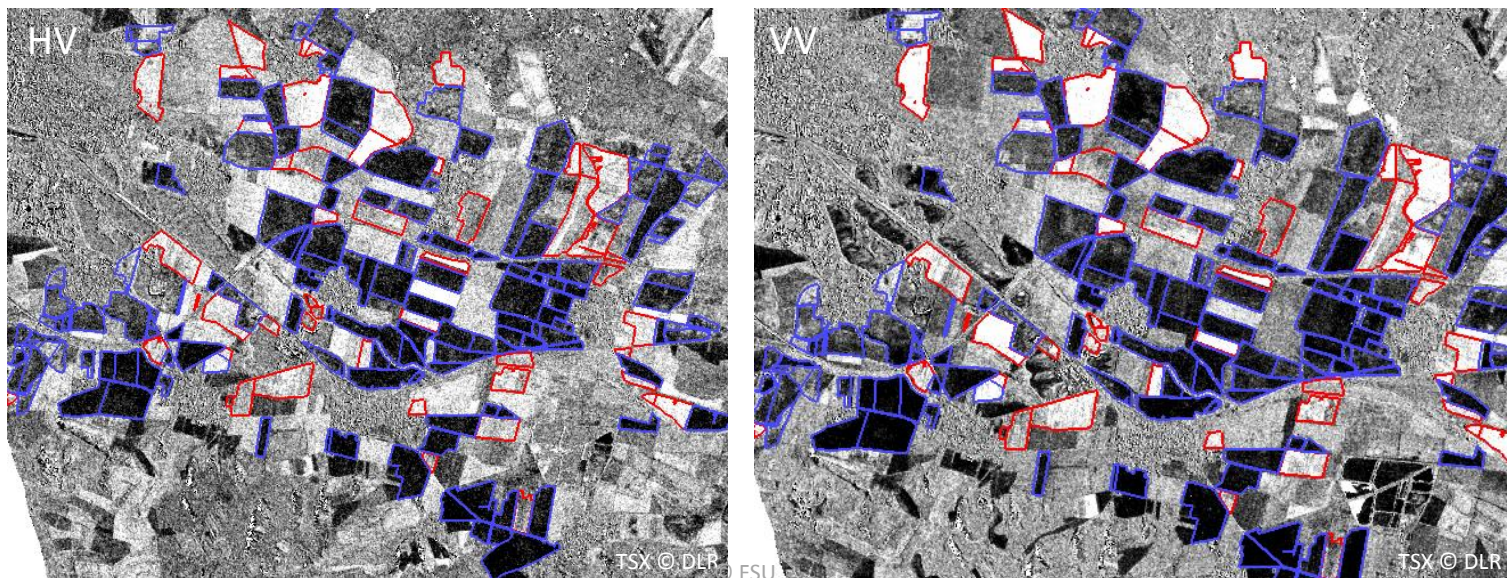


Fig.: TerraSAR-X data for the differentiation of wheat and barley – ratio of data acquired on April 19 and July 16 over the Nordhausen test site, Thuringia, Germany (ratio: (July-April)/(July+April)). Cultivated winter wheat fields are highlighted in blue and winter barley in red (© FSU)

Crop type mapping – selected image features

Winter cereals: wheat vs. barley

- ↗ X-band, VV-polarization (or HV if VV is not available)
- ↗ Ratio of April and July data
- ↗ Winter barley
 - ↗ Earlier ripening → increase in radar backscatter
 - ↗ Strong ear bending → rise in HV

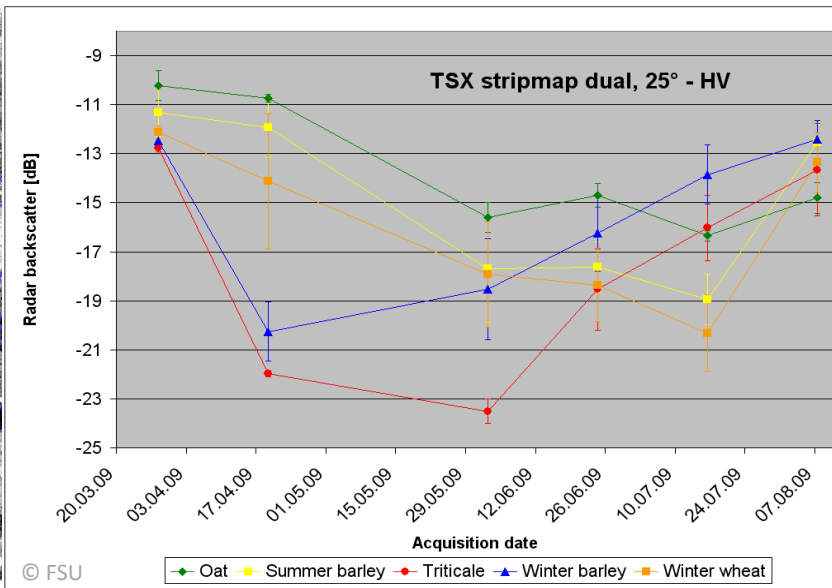
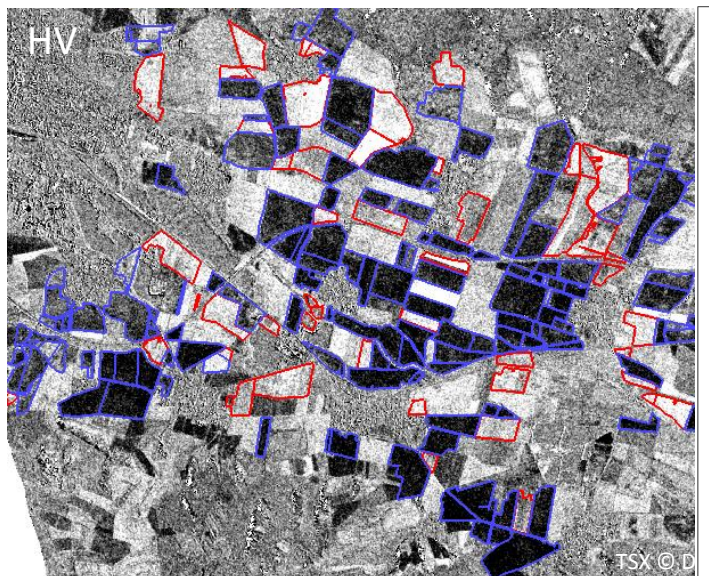


Fig.: TerraSAR-X data for the differentiation of wheat and barley – ratio of data acquired on April 19 and July 16 over the Nordhausen test site, Thuringia, Germany (ratio: (July-April)/(July+April)). Cultivated winter wheat fields are highlighted in blue and winter barley in red (© FSU)

Crop type mapping – selected image features

Rape

- C-band, HV polarisation → high radar backscatter

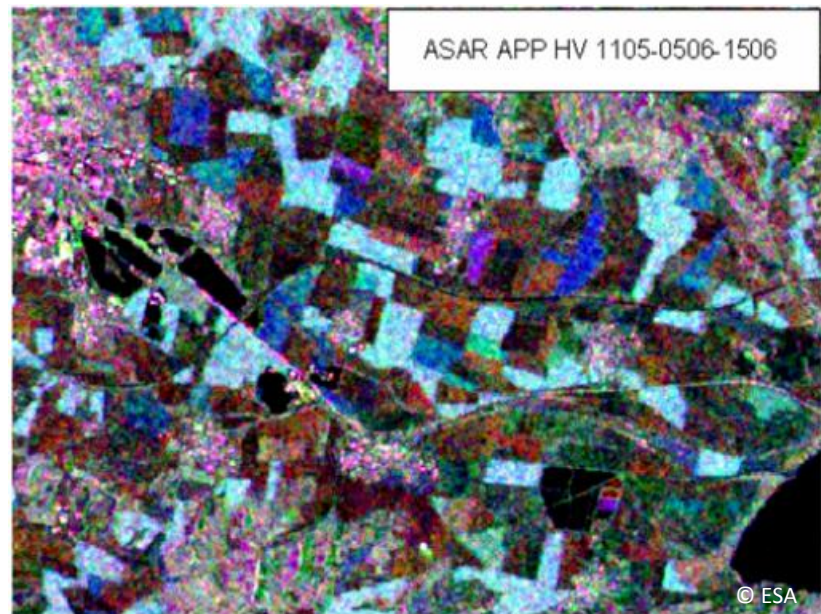
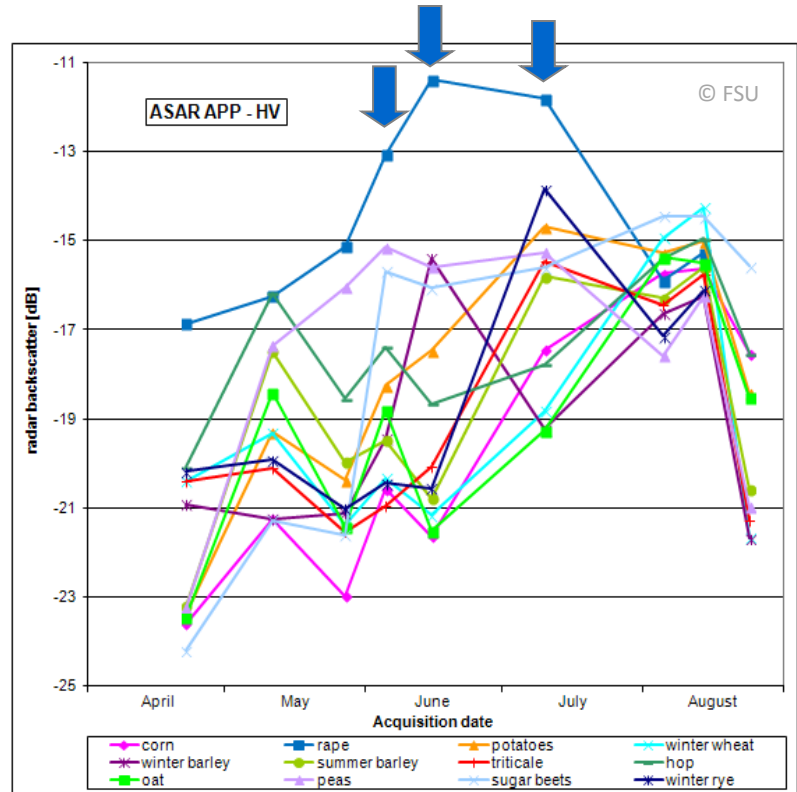


Fig.: Potential of multitemporal, HV-polarized Envisat ASAR data for mapping of rape fields, test site Nordhausen, Thuringia – left: temporal plot , right: RGB composite: 11-05-2005 / 05-06-2005 / 15-06-2005 - rape fields appear in light blue (© FSU)

Crop type mapping – selected image features

Sugar beets

- ↗ X-band, HV polarisation
- ↗ Optimal acquisition time at Nordhausen test site, Germany: August –September

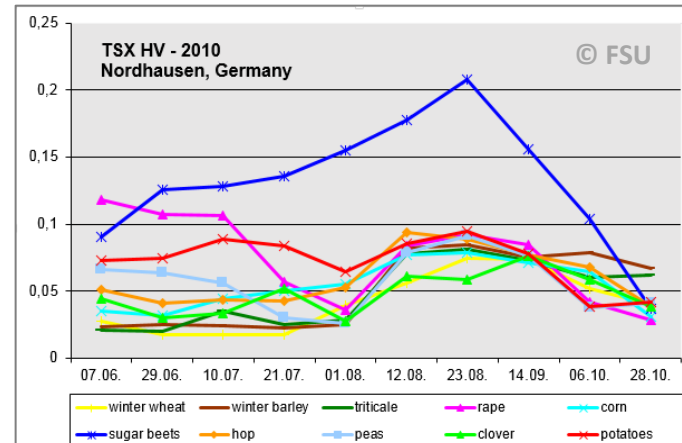
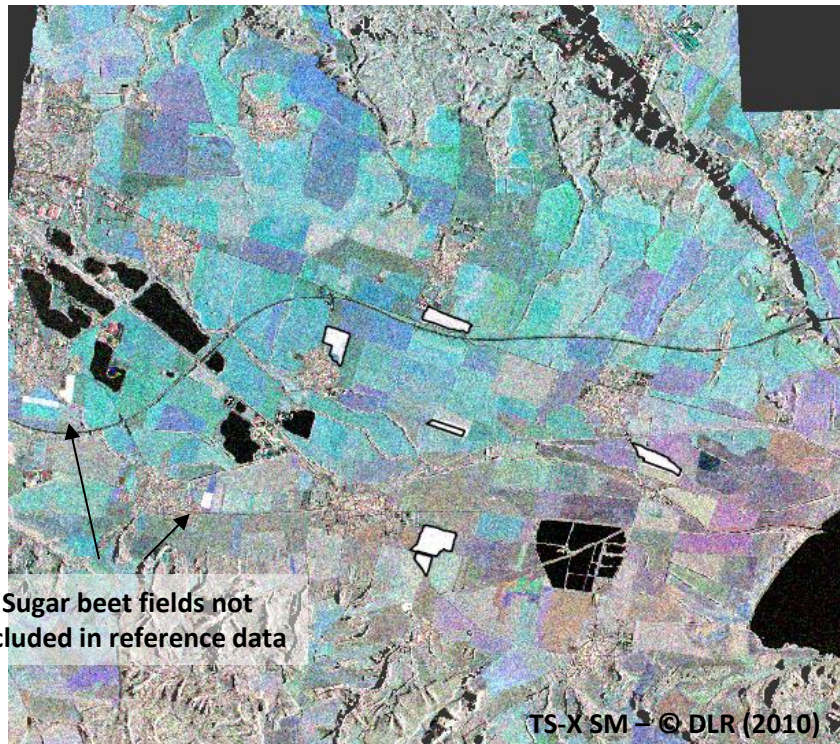


Fig. left: Multitemporal X-HV composite (2010-08-01 / 2010-08-12 / 2010-08-23), sugar beet fields appear in white (reference vector data in black), test site Nordhausen, Thuringia, Germany (© FSU)

Crop type mapping – classification example 1

C-band

- MLK classification of Pauli components & sieve filtering
- Radarsat-2
 - FQ5: 23,4 – 25,3° (5 scenes)
 - FQ19: 38,3 – 39,8° (4 scenes)
 - FQ29: 46,8 – 48° (5 scenes)
- Overall classification accuracies: 83,7% - 85,6%
- Impact of incidence angle on classification accuracy: no clear pattern

Tab. and Fig.: Classification accuracies of single crop types (Liu et al., 2013)

| | 2009 | | 2010 | | |
|------------------|------|------|------|------|------|
| | FQ5 | FQ19 | FQ5 | FQ19 | FQ29 |
| Overall accuracy | 85.1 | 85.6 | 84.5 | 83.7 | 85.5 |
| Hay/pasture | 84.0 | 86.0 | 80.5 | 68.0 | 77.9 |
| Soybean | 88.2 | 87.1 | 77.1 | 74.8 | 87.1 |
| Corn | 87.0 | 86.6 | 89.2 | 89.9 | 88.1 |
| Cereal/wheat | 70.6 | 77.0 | 88.4 | 87.1 | 72.6 |

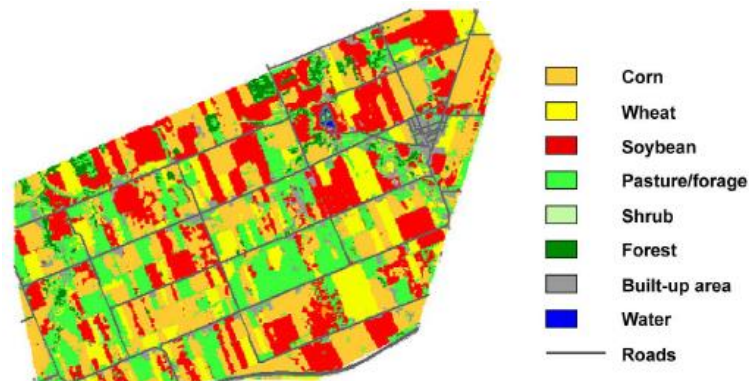
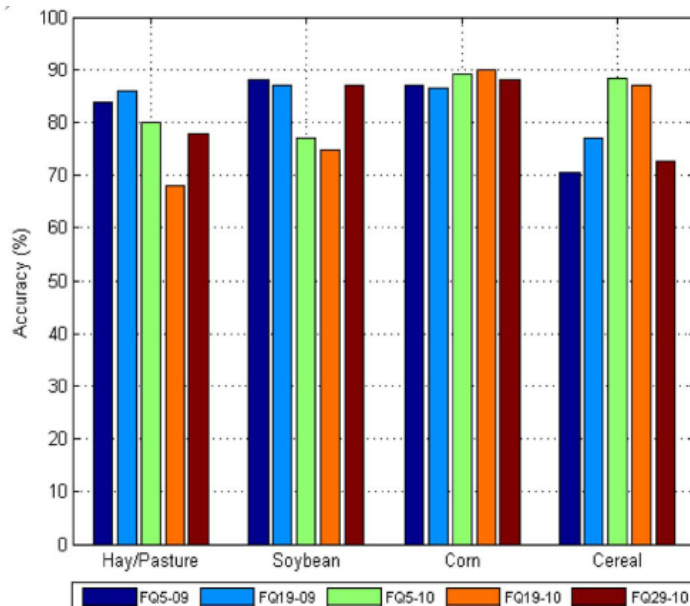


Fig.: FQ5 2010 classification map (Liu et al., 2013)



Crop type mapping – classification example 2

C-band

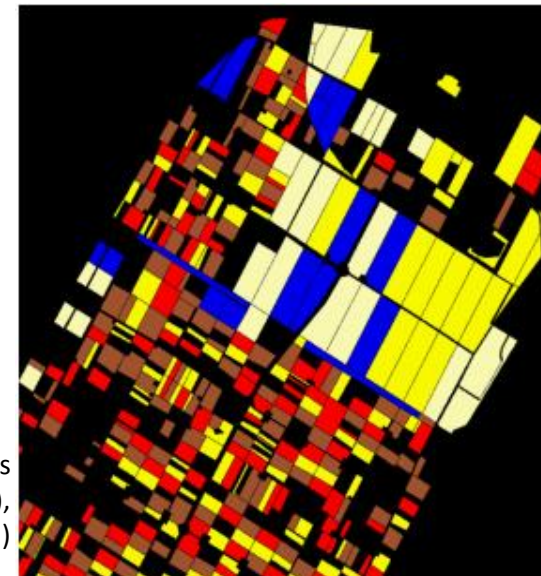
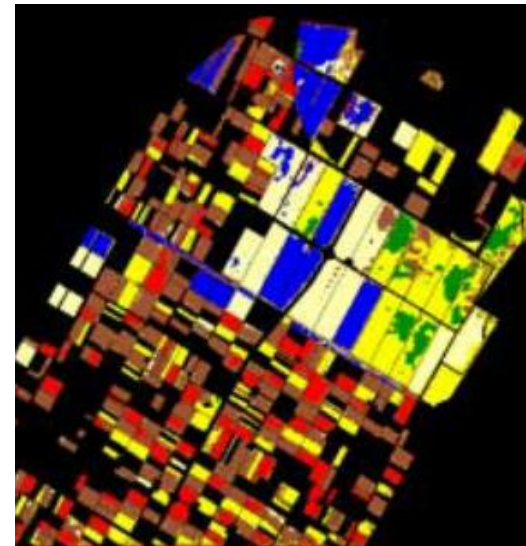
- Decision tree classification
- Airborne AirSAR data acquired on July 12, 1991
- Flevoland test site, the Netherlands



Quegan et al., 2003

Fig.: Decision tree structure (Quegan et al., 2003)

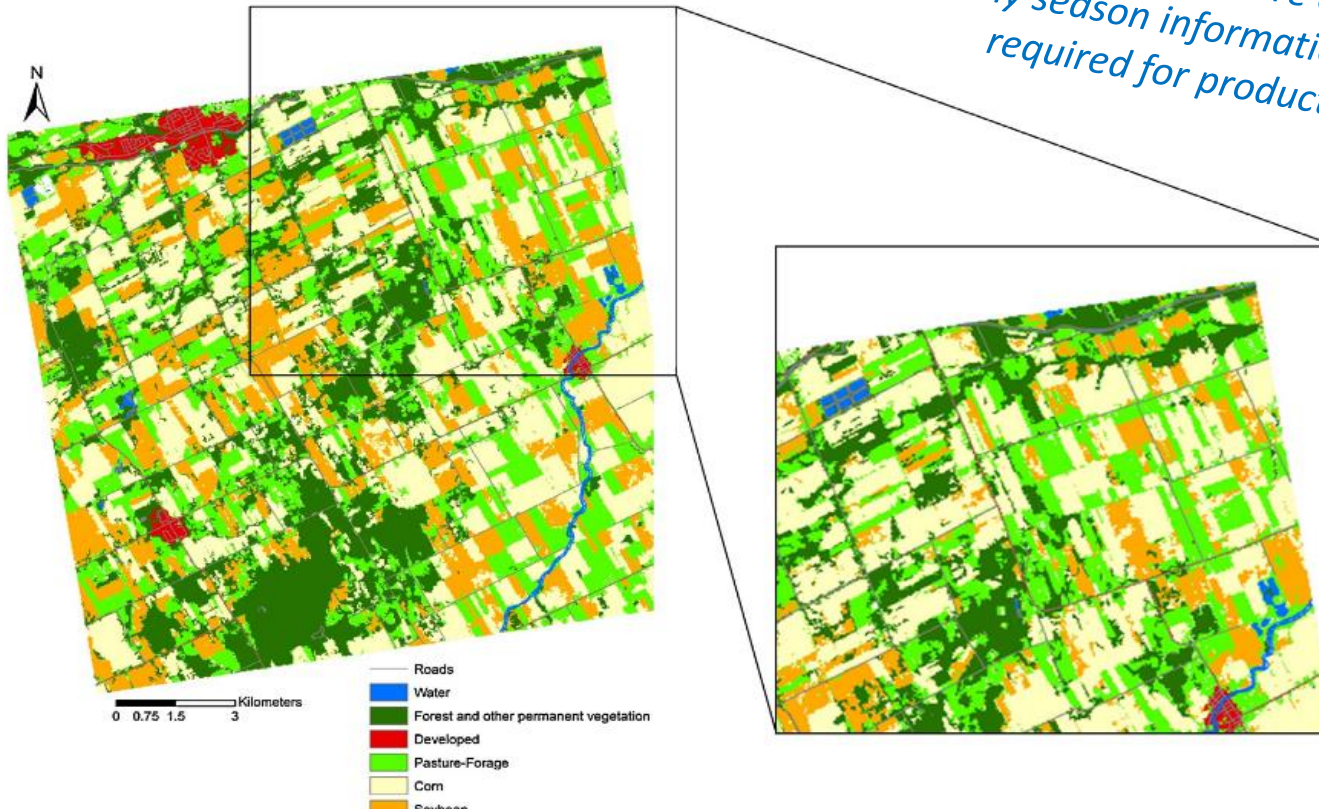
Fig.: Classification result (top) and groundtruth information (bottom) – potatoes (sienna), sugar beet (red), rapeseed (blue), wheat (yellow), barley (pale yellow), and bare soil (green) (Quegan et al., 2003)



Crop type mapping – classification example 3

X-band

- Decision tree classification
- TerraSAR-X data, VV/HV polarisation
- South Nation river basin, Ontario, Canada



*Corn fields could be identified six weeks after planting (growth stage: six fully developed leaf collars) using 3 TerraSAR-X datasets (BUT: only three different crop types were considered)
Early season information on acreage is required for production forecast*

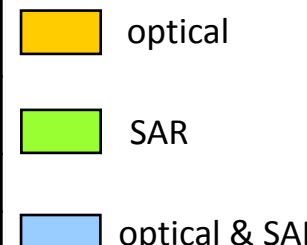
Fig.: End-of-season classification map derived from TerraSAR-X (overall accuracy of 97.2%). Inset shows the early season classification (overall accuracy of 89.2%) (McNairn et al., 2014)

Crop type mapping – classification example 4

C-band

- ↗ Multitemporal ASAR & ERS-2 from 2005
- ↗ Test site Nordhausen, Thuringia, Germany
- ↗ MLK classification

| | Exclud-ing SAR | SAR – HV, VV, texture, HV-min | SAR – HV, VV | SAR – HV, texture, HV-min | SAR – HV | SAR – VV, texture | SAR – VV | |
|-------------------------------|----------------|-------------------------------|--------------|---------------------------|-------------|-------------------|-------------|--|
| SAR | | 80.2 | 77.9 | 73.3 | 71.9 | 64.3 | 65.2 | |
| LS 21.04.05 | 52.8 | 82.8 | 81.8 | 80.4 | 80.4 | 75.8 | 76.8 | |
| LS 10.07.05 | 68.3 | 82.4 | 82.7 | 83.6 | 82.2 | 80.1 | 80.6 | |
| LS 21.04. & 10.07. | 77.9 | 83.7 | 83.7 | 84.0 | 83.8 | 82.9 | 82.5 | |



optical

SAR

optical & SAR

Tab.: Classification results – overall accuracy for 20 land use / land cover classes using 50 randomly distributed reference pixels per class (© FSU)

- Multitemporal, multipolarized SAR-data proves high potential for crop type mapping
- Classification accuracies: SAR > optical (but: only two optical scenes acquired at times unfavourable for crop mapping were considered (April & July); other scenes acquired during growing season were affected by clouds)

Crop type mapping – classification example 4

C-band

- ↗ Multitemporal ASAR & ERS-2 from 2005, test site Nordhausen, Thuringia, Germany

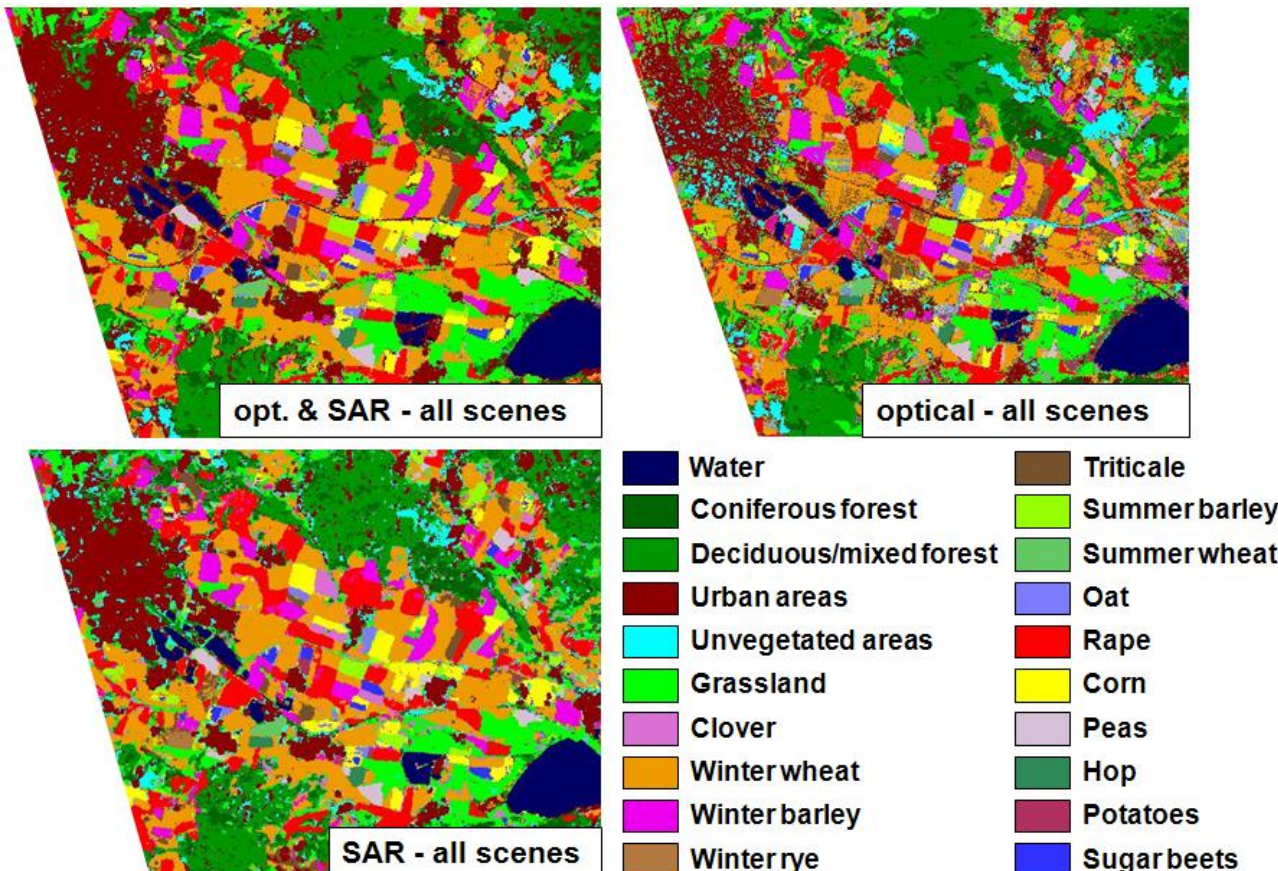


Fig.: Land cover maps – achieved overall accuracies:
optical & SAR: 83,7%;
optical: 77,9%;
SAR: 80,2%
(© FSU, 2007)

Crop type mapping – classification example 5

Automated land cover / land use mapping – the ENVILAND-2 project

Operational services – methodological requirements

- highly automated
- robust and transferable
- time- and cost-effective



ENVILAND-2 - objective

Development of an automated processing chain for the generation of land cover products, utilising optical and SAR data in a synergistic approach

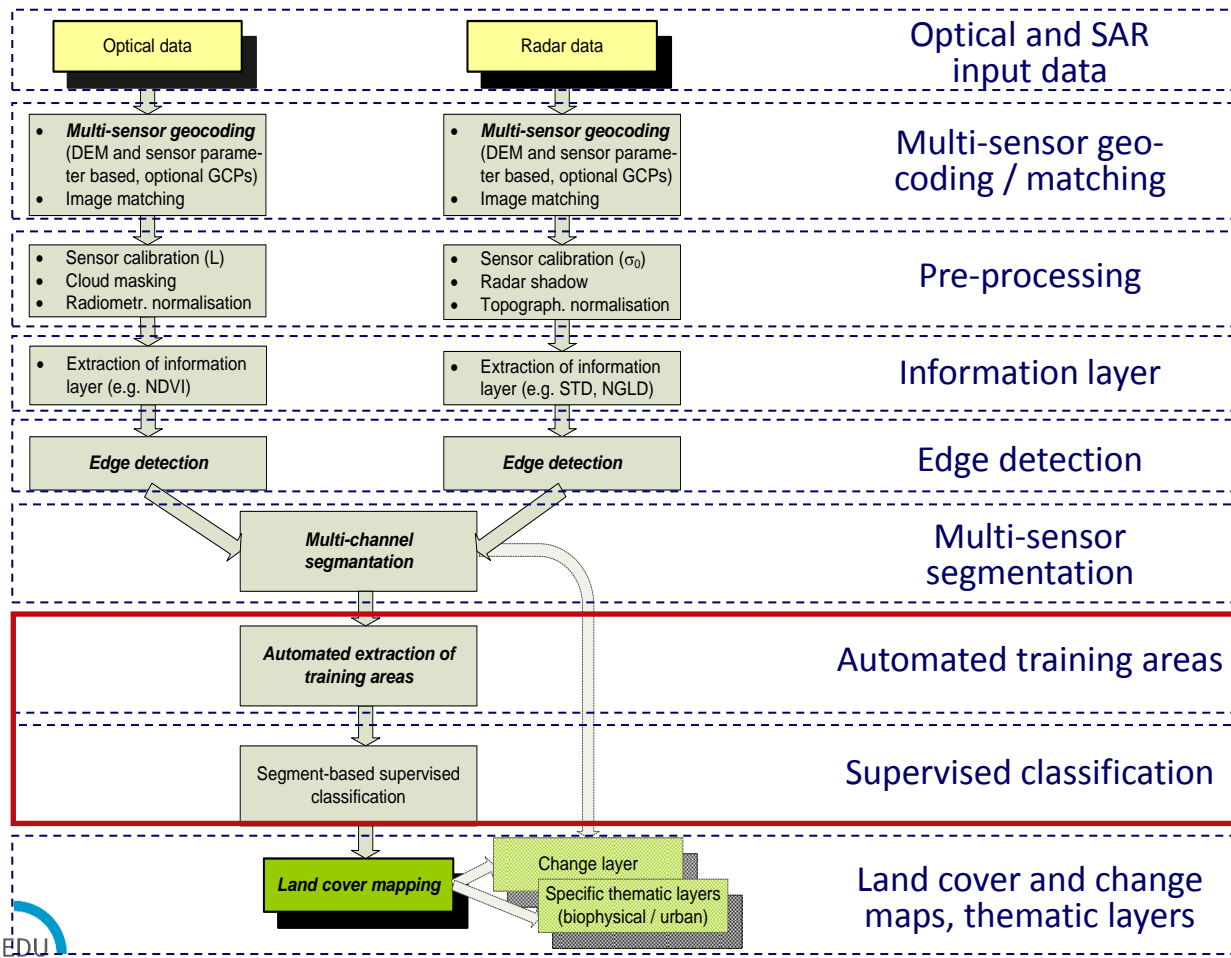
„To date, the automatic or semiautomatic transformation of huge amounts of multisource multiresolution spaceborne imagery into information still remains far below reasonable expectations“

Zamperoni 1996, cited in Baraldi et al. 2010

Crop type mapping – classification example 5

Automated land cover / land use mapping – the ENVILAND-2 project

↗ Processing chain



Classification strategy

- ↗ Training sample selection without any user interaction → automatic classification
- ↗ Flexible with regard to input data: optical, SAR, spatial resolution
- ↗ Robustness and transferability demonstrated for two agricultural test sites in Germany

Crop type mapping – classification example 5

Automated land cover / land use mapping – the ENVILAND-2 project

Classification strategy

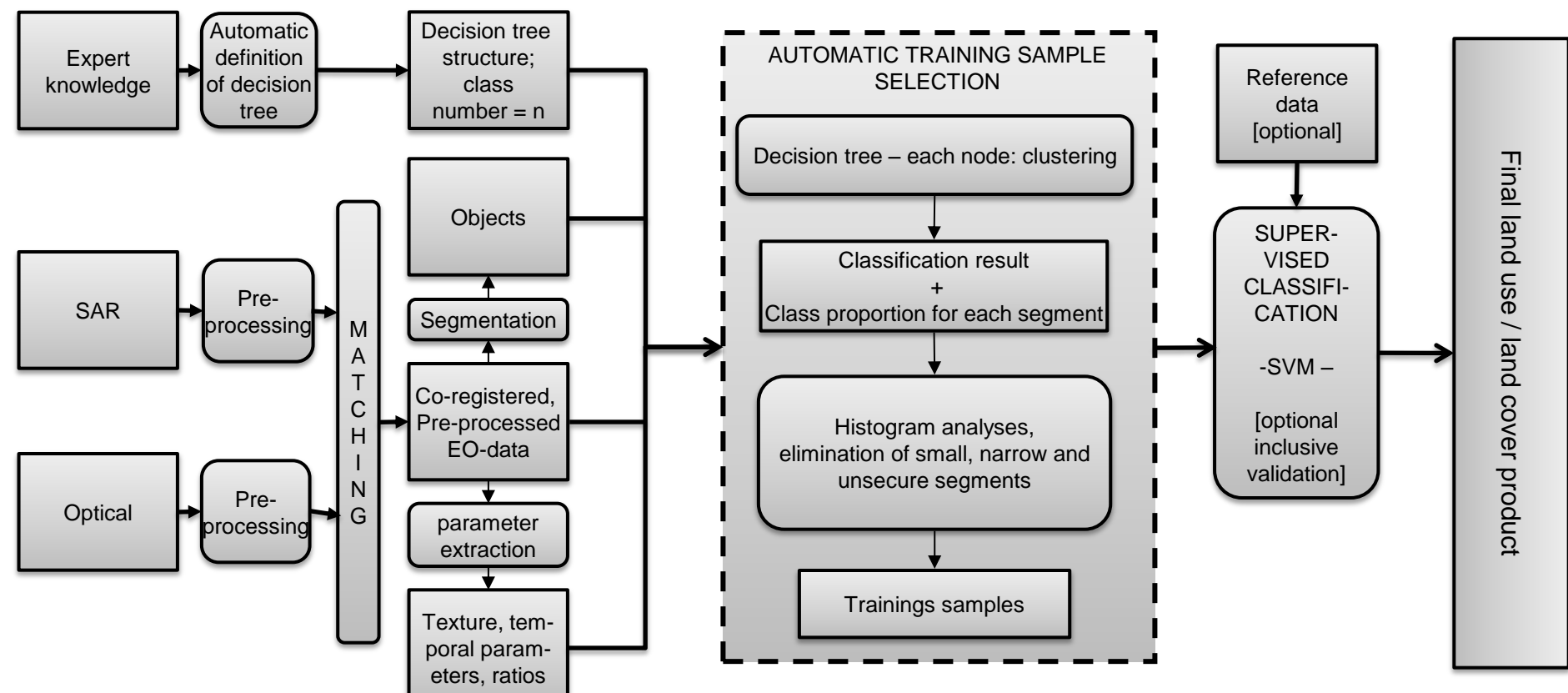
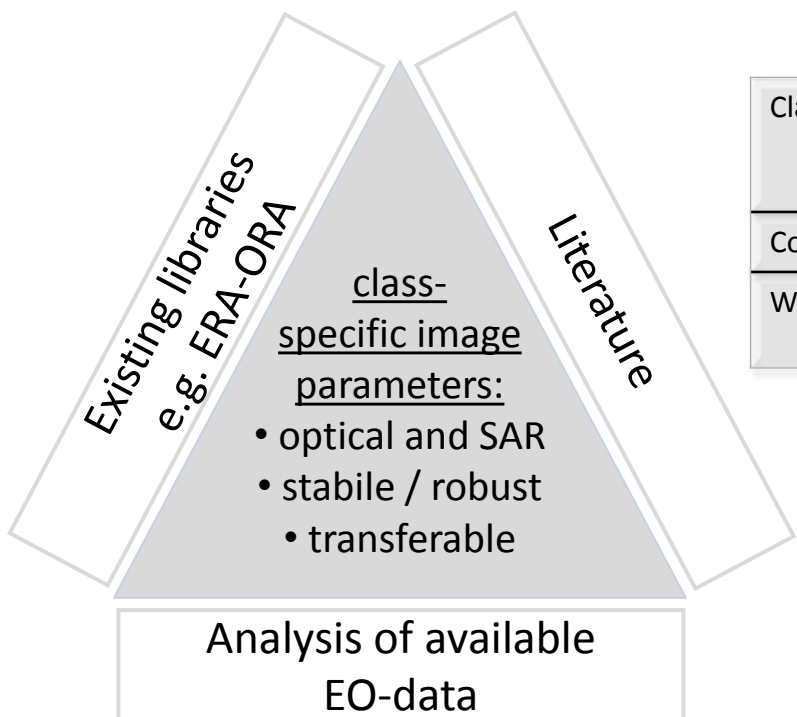


Fig.: © FSU / ZFL Bonn

Crop type mapping – classification example 5

Automated land cover / land use mapping – the ENVILAND-2 project

- Expert knowledge – key element of automatic training sample selection



| Class | Band | Time | Parameter | Separability | | See slides |
|----------|------|-------------------------|-------------|--------------|----------|------------|
| | | | | Corn | W.-wheat | |
| Corn | C-HV | June / July | Backscatter | -1 | 1.78 | 75 |
| W.-wheat | X-VV | April + end June / July | Ratio | 1.15 | -1 | 74 |

Tab.: © FSU



Automatic definition of decision tree structure in dependence from available EO-data

Fig.: © FSU

Crop type mapping – classification example 5

Automated land cover / land use mapping – the ENVILAND-2 project

- ↗ ENVILAND-2 classification – example
- ↗ Input: multitemporal X-, C- and L-band data acquired in 2009 over Nordhausen, Thuringia

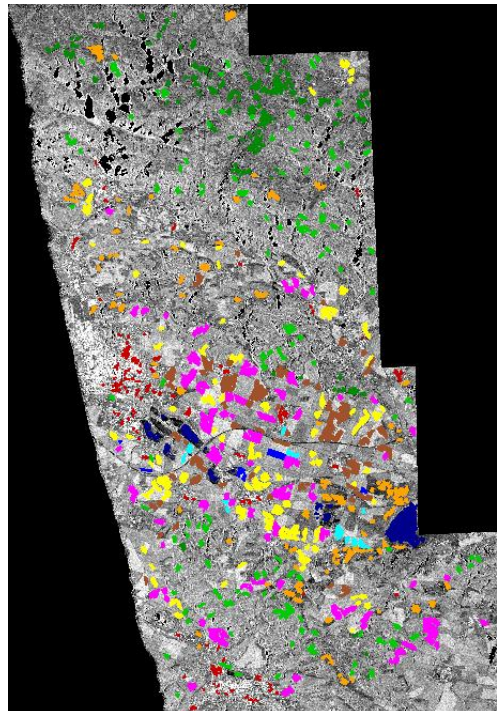


Fig.: Automatically extracted training samples (© FSU)

- Water
- Coniferous forest
- Mixed / deciduous forest
- Urban
- Grassland
- Winter wheat
- Winter barley / triticale
- Rape
- Sugar beets
- Corn
- Other crops

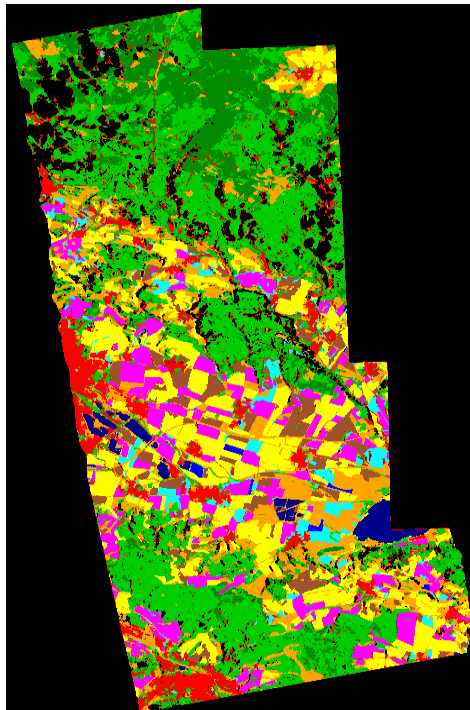
| X-, C-, L-band | Number of training samples [total / reference data available] | Correct training samples [%] |
|---------------------------|--|------------------------------|
| Water | 131 / 59 | 100,00 |
| Coniferous forest | 150 / 75 | 100,00 |
| Mixed / deciduous forest | 150 / 91 | 90,11 |
| Urban | 150 / 121 | 99,17 |
| Grassland | 150 / 86 | 96,51 |
| Winter wheat | 150 / 91 | 100,00 |
| Winter barley / triticale | 150 / 116 | 97,41 |
| Rape | 150 / 83 | 98,80 |
| Sugar beets | 12 / 9 | 100,00 |
| Corn | 20 / 18 | 100,00 |
| Other crops | 38 / 21 | 93,37 |

Tab.: © FSU

Crop type mapping – classification example 5

Automated land cover / land use mapping – the ENVILAND-2 project

- ↗ ENVILAND-2 classification – example
- ↗ Input: multitemporal X-, C- and L-band data acquired in 2009 over Nordhausen, Thuringia



■ Water
■ Coniferous forest
■ Mixed / deciduous forest
■ Urban
■ Grassland
■ Winter wheat
■ Winter barley / triticale
■ Rape
■ Sugar beets
■ Corn

Fig.: Derived land cover / land use map – SVM classification on base of the automatically extracted training samples (© FSU & ZFL)

| X-, C-, L-band | Producer's accuracy [%] | User's accuracy [%] |
|---------------------------|-------------------------|---------------------|
| Water | 86,93 | 96,03 |
| Coniferous forest | 85,86 | 83,86 |
| Mixed / deciduous forest | 57,25 | 83,92 |
| Urban | 85,86 | 79,28 |
| Grassland | 88,17 | 70,71 |
| Winter wheat | 96,38 | 96,63 |
| Winter barley / triticale | 93,44 | 91,81 |
| Rape | 96,91 | 99,37 |
| Sugar beets | 74,81 | 99,82 |
| Corn | 96,47 | 90,74 |
| Overall accuracy | 87,71 | |
| Kappa | 0,86 | |

Crop type mapping – classification example 5

Summary automated land cover / land use mapping – the ENVILAND-2 project

Novel methodology for automatic selection of potential training samples

- ↗ Speed up time- and cost-intensive process of training sample definition
- ↗ Automatic classification

Methodology – key elements

- ↗ Synergy of optical and SAR data (or SAR data only)
- ↗ Knowledge-based approach
- ↗ Combination of pixel- and object-based information
- ↗ Flexible, scene-specific thresholds (no fixed values)
- ↗ Implemented in IDL

Crop type mapping – classification example 5

Summary automated land cover / land use mapping – the ENVILAND-2 project

Optimal acquisition parameters

- ↗ **Forest**
 - ↗ Separation from open land: L-band
 - ↗ Separation coniferous vs. deciduous/mixed forest: ratio X-HV (small incidence angle) and L-HH or X-band (leaf-off)
- ↗ **Grassland** – separation to forest / agriculture: multitemporal C-HV
- ↗ **Crop types**
 - ↗ Critical - availability of SAR data acquired at optimal acquisition times
 - ↗ Critical: small field size for medium resolution SAR data
 - ↗ Broadleaf crops (e.g. rape, corn): C- and L-band
 - ↗ Narrowleaf crops (e.g. cereals), corn, sugar beets: X-band

Crop type mapping – classification example 5

Summary automated land cover / land use mapping – the ENVILAND-2 project

Classification results

- ↗ Class number: up to 12 (up to 11 for SAR data)
Strongly depends on available EO-data!!!
- ↗ Erroneous training samples per class: usually << 10%
- ↗ Supervised classifications: 80 – 90% overall accuracy

Transferability

- ↗ Spatial transferability demonstrated for two agricultural used test sites in Germany
- ↗ Temporal transferability demonstrated for SAR data acquired in 2009 and 2010 and various combinations of input data
- ↗ Applicable for various sensors (Landsat TM/ETM, Spot, RapidEye TerraSAR-X, ERS-2, Envisat ASAR, ALOS PALSAR)

Structure

- ↗ Introduction
- ↗ Major parameters affecting radar backscatter from crops
 - ↗ Sensor parameters
 - ↗ Target parameters
- ↗ Agricultural applications
 - ↗ Crop type mapping
 - ↗ Crop management / biophysical parameter retrieval
 - ↗ Soil parameter retrieval
- ↗ Optimal system configuration for agricultural applications

Crop monitoring / biophysical parameters

Need / main applications

- ↗ Mapping of yield losses caused by lodging, flooding, pests etc.
- ↗ Yield estimation
 - ↗ Yearly variations of up to 30% are not uncommon
 - ↗ Early estimate is of economic importance
 - ↗ Production estimation: acreage * yield
- ↗ Precision farming
 - ↗ Management of irrigation practices, fertilization etc.
→ maximum yield is sought with minimum fertilization etc.
 - ↗ Detection of within field variations / heterogeneities
- ↗ Estimation of input parameter for crop growth models

Crop monitoring / biophysical parameters

Traditional measurement techniques

- ↗ Field inspections → cost and time consuming
- ↗ Point-measurements only → all parameters are highly variable in space and time
- ↗ Methods
 - ↗ Phenological stage → BBCH Code
 - ↗ Height, row distance, row direction etc. → direct measurements in field
 - ↗ Wet and dry biomass, plant water content → labour → **destructive**
 - ↗ LAI → digital plant canopy analyser, e.g. LAI-2000 or direct measurement
 - ↗ Chlorophyll content – plant health → chlorophyll meter, e.g. SPAD
 - ↗ Fractional vegetation cover → visual assessment (subjective!), direct measurement at points, lines, plots or classification of vertical photos

Crop monitoring / biophysical parameters

Remote sensing for crop monitoring

↗ Optical data

- ↗ ***Most common*** instrument used in agricultural remote sensing
- ↗ Well established methodologies
- ↗ Visible and near infrared is related to final yield and crop condition
- ↗ But: problem of cloudiness and thus ***timeliness!!!***

↗ SAR data

- ↗ Main advantage: ***all weather capability*** → overcomes problem of cloudiness
- ↗ But: complex processing & complex interactions of sensor and target parameters

Crop monitoring / biophysical parameters

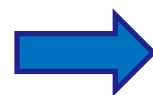
Data requirements

- ↗ **Image product**
 - ↗ RAW / PRI data
 - ↗ SLC data
 - ↗ Polarimetric analyses
 - ↗ PolInSAR: polarimetric single-pass data are required (Lopez-Sanchez et al., 2009)
 - ↗ Critical for many agricultural information: ***timeliness*** → consider repetition and delivery time
- ↗ **Frequency**
 - ↗ Optimal: multifrequency data
 - ↗ Single frequency: depends on crop type
 - ↗ C- (and X-) band most often used
 - ↗ Rice: C-band (Inoue et al., 2002 and Inoue et al., 2014)
 - ↗ Broad-leaf crops: longer wavelengths to minimize saturation effects!!

Crop monitoring / biophysical parameters

Data requirements

- ↗ **Polarization – parameters often used**
 - ↗ HH / VV ratio for cereals (X- or C-band)
 - ↗ HV-data
 - ↗ Various polarimetric parameters
- ↗ **Timing**
 - ↗ For monitoring: multitemporal data
- ↗ **Incidence angle**
 - ↗ Some authors suggest the usage of shallow incidence angles due to reduced soil contribution



See also module 2300:
Radar polarimetry

Crop monitoring / biophysical parameters

Data requirements

- ↗ Spatial resolution
 - ↗ *Critical* parameter!!!
 - ↗ **Very high** spatial resolution is required
 - ↗ Detection of within field variations
 - ↗ Regions with small and mosaic crop fields, e.g. many countries in Asia or Africa

*Example: Suggestion for monitoring rice in Asia: ~1m spatial resolution
(Inoue et al., 2014)*

- *Required resolution is achieved by latest SAR sensors in spotlight mode (TerraSAR-X, COSMO-SkyMed, Radarsat-2)*
- *Limited number of in-depth studies using such high resolution data*

Crop monitoring / biophysical parameters

Methods

- ↗ **Temporal analysis** of backscattering intensities / polarimetric parameters
 - ↗ **Empirical models** → regression analyses
 - ↗ Common approach
e.g. Karjalainen et al., 2008;
 - ↗ Sensitivity analysis
 - ↗ Evaluation of the feasibility of crop parameter extraction
 - ↗ Assessment of optimal SAR parameters for crop information extraction
 - ↗ Inversion unproblematic
 - ↗ Spatial / temporal transferability critical!!!
- Problem: signal saturation
Broad-leaf crops (e.g. corn, soybean): very early (e.g. corn, C-band: 1m height)
Grain crops: dynamic temporal variation, subsequent saturation*

Crop monitoring / biophysical parameters

Methods

- ↗ Empirical models → regression analyses
 - ↗ Several crop-specific polarization and / or dual frequency ratios were developed
 - Examples:*
 - ↗ RVI radar vegetation index at L-band → corn, biomass
Yunjin & Van Zyl, 2009
 - ↗ L-HV / L-VV → soybean, water content
De Roo, 2001
 - ↗ VV / HV at S- and C-band → corn, height & biomass
Della Vecchia et al., 2008
 - ↗ C-HV / C-HH → sugarcane, LAI
Lin et al., 2009
 - ↗ Increasing usage of polarimetric parameters in recent years

Cross-polarization ratios are almost insensitive to soil moisture
(Gherboudji et al., 2011)

Crop monitoring / biophysical parameters

Methods

- ↗ Semi-empirical Water Cloud Model

- ↗ Developed by Attema & Ulaby (1978)



Further application:
see module 3201:
Forests

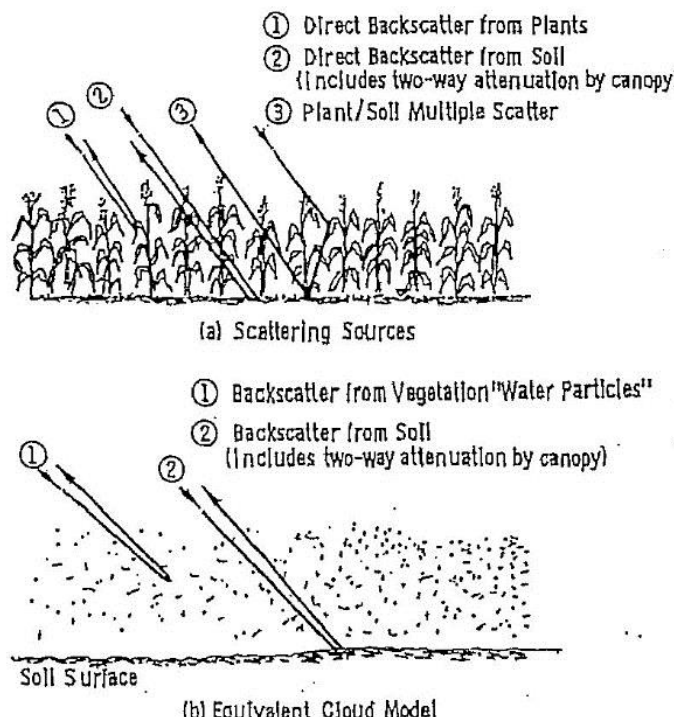


Fig.: Ulaby et al., 1984

Basic assumptions:

- ↗ Vegetation representation: cloud of identical water droplets randomly distributed within the canopy
- ↗ Single scattering is considered only → no multiple scattering
- ↗ Significant variables: volumetric soil moisture, volumetric water content of vegetation and vegetation height

Crop monitoring / biophysical parameters

Methods

↗ Semi-empirical Water Cloud Model

Radar cross-section is expressed as the incoherent sum of the contribution of the vegetation layer and the contribution of the soil, latter being attenuated through the vegetation

$$\sigma^o = \sigma_{veg}^o + \tau^2 \sigma_{soil}^o$$

$$\sigma_{veg}^o = A \cos \theta (1 - \tau^2)$$

$$\sigma_{soil}^o = C + Dm_s$$

$$\tau^2 = \exp(-2Bm_v/\cos \theta) \quad \text{two-way attenuation through canopy}$$

- ↗ A, B, C, D constants – estimation by data fitting
- ↗ m_v – water content of the canopy, i.e. product of volumetric water content times the height of the canopy
- ↗ m_s – soil surface moisture content

Crop monitoring / biophysical parameters

Methods

↗ Semi-empirical Water Cloud Model

↗ Pro:

- ↗ Simple approach
- ↗ Easy model inversion

↗ Cons:

- ↗ Need of data fitting to estimate input constants A, B, C, D
 - ↗ Common approach: regression analysis
 - ↗ Estimation using theoretical models (Graham & Harris, 2002)
- ↗ Data fitting required for each radar configuration
- ↗ Not applicable for polarimetric systems (consideration of phase information)

Crop monitoring / biophysical parameters

Methods

↗ Theoretical models

- ↗ Many studies in the 90's and the early 00's
- ↗ Most models are based on radiative transfer theory
- ↗ Need / motivation
 - ↗ To understand the interaction between radar signal and target → assist data interpretation
 - ↗ To assess the sensitivity of radar backscatter to variations of specific input parameters → specification of optimal radar configuration

⇒ *Required for the development of reliable retrieval algorithms*

Crop monitoring / biophysical parameters

Methods

↗ Theoretical models

- ↗ General approach (Karjalainen et al., 2008)
 - ↗ Subdivision of the canopy into single elements and selection of suitable geometrical shapes (e.g. stems – finite-length cylinders, leaves – plane circular or elliptical discs)

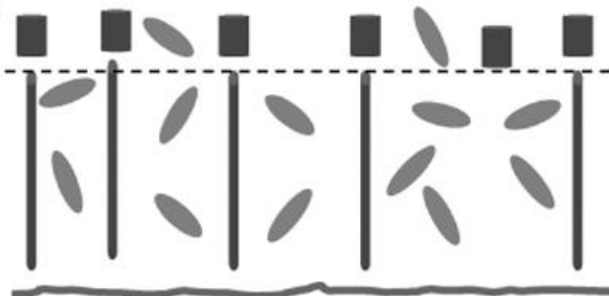


Fig.: Model scheme for wheat
(Karjalainen et al., 2008)

- ↗ Modelling of permittivity, extinction and scattering of elements
- ↗ Combination of single contributions

Crop monitoring / biophysical parameters

Methods

↗ Theoretical models

- ↗ Modelling approaches – combination of single contributions
 - ↗ Single scattering approach, e.g. MIMICS model
 - e.g. *Touré et al., 1994*
 - ↗ Consideration of multiple scattering
 - e.g. *Bracaglia et al., 1995*
 - ↗ Consideration of coherent scattering
 - e.g. *Marliani et al., 2002; Stiles & Sarabandi, 2000*
 - ↗ Consideration of multiple and coherent scattering
 - e.g. *Picard et al., 2003, Chiu & Sarabandi, 2000*

For fully developed cereals multiple scattering should be considered

Crop monitoring / biophysical parameters

Methods

↗ Theoretical models

↗ Major drawbacks

- ↗ Difficulties in the modelling of scattering processes
- ↗ Partly large differences between model predictions and measurements
- ↗ Inherent limitations in model inversion
- ↗ Problems in the determination of the key parameters
- ↗ Overparameterization (e.g., 3-D canopy structure, plant water content, and soil roughness) → parameters often difficult to measure (e.g. destructive only) and strong spatial variations

Fig.: Required input parameters of the MIMICS model to simulate wheat crops (Touré et al., 1994)

| WHEAT | | | |
|---|-----------------------------------|--------|---|
| | Stem | Leaf | Soil |
| gravimetric moisture (m_g) = 0.47–0.79 | $m_g = 0.50\text{--}0.87$ | | $m_v(\text{g/cm}^3) = 0.06\text{--}0.25$ |
| height, $h(\text{m}) = 0 \text{ -- } 0.58$ | length, $l = 120 \text{ mm}$ | C band | $s(\text{cm}) = 0.55(\text{site13}), 0.45(\text{site12})$ |
| diameter, $d = 2 \text{ mm}$ | width, $w = 10 \text{ mm}$ | | $ls = 1.2 \text{ cm}$ |
| density, $N(\text{st./m}^2) = 320(\text{site13}), 200(\text{site12})$ | lai = 0.45 – 2.82 | L band | $s(\text{cm}) = 1.2(\text{site13}), 1.1(\text{site12})$ |
| PDF = vertical | thickness, $th. = 0.2 \text{ mm}$ | | $ls(\text{cm}) = 4.9(\text{site13}), 5(\text{site12})$ |
| | PDF = uniform | | |

Crop monitoring / biophysical parameters

Methods

↗ InSAR



See module 2200:
InSAR

- ↗ Very limited number of InSAR studies for agriculture
 - ↗ **Why?** Extreme temporal decorrelation due to rapid changes in crop and soil conditions
 - ⇒ *Necessity of single-pass interferometric systems*
- ↗ Selected studies
 - ↗ Blaes & Defourny, 2003 → crop height using tandem ERS-1/-2 data
 - ↗ Engdahl et al., 2001 → crop height
 - ↗ Wegmüller & Werner, 1997 → fractional coverage & crop growth

Crop monitoring / biophysical parameters

Methods

↗ Polarimetric SAR interferometry

↗ Investigation of the 3D structure of natural volume scatterers

↗ Methodological background

→ See module 2300:
Radar polarimetry

↗ Successfully used for forest height extraction

→ See module 3201:
Forests

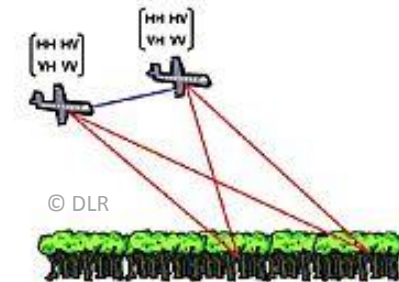


Fig.: Pol-InSAR acquisition geometry:
Scattering matrix recorded from two
different observation angles (© DLR -
http://www.dlr.de/hr/en/desktop/default.aspx/tabcid-2470/3731_read-5663/)

But: adoption of forest concepts for agriculture applications is questionable and ineffective (significant differences in vegetation height and scattering behaviour)

Crop monitoring / biophysical parameters

Methods

↗ Polarimetric SAR interferometry - Agriculture

- ↗ Early development stage
 - ↗ Indoor experiments at the European Microwave Signature Laboratory at JRC-Ispra, Italy (Ballester-Berman et al., 2005)
 - ↗ First demonstration study using airborne SAR data was published in 2012b (Lopez-Sanchez et al., see slide 120)
- ↗ Potential applications
 - ↗ Height extraction
 - ↗ Important parameter for biomass estimation
 - ↗ Indicator for phenological stage of most cereals and some other crops, (particular) in the vegetative phase
 - ↗ Height monitoring → health and yield estimation
 - ↗ Extinction of vegetation layer → vegetation moisture content, LAI
 - ↗ Soil moisture retrieval – potential is currently investigated

Crop monitoring / biophysical parameters

Plant parameters of interest

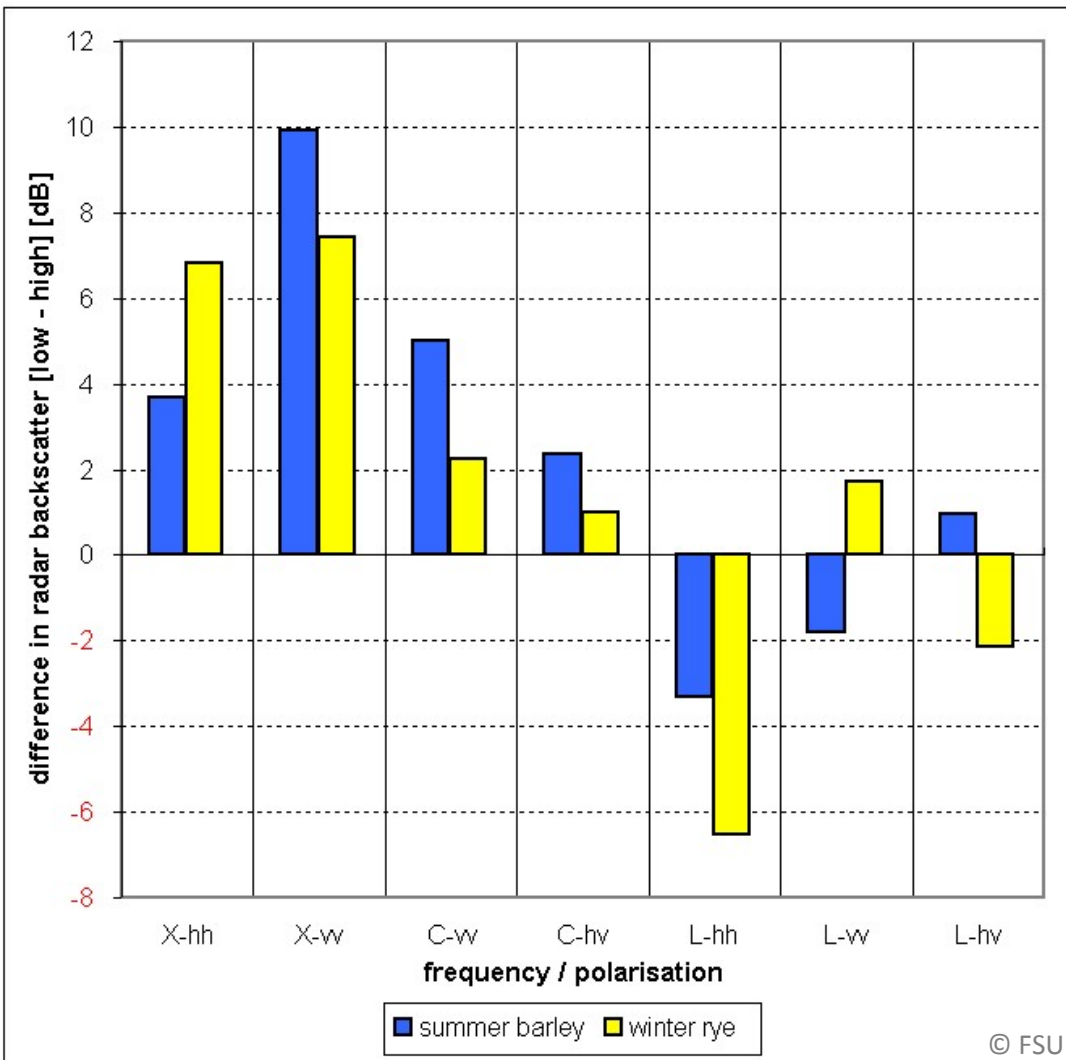
- ↗ Phenology
- ↗ Plant height
- ↗ Leaf Area Index (LAI)
- ↗ Plant biomass
- ↗ Water content
- ↗ fAPAR
- ↗ ...

Crop monitoring / biophysical parameters

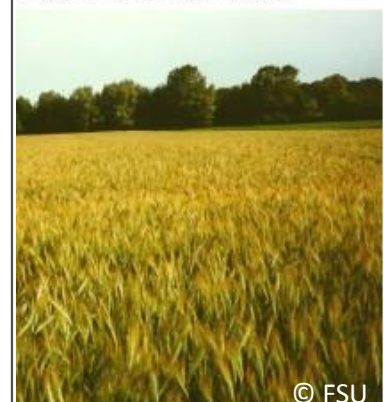
Could we recognize cultivation problems / field heterogeneities in SAR data? Example 1



summer barley
south: 60 – 70 cm / north:



winter rye
20 cm / north: 30 – 60 cm



Crop monitoring / biophysical parameters

Could we recognize cultivation problems / field heterogeneities in SAR data? Example 2

TerraSAR-X data

- ↗ Test site: mouth of the Guadalquivir river, SW of Spain
- ↗ Common problems in study area: plagues and effects of highly salty water used for irrigation
- ↗ Lower plant density & phenological delay
- ↗ Crop type: rice

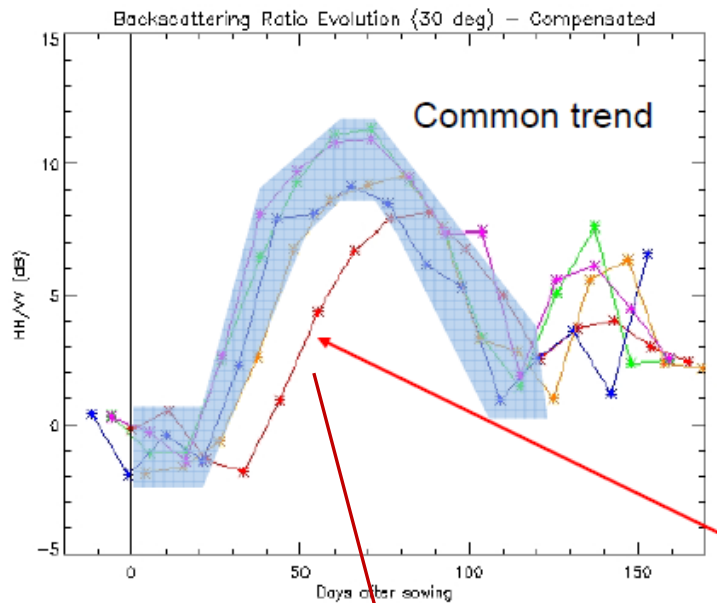
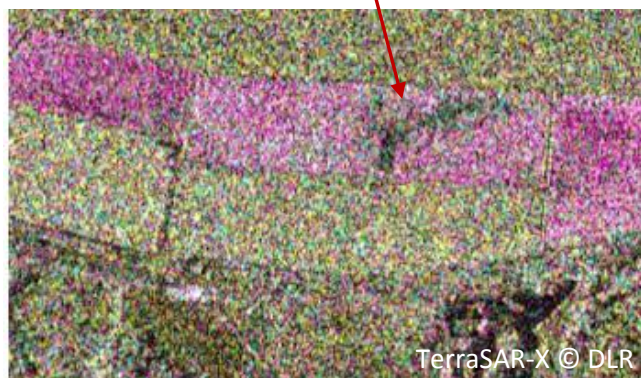


Fig.: Lopez-Sanchez et al., 2012c



TerraSAR-X © DLR

Fig.: TerraSAR-X false colour composite acquired on July 24, 2008 – HH / VV / HH-VV (Lopez-Sanchez et al., 2011)

Biophysical parameter - application example 1

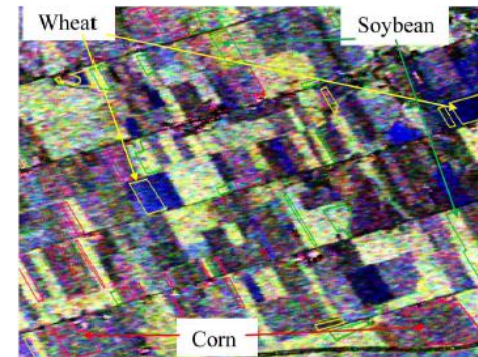
Temporal analysis of Pauli components



See module 2300:
Radar polarimetry

- ↗ Radarsat-2 fine quad mode data, 2008 - 2010
- ↗ Study area: Eastern Ontario, Canada
- ↗ Crop types: corn, spring wheat, soybeans

Fig.: RGB Pauli composite acquired on
August 30, 2008 – HH-VV / HV / HH+VV
(Liu et al., 2013)



Key findings:

- ↗ Strong indicator for crop growth development → Pauli **volume (HV)** and Pauli **double bounce (HH-VV)** component
 - ↗ Emergence: very low
 - ↗ Vegetative phase: significant rise
 - ↗ Plant maturity: plateau is reached
 - ↗ Senescence: decline
 - ↗ Harvest: significant decrease → estimation of harvest date

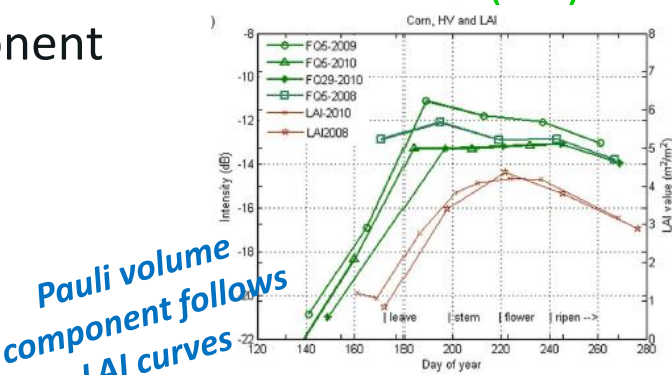


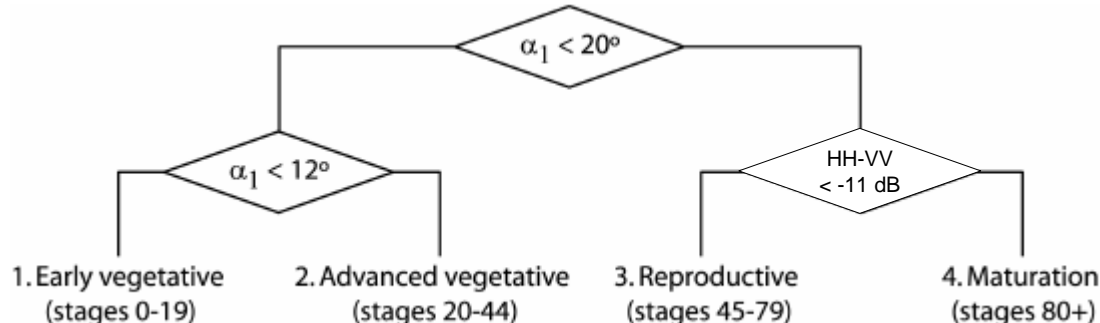
Fig.: Liu et al., 2013

Biophysical parameter - application example 2

Phenology retrieval - temporal analysis

- ↗ Radarsat-2 (20 images), ESA AgriSAR campaign 2009
- ↗ Study area: Indian Head, Canada
- ↗ Cereals: wheat, barley, oat
- ↗ Alpha angle and HH-VV

See module 2300:
Radar polarimetry



Lopez-Sanchez et al., 2012c

Problems:
- Transition between reproductive phase and maturation
- Extreme incidence angles

Fig.: Lopez-Sanchez et al., 2012c

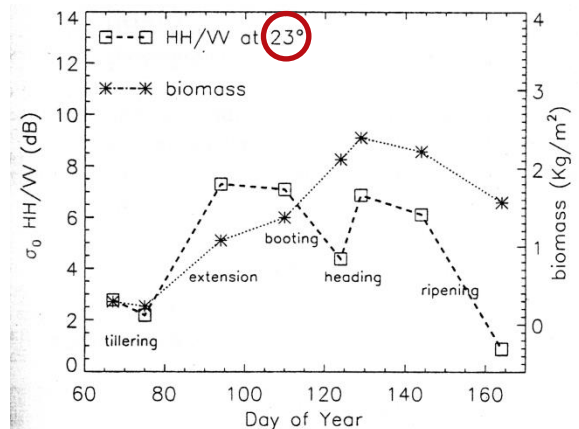
Key findings:

- ↗ Applicable for wheat and barley (correct: 18 resp. 19 out of 20 images)
- ↗ Insensitive for oat

Biophysical parameter - application example 3

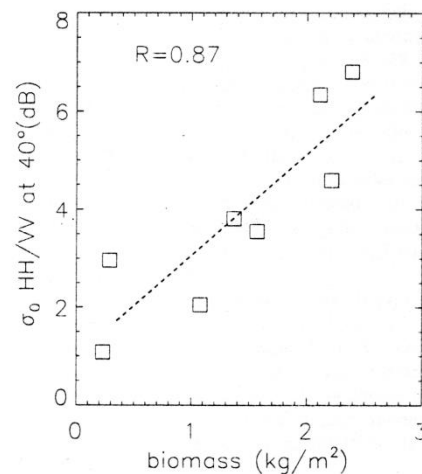
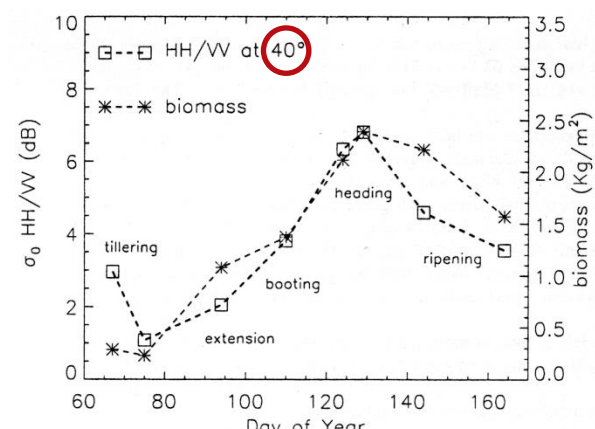
Biomass retrieval – empirical models

Ratio HH/VV - example 1: wheat, scatterometer data, C-band



no correlation

Shallow incidence angles are required



**Mattia et al.,
2003**

Biophysical parameter - application example 4

Biomass retrieval – empirical models

Ratio HH/VV - example 2: rice

↗ C-band, Envisat-ASAR data

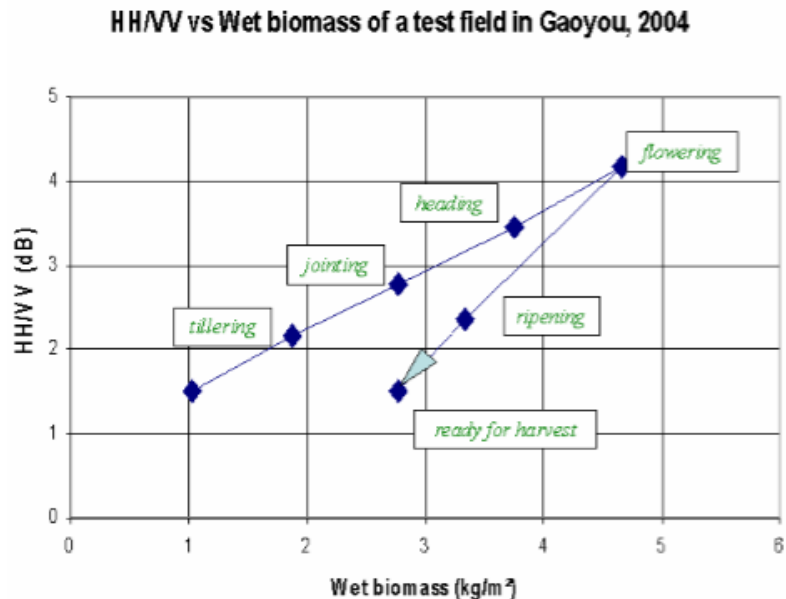


Fig.: Temporal variation of HH/VV over a rice field as a function of rice wet biomass in Gaoyou, 2004 (LeToan et al., 2005)

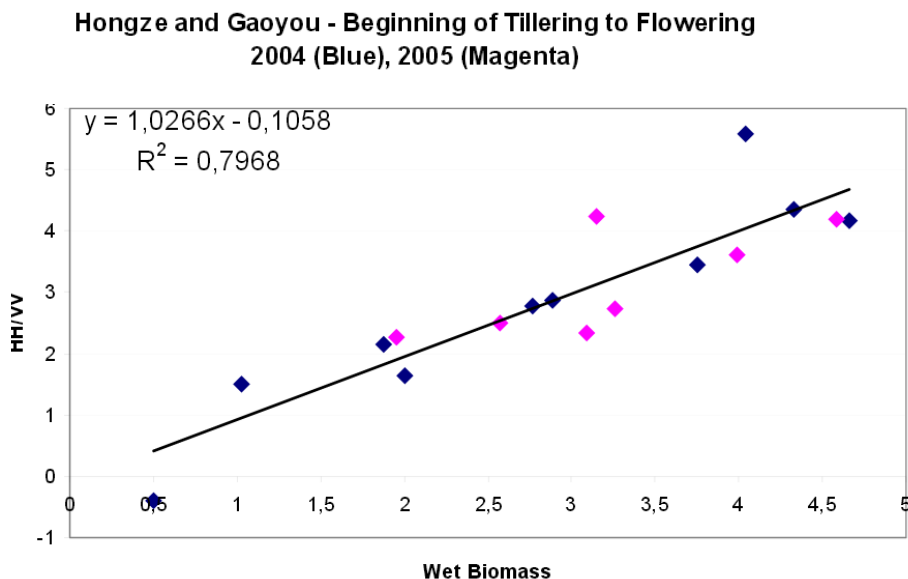


Fig.: Relation between HH/VV and wet biomass of rice fields in Hongze and Gaoyou (LeToan et al., 2005)

Biophysical parameter - application example 5

LAI retrieval – empirical and semi-empirical models

Step 1: sensitivity analysis → linear regressions

- ↗ C-band, Radarsat-2 data
- ↗ Indian Head, Canada

*Linear regressions
were found for LAI
< 3 m²/m²*

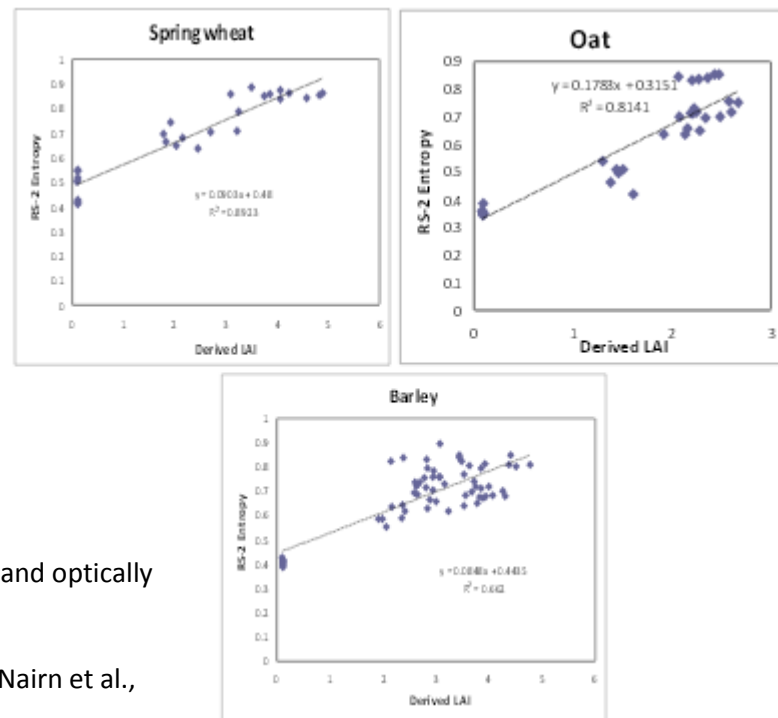


| SAR parameter | Wheat | Oats | Barley |
|-------------------|-------|-------|--------|
| HH | 0.58 | 0.41 | 0.26 |
| HV | 0.91 | 0.89 | 0.52 |
| VV | 0.26 | -0.28 | -0.46 |
| HV/HH ratio | -0.78 | -0.73 | -0.75 |
| HV/VV ratio | 0.84 | 0.71 | 0.80 |
| HH/VV ratio | 0.69 | 0.75 | 0.80 |
| entropy | 0.94 | 0.90 | 0.81 |
| pedestal height | 0.87 | 0.70 | 0.63 |
| total power | 0.62 | 0.28 | 0.08 |
| volume scattering | 0.86 | 0.89 | 0.39 |

See module
2300: radar
polarimetry

Tab.: Correlation coefficients (R) between RADARSAT-2 response and optically derived LAI (McNairn et al., 2012)

Fig.: Relationship between entropy and optically derived LAI (McNairn et al., 2012)



McNairn et al., 2012

Biophysical parameter - application example 5

LAI retrieval – empirical and semi-empirical models

Step 2: Water cloud model

- Entropy → strongest sensitivity to optically derived LAI
- Water cloud model modified by Prevot et al. (1993) for wheat canopies were used → incorporation of LAI

$$\sigma^0 = \underbrace{AL^E \cos\theta(1 - \exp(-2RL \cos\theta))}_{\text{Vegetation contribution}} + \underbrace{\sigma_{soil}^0 \exp(-2RL \cos\theta)}_{\text{Two-way attenuation through the canopy layer}}$$

Soil contribution

$$\sigma_{soil}^0 = C + DM_s$$

L → LAI

A, B, E → Parameters depending on canopy type, fitted by experimental data

M_s → Volumetric soil moisture content

C, D → Parameters depending on soil moisture → parameterization of Jiao et al. (2011) were used

θ → Incidence angle

Biophysical parameter - application example 5

LAI retrieval – empirical and semi-empirical models

Step 2: Water cloud model

- ↗ Parameterization using LAI, soil moisture and SAR data
- ↗ Model inversion based on look-up-table approach -> final LAI map

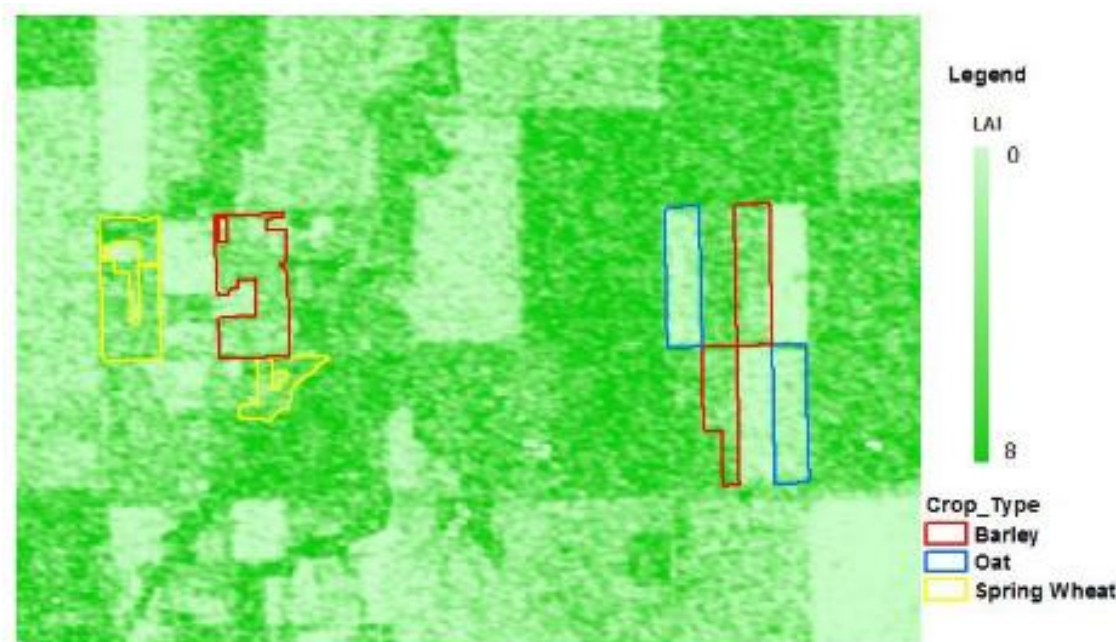
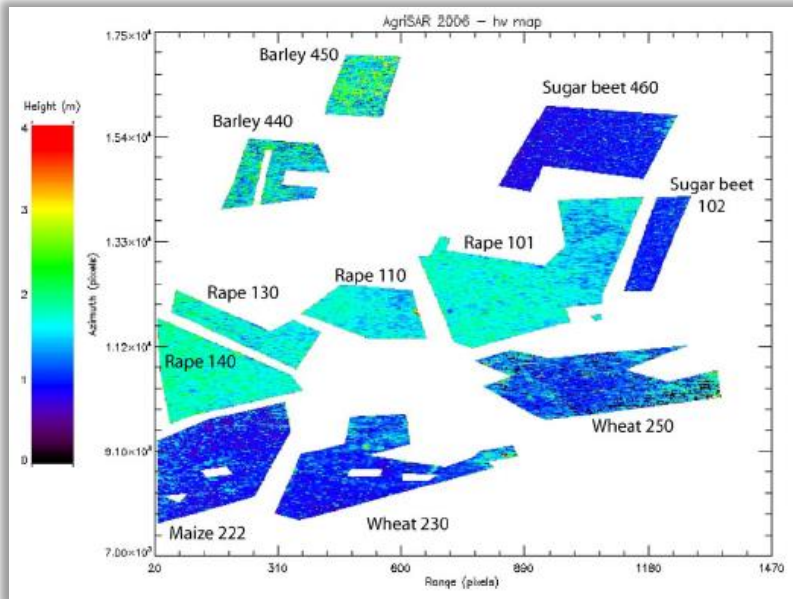


Fig.: RADARSAT-2 derived LAI map – June 24th (McNairn et al., 2012)

Biophysical parameter - application example 6

Retrieval of vegetation height – polarimetric SAR interferometry

- ↗ Airborne E-SAR data acquired at L-band over Demmin, Germany
- ↗ L-band not optimal → strong soil contribution



| Field | Mean (m) | Std.dev. (m) | Ground data (m) |
|----------------|----------|--------------|------------------|
| Rape 101 | 1.61 | 0.22 | 1.70, 1.72, 1.75 |
| Rape 110 | 1.60 | 0.24 | N.A. |
| Rape 130 | 1.67 | 0.25 | N.A. |
| Rape 140 | 1.76 | 0.20 | 1.45, 1.50, 1.55 |
| Maize 222 | 0.98 | 0.31 | 0.90, 1.05, 1.10 |
| Wheat 230 | 1.06 | 0.33 | 0.77, 0.79, 0.82 |
| Wheat 250 | 1.31 | 0.47 | 0.78, 0.80, 0.87 |
| Barley 440 | 1.61 | 0.47 | 0.96, 0.97, 1.10 |
| Barley 450 | 1.89 | 0.61 | 0.91, 0.95, 0.98 |
| Sugar beet 102 | 1.02 | 0.25 | 0.40, 0.50, 0.50 |
| Sugar beet 460 | 0.93 | 0.31 | 0.13, 0.20, 0.25 |

Tab.: Comparison between vegetation height estimates h_v at field level and ground measurements (Lopez-Sanchez et al., 2012b)

Fig.: Retrieved vegetation heights (Lopez-Sanchez et al., 2012b)

- ↗ Accurate estimates for winter rape and maize
- ↗ No valid estimates for wheat, barley and sugar beet (reasons: RVoG model used, available baseline, SNR, phenological stage)

Structure

- ↗ Introduction
- ↗ Major parameters affecting radar backscatter from crops
 - ↗ Sensor parameters
 - ↗ Target parameters
- ↗ Agricultural applications
 - ↗ Crop type mapping
 - ↗ Crop management / biophysical parameter retrieval
 - ↗ Soil parameter retrieval
- ↗ Optimal system configuration for agricultural applications

Soil parameter retrieval

Agricultural fields – three main stages

↗ Soil covered by vegetation



Fig.: Corn field, test site Nordhausen, Germany – date: July 10, 2005 (© FSU)

↗ Soil covered by crop residue



Fig.: Harvested corn field, one part freshly plowed, test site Nordhausen, Germany – date: September 28, 2005 (© FSU)

↗ Bare soil

See module 3402:
Hydrosphere – soil
moisture

Soil parameter retrieval

Need / main applications

➢ Soil moisture

- Economic importance: reduced productivity due to droughts / excessive moisture / floods
 - e.g. drought in Canada in 2001 / 2002 – costs: 5.8 billion \$
 - e.g. excessive moisture in Canadian Prairies in 2010 – costs: 2.4 billion \$
- Optimal crop / irrigation management (precision farming)
- Important parameter for predictive hydrological modelling → flood forecasting

Traditional measurement techniques



See module 3402: Hydrosphere
– soil moisture

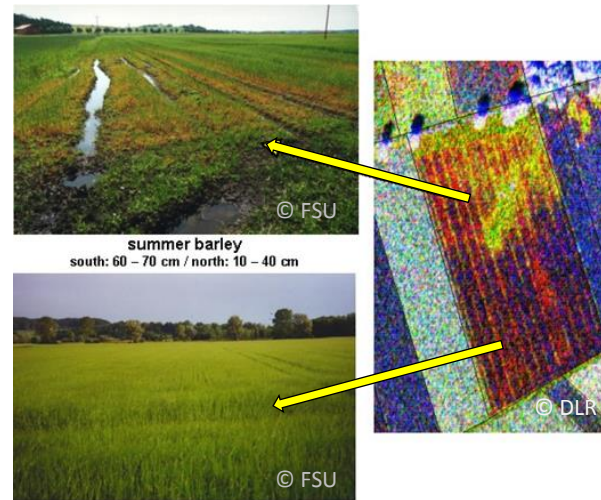


Fig.: Reduced crop productivity and its representation in airborne E-SAR data (© FSU)

McNairn

http://www.fia.cl/Portals/0/UCP/Senarios/Agricultura%20Precisi%C3%B3n/0002%20_20Heather_Talca%20Earth%20Observation%20McNairn.pdf

Soil parameter retrieval

Need / main applications



↗ Surface roughness

- ↗ Estimation of harvest date
- ↗ Monitoring of residue cover
- ↗ Monitoring of tillage practices

McNairn

http://www.fia.cl/Portals/0/UCP/Seminarios/Agricultura%20Precisi%C3%B3n/0002%20_%20Heather__Talca%20Earth%20Observation%20McNairn.pdf

Benefits of reduced tillage / no-till practices

- ↗ Reduction in wind and water erosion
- ↗ Increase / maintenance of soil organic matter
- ↗ Improved biological activity / soil structure
- ↗ Increase / maintenance of soil carbon and its sequestration

Traditional measurement techniques

See module 3402: Hydrosphere

- soil moisture

Soil parameter retrieval

Role of remote sensing – current status

- ↗ Bare surfaces → satisfactory estimation results using empirical, semi-empirical or theoretical approaches



See module 3402:
Hydrosphere – soil
moisture

BUT:

- ↗ Agricultural fields are covered by different crop types over large periods of the year
- ↗ For many applications soil parameters under vegetation are needed, e.g. irrigation management
- ↗ General very complex and challenging task
- ↗ No nearly operational methods exists
- ↗ Strong need for research

*Effects of surface roughness,
crop cover, and soil texture
(suggested by some authors)
have to be considered in the soil
moisture retrieval process*

Soil moisture under vegetation

Data need

General:

- (1) One radar configuration is not sufficient to estimate soil moisture under vegetation**
- (2) Multi-configuration SAR data are required (multi-temporal, multi-frequency, multi-angular, multi-polarization)**

Frequency

- Longer wavelengths (e.g. L-band) → stronger soil contribution
- Multi-frequency SAR data
 - Combination of higher and lower frequencies, e.g.:
 - Ku- and C-band (Moran et al., 1998)
 - C- and L-band (De Roo et al., 2001)

Soil moisture under vegetation

Data need

Polarisation

- ↗ VV → L-VV radar band with best correlation to soil moisture
- ↗ Multi-polarized SAR data, e.g. combination of L-VV and cross-co-polarized C-band ratio (the latter for biomass correction)

Incidence angle

- ↗ Steep incidence angle → higher soil contribution
- ↗ Combination of steep and shallow incidence angles

Temporal resolution

- ↗ High temporal frequency of data acquisition → soil moisture very variable in space and time

Soil moisture under vegetation

Methods

- ↗ Empirical models
- ↗ Semi-empirical models
 - ↗ Water cloud model (e.g. Gherboudj et al., 2011; Moran et al., 1998)
 - ↗ Adapted MIMICS model (e.g. de Roo et al., 2001)
- ↗ SAR polarimetry (e.g. Hajnsek et al., 2009, Jagdhuber, 2012)
- ↗ PollInSAR → potential is addressed in current studies
- ↗ Multitemporal signal analysis → applicability of change detection approach for large area surface moisture mapping to high-resolution SAR data is addressed in current studies

Common approach: combination of various SAR parameters

(1) SAR parameter(s) with high sensitivity to soil moisture
 (2) SAR parameter(s) to correct for vegetation effects



Methodology see module 3402:
 Hydrosphere – soil moisture

Crop residue / soil surface roughness under vegetation

Crop residue

- ↗ **Optical** data were used, but residue management practices are time-critical → problem of cloudiness
- ↗ **SAR** data
 - ↗ Crop residue → alteration of soil surface roughness → SAR data are sensitive to roughness characteristics
 - ↗ But: very few studies only

Crop residue / soil surface roughness under vegetation

- ↗ Effect of crop residue on radar backscatter
 - ↗ Polarization / other SAR parameters
 - ↗ C-HV strongest correlation with residue condition (further advantage: less sensitive to radar look direction effects)
 - ↗ C-VV: least sensitivity
 - ↗ Other SAR parameters sensitive to volume and multiple scattering are correlated to crop residue, e.g. circular co-polarization

Crop residue / soil surface roughness under vegetation

- ↗ Effect of crop residue on scattering mechanism (McNairn et al., 2002)
 - ↗ Depends on crop type
 - ↗ Lentil, pea: smooth soil surface, sparse and fine residue cover → dominant surface scattering
 - ↗ Corn, sunflowers: large pieces of residue (cover > 50%) → dominant multiple scattering
 - ↗ Grain residue (cover > 50%) → dominant multiple scattering
 - ↗ Methodology: analysis of polarimetric parameters
- ↗ Surface roughness under vegetation
 - ↗ SAR polarimetry → Jagdhuber, 2012

Soil parameter retrieval – application example 1

Soil moisture under vegetation – empirical models

- Truck-mounted radar system, fully polarimetric C- and L-band data from 1996
- Test site: Kellogg Biological Station, Hickory Corners, Michigan, US
- Crop type: soybean

sensitive to soil moisture changes

$$m_v = 0.2338 + 0.0244 \sigma^0_{L-VV} - 0.0142 (\sigma^0_{C-HV} - \sigma^0_{C-VV})$$

correction for biomass effects

De Roo et al., 2001

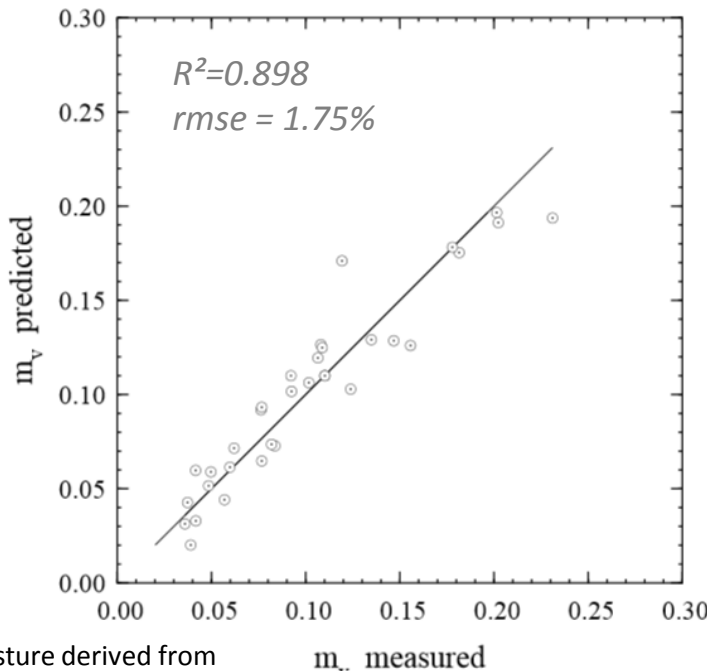


Fig.: Comparison of the measured and inverted soil moisture derived from radar measurements using the given expression (De Roo et al., 2001)

Soil parameter retrieval – application example 2

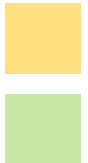
Soil moisture under vegetation – combination of high and low frequencies

- ↗ SAR-data used: Ku – and C-band (airborne SNL data & ERS-1)
 - ↗ Ku-band, shallow incidence angle: SAR signal is primarily sensitive to vegetation parameters
 - ↗ C-band, steep incidence angles: sensitivity to soil moisture (though signal attenuation by vegetation canopy)
- ↗ Retrieval approach: water cloud model
 - ↗ Step 1: Model calibration for Ku- and C-band

| Radar configuration | | Vegetation Parameters | | | Soil Parameters | |
|---------------------|------|-----------------------|-------|------|-----------------|-------|
| | | A | B | E | C | D |
| C-band 23°,VV | Mean | CE: | 0.000 | 0.09 | 0.00 | -11 |
| | | CN: | 0.000 | 0.09 | 0.00 | -8.5 |
| | | Alf: | 0.000 | 0.09 | 0.00 | -13 |
| Ku-band 55°,VV | Mean | CE: | 0.048 | 0.8 | 1.0 | -12 |
| | | CN: | 0.125 | 0.8 | 1.0 | -10.7 |
| | | Alf: | 0.030 | 0.8 | 1.0 | -14 |

$$\sigma_{soil}^o = C + Dm_s$$

C: equal to values for dry, bare soil



D=0: Ku-band not sensitive to soil moisture

Tab.: Parameterization of water cloud model – CE: cotton EW rows, CN: cotton NS rows, Alf: Alfalfa (Moran et al., 1998)

Moran et al.,
1998

Soil parameter retrieval – application example 2

Soil moisture under vegetation – combination of high and low frequencies

- ↗ Retrieval approach: water cloud model
- ↗ Step 2: Computation of Ku- and C-band σ^0 values for varying combinations of GLAI and soil moisture → construction of mesh graph
- ↗ Step 3: Production of maps of soil moisture and GLAI → plotting of measured radar signal within the mesh graph allows estimation of soil moisture and GLAI for each pixel

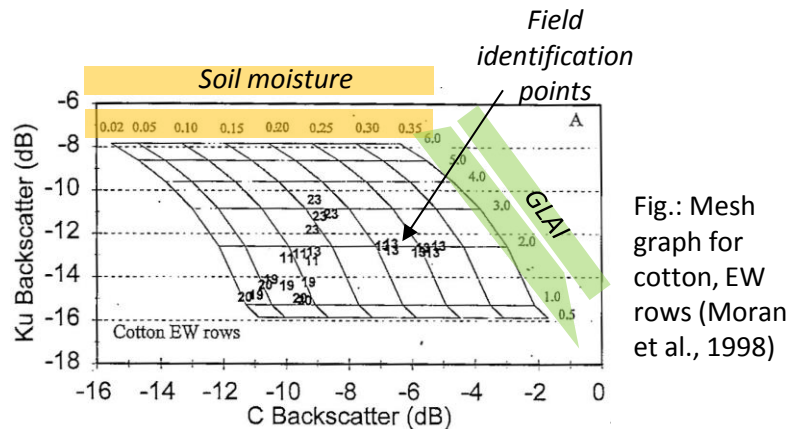


Fig.: Mesh graph for cotton, EW rows (Moran et al., 1998)

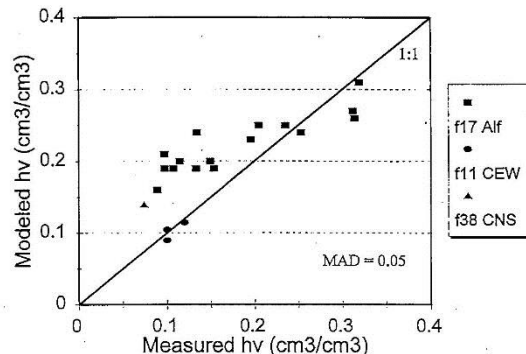


Fig.: Comparison of modelled vs. measured soil moisture (Moran et al., 1998)

Limitations of approach:

- ↗ **Ku- and C-band are sensitive to soil roughness → similar soil roughness, row direction is required**
 - ↗ **Saturation of Ku-band with increasing GLAI**

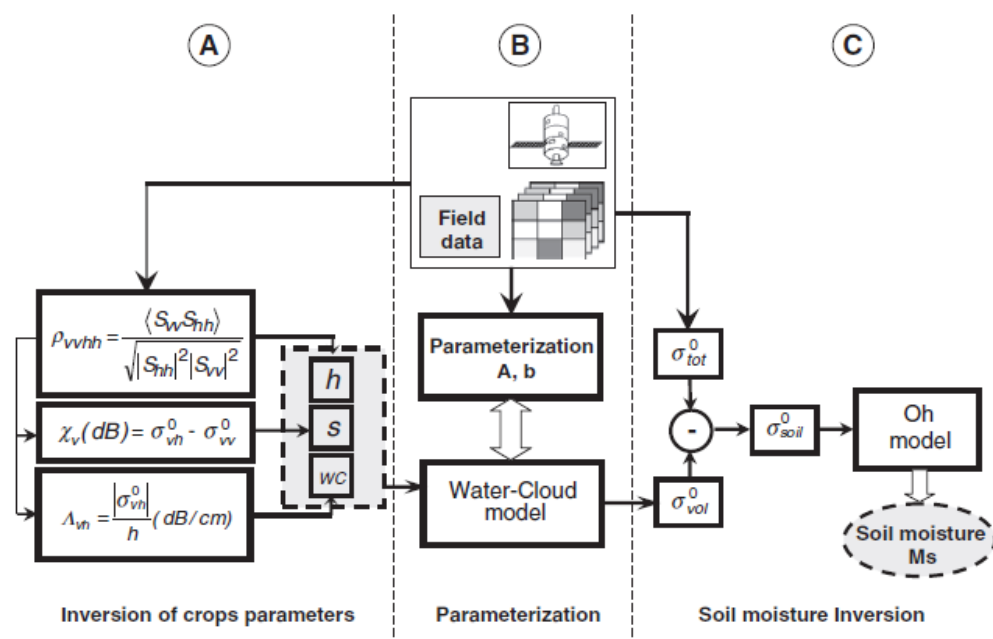
Soil parameter retrieval – application example 3

Soil moisture under vegetation – semi-empirical modelling

- ↗ Radarsat-2 data – C-band
- ↗ Test-site: south of Saskatoon, Canada
- ↗ Various mature crop types

Oh model
see module 3402:
Hydrosphere – soil moisture

Polarimetric parameters
see module 2300:
Radar polarimetry



h – crop height

s – surface roughness

wc – vegetation water content

ρ_{VVHH} – co-polarized correlation coefficient

χ_v – depolarization ratio

Fig.: Schematic diagram of the proposed soil moisture inversion approach (Gherboudj et al., 2011)

Gherboudj et al., 2011

Soil parameter retrieval – application example 3

Soil moisture under vegetation – semi-empirical modelling

- ↗ Retrieved soil moisture - average relative errors: 32%

- ↗ Suggestions for improved soil moisture retrieval
 - ↗ Usage of L-band SAR data
 - ↗ Consideration of soil-vegetation interactions in the modelling approach

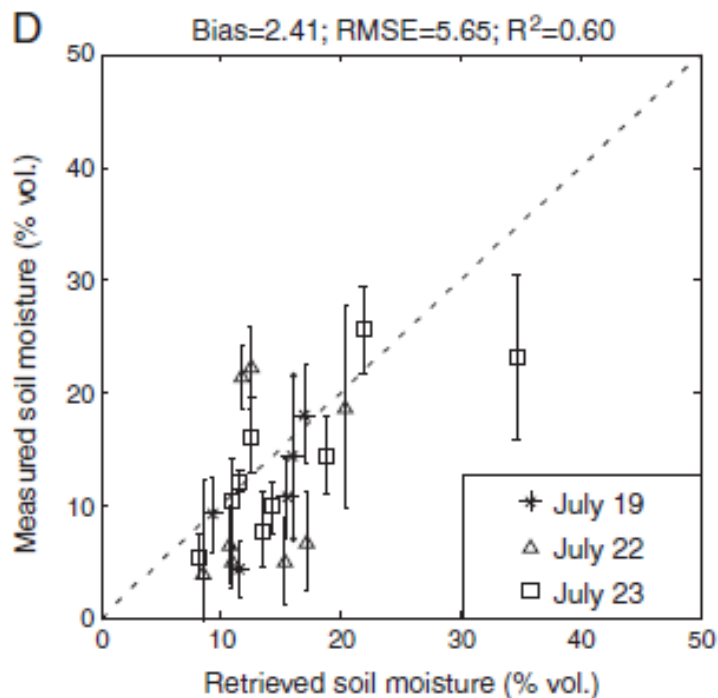


Fig.: Comparison of measured and retrieved soil moisture (Gherboudj et al., 2011)

Soil parameter retrieval – application example 4

Soil moisture under vegetation – SAR polarimetry

- ↗ Airborne L-band E-SAR data acquired within the AgriSAR, OPAQUE and SARTEO campaign over three test sites in Germany
- ↗ Comparison of different decomposition approaches

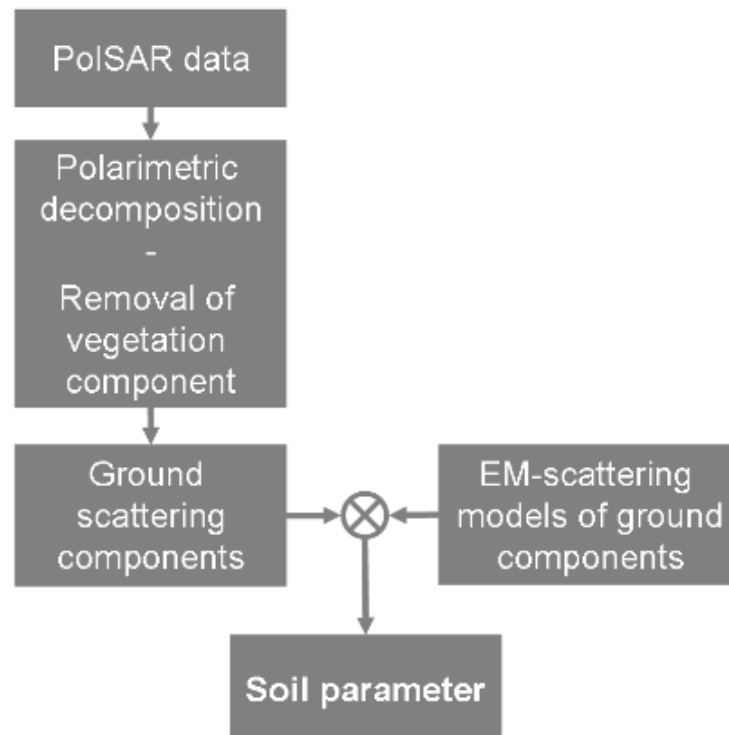


Fig.: General workflow of soil parameter retrieval from polarimetric SAR data using polarimetric decomposition techniques (Jagdhuber, 2012)

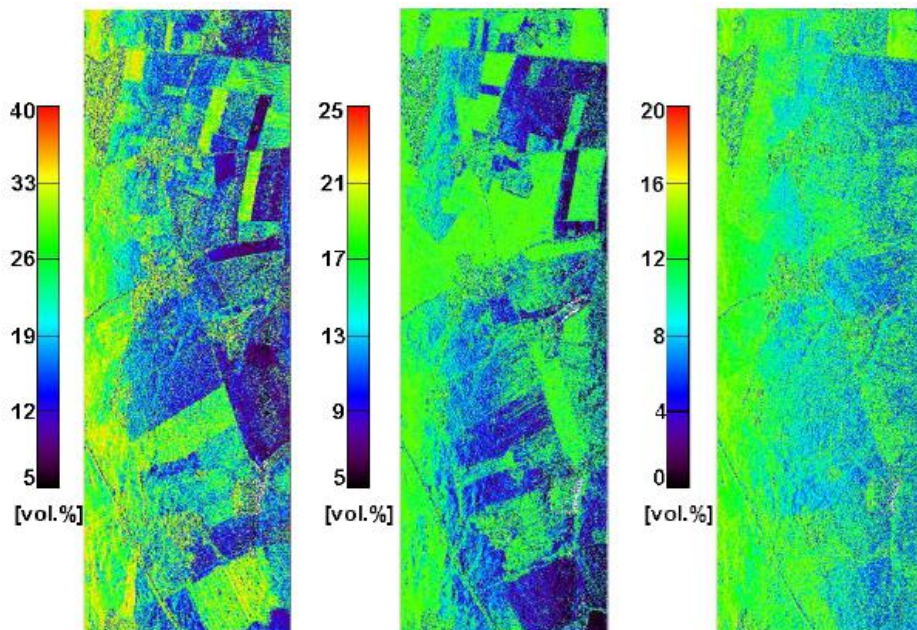
Jagdhuber, 2012

Soil parameter retrieval – application example 4

Soil moisture under vegetation – SAR polarimetry

↗ Results

- ↗ High potential → single angular hybrid decomposition approach (rmse: 5-11%; inversion rate: 97%)
- ↗ Further improvement using multi-angular SAR data (not necessarily true)



For more details
see module 2300:
radar polarimetry

Fig.: Results for soil moisture inversion under vegetation cover using a single angular hybrid decomposition and inversion approach – AgriSAR campaign. Left – April 19, 2006; middle: June 7, 2006; right: July 5, 2006; SO – summer oat, WW – winter wheat (Jagdhuber, 2012)

Soil parameter retrieval – application example 5

Soil surface roughness under vegetation – SAR polarimetry

- ↗ Airborne L-band E-SAR data acquired within the AgriSAR campaign over Demmin, Germany
- ↗ Methodology: modified X-Bragg ratio

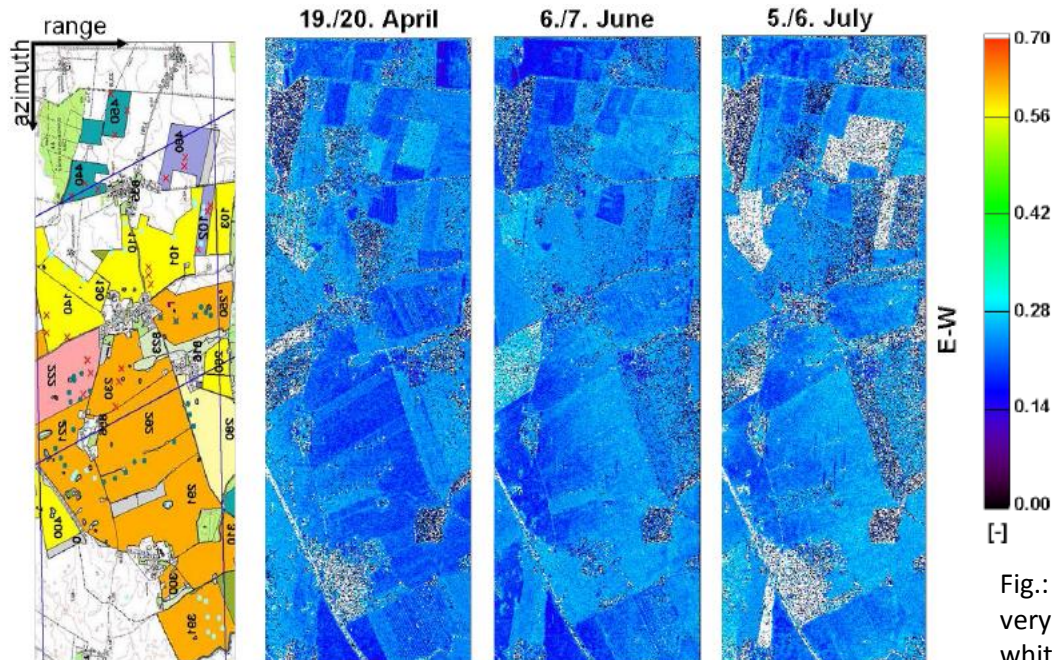


Fig.: Estimated soil roughness (ks). Areas with very rough soil conditions ($ks>0.7$) are masked white (Jagdhuber, 2012)

Soil parameter retrieval – application example 6

Crop residue – impact on soil moisture retrieval

- Radarsat-2 data → C-band acquired within the AgriSAR2009 campaign over Flevoland, The Netherlands
- Field covered by cereal stubbles

| Polarization | Roughness | Mean R^2 | Stdv. R^2 | Min R^2 | Max R^2 |
|--------------|-----------|------------|-------------|-----------|-----------|
| HH | Smooth | 0.477 | 0.185 | 0.247 | 0.800 |
| | Medium | 0.682 | 0.150 | 0.333 | 0.947 |
| | Stubbles | 0.426 | 0.173 | 0.069 | 0.699 |
| VV | Smooth | 0.482 | 0.166 | 0.269 | 0.806 |
| | Medium | 0.680 | 0.163 | 0.339 | 0.951 |
| | Stubbles | 0.413 | 0.190 | 0.102 | 0.707 |

Tab.: Correlation between RADARSAT-2 backscatter and soil moisture for different roughness classes (Lievens & Verhoest, 2012)

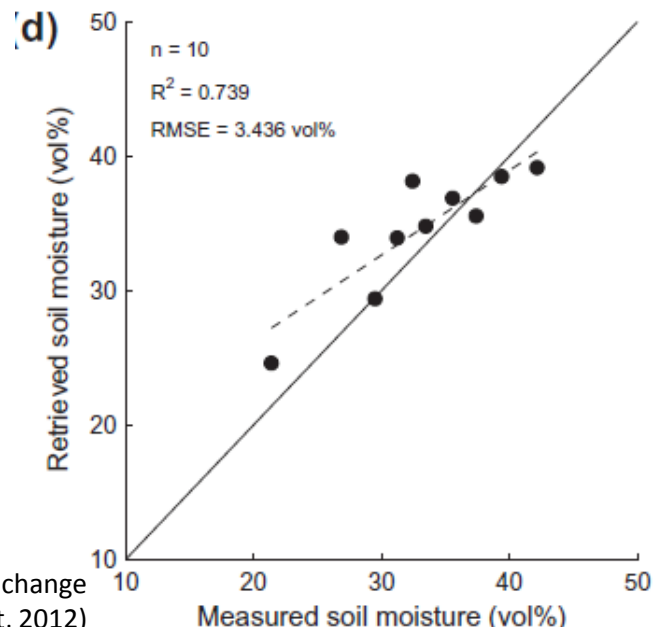


Fig.: Measured vs. retrieved soil moisture using a change detection approach, VV-polarization (Lievens & Verhoest, 2012)

Cereals crop remains → reduced sensitivity of the backscatter to soil moisture content observed

Lievens & Verhoest, 2012

Structure

- Introduction
- Major parameters affecting radar backscatter from crops
 - Sensor parameters
 - Target parameters
- Agricultural applications
 - Crop type mapping
 - Crop management / biophysical parameter retrieval
 - Soil parameter retrieval
- Optimal system configuration for agricultural applications

Optimal system configuration & current satellites

Revisit time

- ↗ Very critical parameter for agricultural applications
 - ↗ **Timeliness** of information
 - ↗ Significant variations of radar backscatter within short time
- ↗ **Dense time series** are required for many applications → acquisitions every few days, for soil moisture monitoring some authors suggest every day (e. g. Moran et al., 2012)

Phenological cycle of crops spans from 1 to few months

| | | | | | | |
|----------------------|--------|-------------|-------------|-------------|-------------|-------------|
| Satellite | ALOS-2 | Sentinel-1A | Tandem-X | Radarsat-2 | TerraSAR-X | |
| Life time | 2014 - | 2014 - | 2010 - | 2007 - | 2007 - | |
| Revisit time in days | 14 | 12 | 11 | 24 | 11 | |
| Satellite | Cosmo* | ALOS | Envisat | Radarsat-1 | ERS-2 | ERS-1 |
| Life time | 2007 - | 2006 - 2011 | 2002 - 2012 | 2005 - 2013 | 1995 - 2012 | 1991 - 2000 |
| Revisit time in days | 16 | 46 | 35 | 24 | 35 | 35 |

Tab.: Orbital revisit times of former & current satellites (© FSU)

* 4 satellites, launched in 2007, 2008 and 2010

Optimal system configuration & current satellites

Revisit time

- Revisit times of 1 to few days could be achieved by combining data acquired at different tracks / frames and ascending / descending orbits → but: additional angular scattering effects

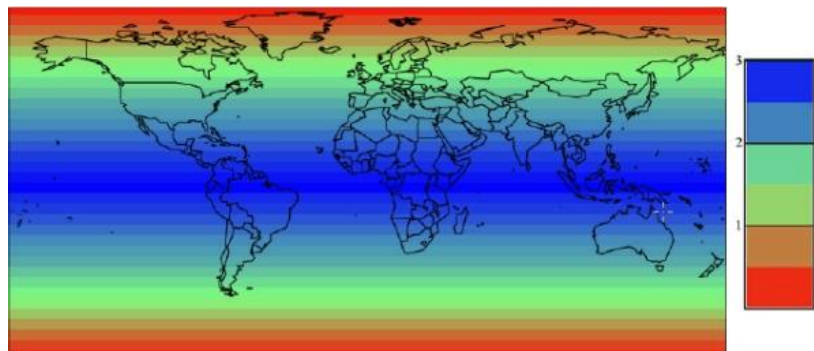


Fig.: Revisit frequency for Sentinel-1A and Sentinel-1B in days
<https://sentinel.esa.int/web/sentinel/user-guides/sentinel-1-sar/revisit-and-coverage>

- ✓ Two satellites in a 12 day orbit
- ✓ Repeat frequency: 6 days (important for coherence)
- ✓ Revisit frequency: (asc/desc & overlap): 3 days at the equator, <1 day at high latitudes (Europe ~ 2 days)

- Common problem: conflicts among different user requests → cancellation of acquisitions (e.g. TerraSAR-X, Envisat ASAR)

Systematic, pre-defined acquisition strategy

Goal: spatially and temporally consistent global data archive

e.g. ALOS PALSAR, ALOS-2 PALSAR-2 (Rosenqvist et al, 2014), Sentinel-1

Optimal system configuration & current satellites

Spatial resolution

- ↗ Very critical parameter
- ↗ Required spatial resolution:
 - ↗ Field-based investigations → depends on parcel size
General: high spatial resolution compared to parcel size
 - ↗ Intra-field variations / precision farming: very high

SAR data analyses require correction for inherent speckle → further decrease in spatial resolution

⇒ *For many regions of the world / many agricultural applications SAR data with a spatial resolution of one to a few meters are required*

Optimal system configuration & current satellites

Spatial resolution

Tab.: Spatial resolution of former & current satellites (© FSU)

| Satellite | ALOS-2 | Sentinel-1A | Tandem-X | Radarsat-2 | TerraSAR-X |
|------------------------|----------|---------------------|----------|------------|------------|
| Life time | 2014 - | 2014 - | 2010 - | 2007 - | 2007 - |
| Spatial resolution [m] | 3 – 100 | 5 – 50 ¹ | 1 – 16 | 3 – 100 | 1 – 16 |
| Swath width [km] | 25 - 350 | 20 - 400 | 10-100 | 10 - 500 | 10-100 |

| Satellite | Cosmo* | ALOS | Envisat | Radarsat-1 | ERS-2 | ERS-1 |
|------------------------|----------|-------------|-------------|-------------|-------------|-------------|
| Life time | 2007 - | 2006 - 2011 | 2002 - 2012 | 2005 - 2013 | 1995 - 2012 | 1991 - 2000 |
| Spatial resolution [m] | ~1 - 100 | 10 - 100 | 25 – 1000 | 10 – 100 | 25 | 25 |
| Swath width [km] | 10 - 200 | 70 - 360 | 100 - 400 | 50 - 500 | 100 | 100 |

* 4 satellites, launched in 2007, 2008 and 2010

¹ pre-defined mode over land: IW – 20m resolution

⇒ Latest SAR systems provide data with very high spatial resolution

⇒ In practice: often compromise between spatial resolution and area coverage

Optimal system configuration & current satellites

Polarization

- ↗ Data need sufficient for most studies / applications
 - ↗ Dual-pol SAR data including cross-polarisation
 - ↗ Polarimetry: increasing usage in recent years
→ fully-polarimetric SAR data

↗ Partial SAR polarimetry
see module 2300:
radar polarimetry

| | | | | | |
|---------------------|--------|-------------|----------------|------------|----------------|
| Satellite | ALOS-2 | Sentinel-1A | Tandem-X | Radarsat-2 | TerraSAR-X |
| Life time | 2014 - | 2014 - | 2010 - | 2007 - | 2007 - |
| Dual pol (incl. HV) | ✓ | ✓ | ✓ | ✓ | ✓ |
| Quad pol | ✓ | ✗ | ✓ ¹ | ✓ | ✓ ¹ |

| | | | | | | |
|---------------------|--------|-------------|-------------|-------------|-------------|-------------|
| Satellite | Cosmo* | ALOS | Envisat | Radarsat-1 | ERS-2 | ERS-1 |
| Life time | 2007 - | 2006 - 2011 | 2002 - 2012 | 2005 - 2013 | 1995 - 2012 | 1991 - 2000 |
| Dual pol (incl. HV) | ✓ | ✓ | ✓ | ✓ | ✗ | ✗ |
| Quad pol | ✗ | ✓ | ✗ | ✓ | ✗ | ✗ |

Tab.: Acquisition modes of former and current satellites (© FSU)

* 4 satellites, launched in 2007, 2008 and 2010

¹ experimental mode only

Optimal system configuration & current satellites

PollInSAR requirements

- ↗ C- or X-band
- ↗ Single-pass mode → to overcome temporal decorrelation
- ↗ Baseline: larger baselines are required → further studies are needed to define minimum baseline

Lopez-Sanchez et al.,
2009

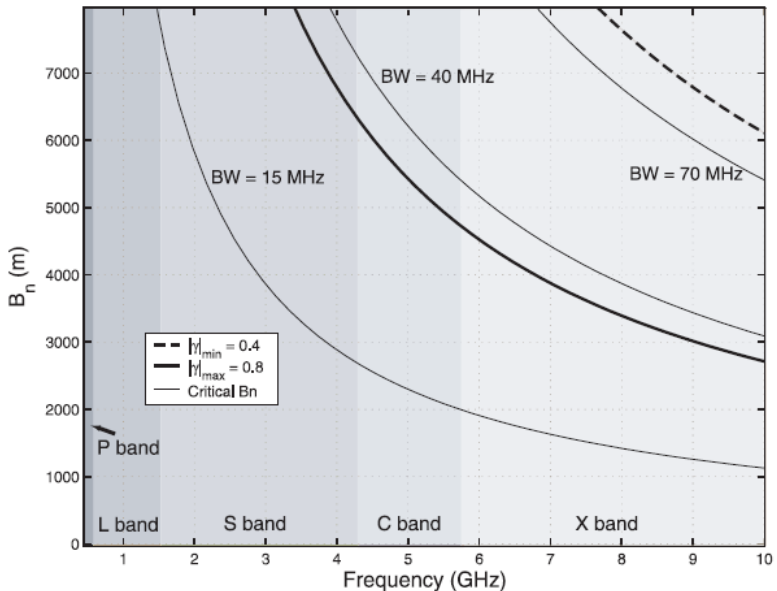


Fig.: Valid range of normal baseline as a function of frequency, derived from results with a 75 cm tall rice sample. Thick lines show the limits by low coherence (dashed) and volume sensitivity (solid). Thin lines represent the critical baseline for different bandwidths. Parameters: $\theta = 45^\circ$, $H = 550$ km (Lopez-Sanchez et al., 2009)

Optimal system configuration & current satellites

Summary

- ↗ SAR data availability by current spaceborne satellites
 - ↗ X-, C- and L-band
 - ↗ Very high spatial resolution
 - ↗ Short revisit time
- ↗ Sentinel-1A und Sentinel-1B data → free access, i.e. no costs!
 - ↗ Important for improvement of existing methods and operational applications → ESA expects breakthrough in the use of satellite data for specialised users, but also for the general public
- ↗ Fixed / systematic acquisition strategy → important for operational applications (e.g. Sentinel-1, ALOS-2 PALSAR-2)
 - ↗ Overcome problem of cancelled acquisitions
 - ↗ Built-up of comprehensive and consistent time series

*General problem:
spatial resolution vs. area coverage*

Optimal system configuration & current satellites

Summary

- ↗ Crop-type mapping
 - ↗ Latest SAR sensors provide a good database for classification approaches
- ↗ Retrieval of biophysical and soil parameters
 - ↗ More in-depth studies using high resolution data are needed to improve existing methods and retrieval algorithms

Important for wider usage / acceptance of SAR data (scientists and public users) and the development of operational applications

- Easy data access
- Access to pre-processed data
- No / low data costs
- Frequent, consistent data acquisition (no cancellations due to user conflicts)

References

- Attema, E. P. W., & Ulaby, F. T. (1978). Vegetation modeled as a water cloud. *Radio Science*, 13(2), 357-364.
- Atzberger, C. (2013). Advances in remote sensing of agriculture: context description, existing operational monitoring systems and major information needs. *Remote Sensing*, 5, 949-981.
- Ballester-Berman, J. D., Lopez-Sanchez, J. M., & Fortuny-Guasch, J. (2005). Retrieval of biophysical parameters of agricultural crops using polarimetric SAR interferometry. *IEEE Transaction on Geoscience and Remote Sensing*, 43(4), 683-694.
- Baraldi, A., Durieux, L., Simonetti, D., Conchedda, G., Holecz, F., & Blonda, P. (2010). Automatic spectral-rule-based preliminary classification of radiometrically calibrated SPOT-4/-5/IRS, AVHRR/MSG, AATSR, IKONOS/QuickBird/OrbView/GeoEye, and DMC/SPOT-1/-2 imagery – Part I: system design and implementation. - *IEEE Transactions on Geoscience and Remote Sensing*, 48(3), 1299-1325.
- Blaes, X., & Defourny, P. (2003). Retrieving crop parameters based on tandem ERS ½ interferometric coherence images. *Remote Sensing of Environment*, 88(4), 374-385.
- Bouman, B. A. M., & van Kasteren, H. W. J. (1990): Ground-based X-band (3-cm wave) radar backscattering of agricultural crops. II. wheat, barley, and oats; the impact of canopy structure. *Remote Sensing of Environment*, 34(2), 107-118.
- Bouvet, A., LeToan, T., Nguyen, L.-D. (2009). Monitoring of the rice cropping system in the Mekong Delta using ENVISAT/ASAR dual polarization data. *IEEE Transaction on Geoscience and Remote Sensing*, 47(2), 517-526.
- Bracaglia, M., Ferrazzoli, P., & Guerriero, L. (1995). A fully polarimetric multiple scattering model for crops. *Remote Sensing of Environment*, 54, 170-179.

References

- Brisco, B. & R.J. Brown (1998): Agricultural Applications with Radar. In: Henderson, F.M. & A.J. Lewis (Eds.): Principles & Applications of Imaging Radar. Manual of Remote Sensing. Third Edition, Volume 2. Wiley & Sons, New York.
- Chiu, T., & Sarabandi, K. (2000). Electromagnetic scattering from short branching vegetation. . *IEEE Transaction on Geoscience and Remote Sensing*, 38(2), 911-925.
- De Roo, R. D., Du, Y., Ulaby, F. T., & Dobson, M. C. (2001). A semi-empirical backscattering model at L-band and C-band for a soybean canopy with soil moisture inversion. *IEEE Transactions on Geoscience and Remote Sensing*, 39(4), 864–872.
- Della Vecchia, A., Ferrazzoli, P., Guerriero, L., Ninivaggi, L., Strozzi, T., & Wegmüller, U. (2008). Observing and modeling multifrequency scattering of maize during the whole growth cycle. *IEEE Transactions on Geoscience and Remote Sensing*, 46(11), 3709–3718.
- Deschamps, B., McNairn, H., Shang, J., & X. Jiao (2012). Towards operational radar-only crop type classification: comparison of a traditional decision tree with a random forest classifier. *Canadian Journal of Remote Sensing*, 38(1), 60-68.
- Engdahl, M. E., Borgeaud, M., & Rast, M. (2001). The use of ERS-1/2 tandem interferometric coherence in the estimation of agricultural crop heights. *IEEE Transactions on Geoscience and Remote Sensing*, 39(8), 1799–1806.
- FAO (2013a): *Food wastage footprint. Impacts on natural resources. Summary report*. Retrieved on October 9, 2013 from <http://www.fao.org/docrep/018/i3347e/i3347e.pdf>
- FAO (2013b). *FAOSTAT*. Retrieved on February 24, 2014 from <http://faostat3.fao.org/faostat-gateway/go/to/download/Q/QC/E>

References

- Ferrazzoli, P. (2001). SAR for agriculture: advances, problems and prospects. In: *Proceedings of the Third International Symposium on Retrieval of Bio- and Geophysical Parameters from SAR Data for Land Applications* (ESA SP-475, pp. 47-56), September 11-14, 2001, Sheffield, UK.
- Foley, J. A., Ramankutty, N., Brauman, K. A., Cassidy, E. S., Gerber, J. S., Johnston, M., Mueller, N. D., O'Connell, C., Ray, D. K., West, P. C., Balzer, C., Bennett, E. M., Carpenter, S. R., Hill, J., Monfreda, C., Polasky, S., Rockstrom, J., Sheehan, J., Siebert, S., Tilman, D., & Zaks, D. P. M. (2011). Solutions for a cultivated planet. *Nature*, 478, 337-342.
- Gherboudj, I., Magagi, R., Berg, A. A., & Toth, B. (2011). Soil moisture retrieval over agricultural fields from multi-polarized and multi-angular RADARSAT-2 SAR data. *Remote Sensing of Environment*, 115, 33-43.
- Government of Canada (2010). International GEO workshop on synthetic aperture radar (SAR) to support agricultural monitoring, 2. – 4. November 2009, Kananaskis, Alberta, Canada – Workshop report. Retrieved on 2013-11-19 from http://www.earthobservations.org/documents/cop/ag_gams/200911_02/20091102_sar_for_ag_monitoring_workshop_report.pdf
- Graham, A. J., & Harris, R. (2002). Estimating crop and waveband specific water cloud model parameters using a theoretical backscatter model. *International Journal of Remote Sensing*, 23(23), 5129-5133.
- Hajnsek, I., Jagdhuber, T., Schön, H., & Papathanassiou, K. P. (2009). Potential of estimating soil moisture under vegetation cover by means of PolSAR. *IEEE Transaction on Geoscience and Remote Sensing*, 47(2), 442-454.
- Inoue, Y., Sakaiya, E., & Wang, C. (2013). Capability of C-band backscattering coefficients from high-resolution satellite SAR sensors to assess biophysical variables in paddy rice fields. *Remote Sensing of Environment*, 140, 257 -266.

References

- Inoue, Y., Kurosu, T., Maeno, H., Uratsuka, S., Kozu, T., Dabrowska-Zielinska, K., & Qi, J. (2002). Season-long daily measurements of multifrequency (Ka, Ku, X, C, and L) and full-polarization backscatter signatures over paddy rice field and their relationship with biological variables. *Remote Sensing of Environment*, 81(2-3), 194 – 204.
- Jagdhuber, T. (2012). *Soil Parameter Retrieval under Vegetation Cover Using SAR Polarimetry*. Dissertation, University of Potsdam. Retrieved on 2014-02-10 from <http://opus.kobv.de/ubp/volltexte/2012/6051/>.
- Jensen, J. R. (2000). *Remote Sensing of the Environment: An Earth Resource Perspective*. Upper Saddle River, New Jersey: Prentice Hall.
- Jiao, X., McNairn, H., Shang, J., Pattey, E., Liu, J., & Chamagne, C. (2011). The sensitivity of RADARSAT-2 polarimetric SAR data to corn and soybean Leaf Area Index (LAI). *Canadian Journal of Remote Sensing*, 37, 69-81.
- Karjalainen, M., Kaartinen, H., & Hyppä, J. (2008). Agricultural monitoring using Envisat alternating polarization SAR images. *Photogrammetric Engineering & Remote Sensing*, 74(1), 117-126.
- LeToan, T. (2008). Use of SAR data for agricultural applications – Advanced training course in land remote sensing, DRAGON-2 project, 13. – 18. October 2008, Wuhan University, China. Retrieved on November, 21, 2013 from http://dragon2.esa.int/landtraining2008/pdf/D4L2_Agriculture_LeToan.pdf
- LeToan, T., Bouvet, A., Bingxiang, T., Zengyuan, L., Wie, H., Bingbai, L., Pingping, Z., & Bondeau, A. (2005). Rice monitoring in China – mid-term report. In: *Proceedings of the Dragon Symposium „Mid-Term Results“ (ESA SP-611)*, June 27 – July 1, 2005, Santorini, Greece.

References

- Lievens, H., & Verhoest, N. E. C. (2012). Spatial and temporal soil moisture estimation from RADARSAT-2 imagery over Flevoland, The Netherlands. *Journal of Hydrology*, 456-457, 44-56.
- Lin, H., Chen, J., Pei, Z., Zhang, S., & Hu ,X. (2009). Monitoring sugarcane growth using ENVISAT ASAR data. *IEEE Transactions on Geoscience and Remote Sensing*, 47(8), 2572–2580.
- Liu, C., Shang, J., Vachon, P. W., & McNairn, H. (2013). Multiyear crop monitoring using polarimetric RADARSAT-2 data. *IEEE Transaction on Geoscience and Remote Sensing*, 51(4), 2227 -2240.
- Lopes, A.,I (1983). *Etude experimentale et theorique de l'attenuation et de la retrodiffusion des micro-ondes par un couvert de ble. Application a la teledetection.* Ph.D. Dissertation, l'Universite Paul Sabatier de Toulouse.
- Lopez-Sanchez, J. M., Cloude, S. R., Ballester-Berman, J. D. (2012a). Rice phenology monitoring by means of SAR polarimetry at X-band. *IEEE Transaction on Geoscience and Remote Sensing*, 50(7), 2695 -2709.
- Lopez-Sanchez, J. M., Hajnsek, I., & Ballester-Berman, J. D. (2012b): First demonstration of agriculture height retrieval with PollInSAR airborne data. *IEEE Geoscience and Remote Sensing Letters*, 9(2), 242-246.
- Lopez-Sanchez, J. M., Ballester-Berman, J. D., Vicente, F., & Cloude, S. R. (2012c). *Recent advances in applications of SAR polarimetry – Agriculture: phenology retrieval.* 2nd Advanced Course on Radar Polarimetry, January 25, 2012, Frascati, Italiy. Retrieved on January 15, 2014 from https://earth.esa.int/documents/10174/669756/Phenology_retrieval.pdf
- Lopez-Sanchez, J. M., Ballester-Berman, J. D., & Hajnsek, I. (2011). First results of rice monitoring practices in Spain by means of time series of TerraSAR-X dual-pol images. *IEEE Journal of Selected Topics in Applied Earth Observations and Remote Sensing*, 4(2), 412-422.

References

- Lopez-Sanchez, J. M (2010). Agriculture monitoring using time series of satellite radar polarimetric images. *EEO-AGI Series Programme 2010-2011*, September 24, 2010, Edinburgh, Scotland. Retrieved on January 13, 2014 from http://www.geos.ed.ac.uk/~gisteac/eeo_agi/2010-11/1_lopez-sanchez_24092010.pdf
- Lopez-Sanchez, J. M., & Ballester-Berman, J. D. (2009). Potentials of polarimetric SAR interferometry for agriculture monitoring. *Radio Science*, 44(2), DOI: 10.1029/2008RS004078.
- Loosvelt, L., Peters, J., Skriver, H., De Baets, B., & Verhoest, N.E.C. (2012). Impact of Reducing Polarimetric SAR Input on the Uncertainty of Crop Classifications Based on the Random Forests Algorithm. *IEEE Transactions on Geoscience and Remote Sensing*, 50(10), 4185 - 4200.
- Marliani, F., Paloscia, S., Pampaloni, P., & Kong, J. A. (2002). Simulating coherent backscattering from crops during the growing season. *IEEE Transaction on Geoscience and Remote Sensing*, 40(1), 162-177.
- Mattia, F., Le Toan, T., Picard, G., Posa, F. I., D'Alessio, A., Notarnicola, C., Gatti, A. M., Rinaldi, M., Satalino, G., & Pasquariello, G. (2003). Multitemporal C-band radar measurements on wheat fields. *IEEE Transaction on Geoscience and Remote Sensing*, 41(7), 1551 -1559.
- McNairn, H., Kross, A., Lapen, D.R., Caves, R., & Shang, J. (2014). Early season monitoring of corn and soybeans with TerraSAR-X and RADARSAT-2. *International Journal of Applied Earth Observation and Geoinformation*, 28, 252-259. doi : 10.1016/j.jag.2013.12.015
- McNairn, H., Shang, J., Jiao, X., & Deschamps, B. (2012). Establishing crop productivity using RADARSAT-2. *International Archives of the Photogrammetry, Remote Sensing and Spatial Information Sciences* (Volume XXXIX-B8, 2012), XXII ISPRS Congress, 25 August – 01 September 2012, Melbourne, Australia.

References

- McNairn, H., Shang, J., Jiao, X., & Champagne, C. (2009). The contribution of ALOS PALSAR multipolarization and polarimetric data to crop classification. *IEEE Transaction on Geoscience and Remote Sensing*, 47(12), 3981 -3992.
- McNairn, H., Duguay, C., Brisco, B., & Pultz, T.J. (2002). The effect of soil and crop residue characteristics on polarimetric radar response. *Remote Sensing of Environment*, 80(2), 308-320.
- Moran, M. S., Alonso, L., Moreno, J. F., Mateo, M. P. C. de la Cruz, D. F., & Montoro, A. (2012). A RADARSAT-2 quad-polarized time series for monitoring crop and soil conditions in Barrax, Spain. *IEEE Transactions on Geoscience and Remote Sensing*, 50(4), 1057-1070.
- Moran, M. S., Vidal, A., Troufleau, D., Inoue, Y., & Mitchell, T. A. (1998). Ku- and C-band SAR for discriminating agricultural crop and soil conditions. . *IEEE Transactions on Geoscience and Remote Sensing*, 36(1), 265-272.
- OECD-FAO (2012). *OECD-FAO Agricultural Outlook 2012-2021*. OECD Publishing and FAO.
- Picard, G., Le Toan, T., Mattia, F. (2003). Understanding C-band radar backscatter from wheat canopies using a multiple scattering coherent model. *IEEE Transaction on Geoscience and Remote Sensing*, 41(7), 1583-1591.
- Prevot, L., Champion, I., & Guyet, G. (1993). Estimating surface soil moisture and leaf area index of a wheat canopy using a dual-frequency (c and X bands) scatterometer. *Remote Sensing of Environment*, 46, 331-339.
- Quegan, S., Le Toan, T., Skriver, H., Gomez-Dans, J., Gonzalez-Sampredo, M. C., & Hoekman, D. H. (2003). Crop classification with multitemporal polarimetric SAR data. In: *Proceedings of the International Workshop on Science and Application of SAR Polarimetry and Polarimetric Interferometry (PolInSAR)* (ESA SP-529), January 14 – 16, 2003, Frascati, Italy.

References

- Rosenqvist, A., Shimada, M., Suzuki, S., Ohgushi, F., Tadono, T., Watanabe, M., Tsuzuku, K., Watanebe, T., Kamijo, S., & Aoki, E. (2014). Operational performance of the ALOS global systematic acquisition strategy and observation plans for ALOS-2 PALSAR-2. *Remote Sensing of Environment*, in press.
- Skriver, H., Mattia, F., Satalino, G., Balenzano, A., Pauwels, V. R. N., Verhoest, N. E. C., & Davidson, M. (2011). Crop classification using short-revisit multitemporal SAR data. *IEEE Journal of Selected Topics in Applied Earth Observations and Remote Sensing*, 4(2), 423-431.
- Stankiewicz, K. (2006). The efficiency of crop recognition on ENVISAT ASAR images in two growing seasons. *IEEE Transaction on Geoscience and Remote Sensing*, 44(4), 806 -348.
- Staples, G., Caves, R., Padda, J., Mah, A., & Davidson, G. (2010). RADARSAT-2 and AgriSAR 2009. *Civil Commercial Imagery Evaluation Workshop, JACIE*, March 16-18, 1020, Fairfax, Virginia, US. Retrieved on 2013-12-8 from http://calval.cr.usgs.gov/JACIE_files/JACIE10/Presentations/ThurAM/Staples_Gordon_radarsat2_JACIE.pdf
- Stiles, J. M., & Sarabandi, K. (2000). Electromagnetic scattering from grassland. I: A fully phase-coherent scattering model. *IEEE Transaction on Geoscience and Remote Sensing*, 38, 339 -3992.
- Tan, C. P., Ewe, H. T., & C. H. T. (2011). Agricultural crop-type classification of multi-polarization SAR images using a hybrid entropy decomposition and support vector machine technique. *International Journal of Remote Sensing*, 32(22). 7057-7071.
- Touré, A., Thompson, K. P. B., Edwards, G., Brown, R. J., & Brisco, B. G. (1994). Adaptation of MIMICS backscattering model to the agricultural context – wheat and canola at L- and C-bands. *Transactions on Geoscience and Remote Sensing*, 32(1), 81-95.

References

- Wang, H., Allain, S., Méric, S., & Pottier, E. (2013): Scattering mechanism analysis using multi-angular polarimetric Radarsat-2 datasets. In: *Proceedings of the 6th International Workshop on Science and Application of SAR Polarimetry and Polarimetric Interferometry (PolInSAR)*, January 28 – February 1, 2013, Frascati, Italy.
- Wegmüller, U., Santoro, M., Mattia, F., Balenzano, A., Satalino, G., Marzahn, P., Fischer, G., Ludwig, R., & Flury, N. (2011). Progress in the understanding of narrow directional microwave scattering of agricultural fields. *Remote Sensing of Environment*, 115, 2423-2433.
- Wegmüller, U., & Werner, C. L. (1997). Retrieval of vegetation parameters with SAR interferometry. *IEEE Transactions on Geoscience and Remote Sensing*, 35(1), 18–24.
- Ulaby, F.T. Moore, R.K. & A.K. Fung (1986): Microwave Remote Sensing: Active and Passive, Vol. III, From Theory to Applications. Artech House, Norwood.
- Ulaby, F. T., Allen, C. T., & Eger III, G. (1984). Relating the microwave backscattering coefficient to leaf area index. *Remote Sensing of Environment*, 14, 113-133.
- Yunjin, K., & Van Zyl, J. (2009). A time-series approach to estimate soil moisture using polarimetric radar data. *IEEE Transactions on Geoscience and Remote Sensing*, 47(8), 2519–2527.
- Background photo by on Flickr, J. (2010). Retrieved on November 11, 2013 from <http://www.fotopedia.com/items/flickr-2733264675>

SAR-EDU – SAR Remote Sensing Educational Initiative

<https://saredu.dlr.de/>

Supported by:



Federal Ministry
of Economics
and Technology

on the basis of a decision
by the German Bundestag